On the Application of the Competitive Modes Conjecture

H.A.J. Reijm

Delft University of Technology

h.a.j.reijm@student.tudelft.nl

UNDER THE SUPERVISION OF

Prof. Cornelis Vuik

Delft University of Technology

c.vuik@tudelft.nl

Dr. Sudipto "Roy" Choudhury

University of Central Florida

sudipto.choudhury@ucf.edu

October 22, 2021

Abstract

Modelling natural phenomena via Dynamical System Theory has become commonplace amongst mathematicians, physicists, engineers, and the like. As such, research in this field is currently underway, with a notable focus on chaos. The Competitive Modes Conjecture is a relatively new approach in the field of chaotic Dynamical Systems, aiming to understand why a strange attractor is chaotic or not. Up till now, the Conjecture has only been used to study multipolynomial systems because of their simplicity. As such, the study of non-multipolynomial systems is sparse, filled with ambiguity, and lacks mathematical structure. This paper strives to rectify this dilemma, providing the mathematical background needed to rigorously apply a large set of non-multipolynomial systems to the Competitive Modes Conjecture. Examples of this new theory include application of Lorenz System, the Chua System, and the Wimol-Banlue System. As far as the authors are aware, any previous application of the latter two systems to the Conjecture has not been attempted. Therefore, this paper presents the first applications of a whole new set of dynamical systems to the Conjecture.

Contents

I. Introduction

Change: people embrace it, societies struggle with it, and politicians promise it. Whatever the case may be, one can not deny its overwhelming control. "Times change, and so must I" as the old saying goes. In fact, many of the processes governing the universe can be described by how they change. Perhaps one could ascertain the behavior of a process given its current state and a set of rules governing how the process must change with time. This basic ideology is the cornerstone of the mathematical theory of dynamical systems.

Dynamical systems are an essential part of the modern mathematical and physical community. Their popularity can be attested to in almost all aspects of science. As an example, consider the system of differential equations describing the 1-dimensional motion of an object under the influence of some constant acceleration (or deceleration).

$$\begin{cases} \dot{a}(t) = 0 \\ \dot{v}(t) = a(t) \\ \dot{p}(t) = v(t) \end{cases}$$

Here, $p : \mathbb{R} \to \mathbb{R}$ describes the position of the object, $v : \mathbb{R} \to \mathbb{R}$ describes its velocity, and $a : \mathbb{R} \to \mathbb{R}$ describes its acceleration, all with respect to time $t \in \mathbb{R}$. Assuming that the acceleration (or deceleration) has a constant value $\beta \in \mathbb{R}$, this system differential equation can easy be solved as follows.

$$a(t) = \beta,\ v(t) = \beta t + v(0),\ p(t) = \frac{1}{2}\beta t^2 + v(0)t + p(0) \tag{1}$$

What are these equations used for? Imagine a car manufacturer that is specifically researching the effectiveness of its automotive braking systems. The brakes will apply a deceleration to slow the velocity of a moving vehicle to zero. However, the deceleration needs to be strong enough to stop the car before it collides into a potential obstacle in its path. How strong would the deceleration then need to be?

Imagine a vehicle traveling to the right starts to apply its brakes at time $t = 0$. The vehicle at this moment is at position $p(0)$ and traveling with a velocity of $v(0) > 0$. As the brakes exert a constant deceleration of $\beta < 0$, the vehicle's velocity slows down. Then the time needed for the vehicle to come to a complete stop t_{stop} as well as the distance traveled while doing so $p(t_{stop}) - p(0)$ can be calculated using Equation (1).

$$t_{stop} = -v(0)/\beta > 0, \quad p(t_{stop}) - p(0) = \frac{1}{2}\beta t_{stop}^2 + v(0)t_{stop} > 0$$

Is this breaking distance small enough? That of course depends on the situation. But automotive manufacturers can use Equation (1) to mathematically model each situation independently and ensure the quality of their vehicles' brakes. Perhaps through this process,

a manufacture of automotive brake pads discovers its products perform less than adequately in rainy weather. The manufacturer can now adjust its products accordingly and in doing so protect the safety of motorists.

The set of solutions in Equation (1) is officially referred to as a dynamical system. Through our exemplary thought-experiment we see the purpose of dynamical systems: describing the solutions of differential equations so that society can better understand, predict, and respond to the processes being modeled. We state this more formally with the following definition.

Definition I.1. ***Dynamical System***
Say we have an autonomous[1] *continuous system of differential equations* $\dot{\mathbf{x}} = \mathbf{F}(\mathbf{x})$ *with* $\mathbf{F} : S \to S$*, where* S *is some open subset of* $\mathbb{R}^n$*. Please note that* $\dot{\mathbf{x}}$ *is shorthand notation for the vector* $[\partial \mathrm{x}_1/\partial t, \cdots, \partial \mathrm{x}_n/\partial t]^T$*.*
The dynamical system $\delta : S \times \mathbb{R} \to S$ *with* $\delta(\mathbf{x}_0, 0) = \mathbf{x}_0$ *is a continuously differentiable mapping that defines the solution of our system of differential equations (also known as a trajectory or orbit) that passes through the point* $\mathbf{x}_0 \in S$ *at* $t = 0$ *[27][36].*

Some dynamical systems are much more complicated than Equation (1) and require numerical integration techniques in order to be approximated (direct solutions are often impossible to find). A particularly famous example of such a dynamical system is that of the Lorenz System [31].

$$\begin{cases} \dot{x} = \sigma(y - x) \\ \dot{y} = x(\rho - z) - y \\ \dot{z} = xy - \beta z \end{cases} \tag{2}$$

Here, σ, ρ, and $\beta \in \mathbb{R}$, and x, y, z are real functions of $t \in \mathbb{R}$.

We can numerically approximate the solution to the Lorenz System using an explicit Runge Kutta method (for example, see [16] and [17]). Choosing a specific set of parameters and initial conditions, we plot approximations to specific solution curves in the x,y,z-graph (called a phase space) in Figure 1. As a result, we see a very curious structure forming in the phase space: it seems that the solution curves we plotted endlessly twist and wind around each other, converging to some bounded set in the phase space resembling the wings of a butterfly. This set is called the Lorenz Attractor.

The Lorenz Attractor is a classic example of the more general concept of a strange attractor [27]. Because of their complicated structures and ability to describe steady-state situations, understanding strange attractors is a topic of great interest in the modern dynamical systems community. However, strange attractors can be difficult to analyze. Some dynamical systems do not contain any strange attractor at all, and some systems only contain strange

[1]This paper will focus primarily on autonomous systems of differential equations. Non-autonomous systems can be trivially represented as autonomous ones.

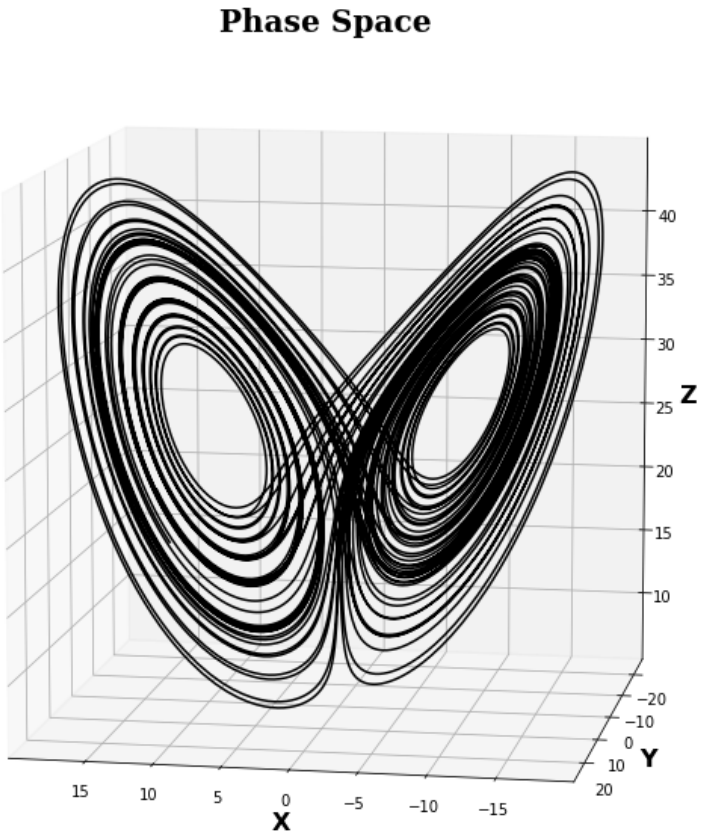

Figure 1: *The Lorenz Attractor, where $\sigma = 10$, $\rho = 28$, and $\beta = 8/3$. The attractor was approximated using an adaptive explicit RK4 numerical integration technique over a time span of 60 time units using an initial position of (10.383, 16.824, 19.325). See Appendix C for coding details.*

attractors for certain values of parameters. Even if the existence of a strange attractor is possible, the location of the attractor can be difficult to pin down.

As such is the case, this document has three purposes. The first few sections are devoted to mathematically describing what a strange attractor is. Furthermore, this paper will go into detail about a property many strange attractors seem to possess: chaos.

From there, this document will move on into underlining some of the current methods used to localize strange attractors. The reason for this is two-fold. Localization techniques require a certain level of understanding; if the attractor can be localized, then it must be because of our understanding of some of its properties. Hopefully these techniques can then provide some more mathematical insight. The second reason for researching localization techniques is understanding their application. It is the authors' opinion that these techniques are complex, and although they can provide results of noteworthy quality, their application can be situational. Perhaps something better can be developed.

This will lead us to the Competitive Modes Conjecture, which is a new attempt at understanding chaotic strange attractors. The latter half of this paper will focus on unpacking this conjecture, providing it a more rigorous mathematical structure, and applying it to systems of differential equations that have never been analyzed in this way before[2]. Furthermore, previous literature has proven that this conjecture can be used of sorts as a more general and easily applicable localization technique.

[2]That is, as far as the authors are aware of as of the writing of this paper

II. Strange Attractors

In Section I, we loosely explained some basic concepts concerning dynamical systems but refrained from concretely defining them. Let us first rectify this.

Definition II.1. ***Attracting Set***
Say we have the dynamical system $\delta : S \times \mathbb{R} \to S$ of a system of differential equations. A closed, invariant set $A \subseteq S$ is called an attracting set of our system if there exists some neighborhood N of A such that for any point $\mathbf{x} \in N$, $\delta(\mathbf{x}, t) \in N$ for all $t \geq 0$. Furthermore $\delta(\mathbf{x}, t)$ limits to A as t limits to infinity. [27]. The maximal neighborhood N_{max} of A where this is the case is called the basin of attraction of A.

Definition II.2. ***Attractor***
Say we have the dynamical system $\delta : S \times \mathbb{R} \to S$ of a system of differential equations. Suppose A is an attracting set of our system. The set A is an attractor if it contains a dense orbit; that is, there exists a trajectory that passes through or comes infinitely close to every point in A. This ensures that A is not the union of two or more distinct attracting sets [27][33].

Attractors are not an uncommon sight in dynamical systems: stable equilibrium points, stable limit cycles, and stable limit tori are all examples of attractors that can occur in a dynamical system. However, defining whether an attractor is strange or not takes some more effort, and it all has to do with the concept of dimension.

Say we have a non-empty set B in $\mathbb{R}^n$. The topological dimension of B is simply the formal name for the well-known, everyday concept of dimensionality. According to topological dimensionality, a point is 0-dimensional, a line is 1-dimensional, a plane is 2-dimensional, and so on. Notice that the topological dimension of B is always an integer value greater or equal to 0, and no greater than n [25].

We must define another concept of dimensionality before we can proceed. Suppose we have the set B defined as before. We define the s-dimensional Hausdorff measure of B as follows [15]:

$$\mathcal{H}^s(B) = \lim_{\varepsilon \to 0} \inf \left\{ \sum_{i=1}^{\infty} ||C_i||^s : \ \{C_i\} \text{ is a } \varepsilon\text{-cover of } B \right\}$$

Here, a ε-cover of B is a countable set $\{C_i\}$ so that $\sup\{||x - y|| : x, y \in C_i\} \leq \varepsilon \ \forall i$ and $B \subseteq \bigcup_{i=1}^{\infty} C_i$. Using this measure, we can define the Hausdorff dimension (or Hausdorff-Besicovitch dimension) of B as follows [15]:

$$dim_{\mathcal{H}}(B) = \inf\{s \geq 0 : \mathcal{H}^s(B) = 0\} \tag{3}$$

Now that we have defined the concepts of topological and Hausdorff dimensionality, we can move on to the defining of a fractal, which are essential structures in strange attractors.

Definition II.3. ***Fractal***
Say we have a non-empty set B in $\mathbb{R}^n$. The set B is a fractal if the Hausdorff dimension of B is strictly greater than the topological dimension of B [25]. Often, this is described as self-similarity: the fractal is constructed of parts that in turn resemble (not necessarily copy) the whole structure [15].

Finally, we can define a strange attractor very simply.

Definition II.4. ***Strange Attractor***
Say we have the dynamical system $\delta : S \times \mathbb{R} \to S$ of a system of differential equations. Suppose A is an attractor of our system. The set A is a strange attractor if its attracting set is fractal in nature. In layman's terms, this means that A has a much more complicated geometric structure than, for example, an equilibrium point, a limit cycle, or limit torus [3][33].

We can further classify strange attractors in two categories: self-excited and hidden. However, in order to formally define these two categories, we must first provide a few more definitions.

Definition II.5. ***Equilibrium Point***
Say we have the system of differential equations $\dot{\mathbf{x}} = \mathbf{F}(\mathbf{x})$. An equilibrium point $\mathbf{x}_e$ of this system is a point in the phase space where $\mathbf{F}(\mathbf{x}_e) = \mathbf{0}$. In order words, the equilibrium point is invariant under the corresponding dynamical system. [27].

Definition II.6. ***Manifolds of Equilibrium Points***
Say we have the dynamical system $\delta : S \times \mathbb{R} \to S$ of a system of differential equations that contains the equilibrium point $\mathbf{x}_e$. Then the equilibrium point has two corresponding sets of S called manifolds [3]:

- *A stable manifold of the equilibrium point $\mathcal{W}^+(\mathbf{x}_e) = \{\mathbf{x} \in S : \lim_{t\to+\infty} \delta(\mathbf{x}, t) = \mathbf{x}_e\}$*
- *A unstable manifold of the equilibrium point $\mathcal{W}^-(\mathbf{x}_e) = \{\mathbf{x} \in S : \lim_{t\to-\infty} \delta(\mathbf{x}, t) = \mathbf{x}_e\}$.*

We can now define self-excited and hidden strange attractors.

Definition II.7. ***Classification of Strange Attractors***
Say we have a system of differential equations that contains equilibrium points. Suppose A is a strange attractor, then

- *A is self-excited if its basin of attraction contains at least one equilibrium point [22].*
- *A is hidden if its basin of attraction contains no equilibrium points [22].*

Per definition, self-excited strange attractors can be easily visualized by simply plotting the unstable manifolds of the equilibrium points. At least one of the unstable manifolds will flow into the strange attractor and, given enough time, will show how the attractor behaves. On

the other hand, finding hidden attractors is much more difficult since they can be located anywhere and are not accessible through the unstable manifolds of equilibrium points. Much more work and time is required to investigate if a hidden attractor is even present in the dynamical system, let alone how it is structured and where it is located. Currently, research is being done on how to locate hidden attractors more easily [21][22][23].

We present a few examples of strange attractors in the following subsection, most of which are self-excited attractors and thus easy to visualize.

i. Lorenz Attractor

As we have seen before in Section I, the Lorenz System is one of the most famous dynamical systems that can contain a strange attractor. For the reader's convenience, we again give the Lorenz System below [12][31].

$$\begin{cases} \dot{x} = \sigma(y - x) \\ \dot{y} = x(\rho - z) - y \\ \dot{z} = xy - \beta z \end{cases} \tag{4}$$

Here, σ, ρ, and β are all real valued parameters.

The first thing we want to do is present a lemma about the symmetrical nature of the Lorenz System.

Lemma II.1 (**Symmetries of the Lorenz System**). *Each of the differential equations in the Lorenz System is odd under the transformation* $(x, y, z) \to (-x, -y, z)$ *[27].*

Proof. The proving this lemma is extremely simple and can be done using the following equivalent statements [27]..

$$\begin{aligned} \dot{x}(-x, -y, z) &= \sigma((-y) - (-x)) = -\dot{x}(x, y, z) \\ \dot{y}(-x, -y, z) &= (-x)(\rho - z) - (-y) = -\dot{y}(x, y, z) \\ \dot{z}(-x, -y, z) &= (-x)(-y) - \beta z = \dot{z}(x, y, z) \end{aligned}$$

□

This means that if a structure appears in the subsection $\{(x, y, z) \in \mathbb{R} : x, y > 0\}$ of the phase space, then that same structure will appear in the subsection $\{(x, y, z) \in \mathbb{R} : x, y < 0\}$. Similarly, any structure that appears in $\{(x, y, z) \in \mathbb{R} : x > 0, y < 0\}$ of will have an equivalent in $\{(x, y, z) \in \mathbb{R} : x < 0, y > 0\}$. This is specifically true for any equilibrium points that the Lorenz System might have.

Speaking of equilibrium points, the Lorenz System under very weak conditions has the following equilibrium points.

Lemma II.2 (**Equilibrium Points of the Lorenz System**). *The equilibrium points* $\{(x_e, y_e, z_e)\}$ *of the Lorenz System given in Equation* (4) *with* $\sigma \neq 0$, $\beta > 0$, *and* $\rho > 1$ *are*
$(0, 0, 0)$ *and* $(\pm\sqrt{\beta(\rho-1)}, \pm\sqrt{\beta(\rho-1)}, \rho - 1)$.

Proof. In the first equation, $\dot{x}_e = \sigma(y_e - x_e) = 0$, meaning that $x_e = y_e$.
In the second equation, $\dot{y}_e = x_e(\rho - z_e) - y_e = 0$, meaning that $y_e = x_e(\rho - z_e)$.
In the third equation, $\dot{z}_e = x_e y_e - \beta z_e = 0$, meaning that $\beta z_e = x_e y_e$.

Combining these three equations, we see that $\beta y_e = y_e(\beta\rho - y_e^2)$, meaning that either $y_e = 0$ or $y_e = \pm\sqrt{\beta(\rho-1)} \in \mathbb{R}$.
Thus, any equilibrium point of the Lorenz System where $\beta \neq 0$ must be either $(0, 0, 0)$ or $(\pm\sqrt{\beta(\rho-1)}, \pm\sqrt{\beta(\rho-1)}, \rho - 1)$. □

Because of this lemma, we will set the parameter $\sigma = 10$, $\beta = 8/3$, and $\rho = 28$; indeed, these are the values that Lorenz himself used when he was first studying this system [12][31]. With these parameters, the equilibrium points are (0, 0, 0), $(6\sqrt{2}, 6\sqrt{2}, 27)$, $(-6\sqrt{2}, -6\sqrt{2}, 27)$.

The question is, what is the stability of the equilibrium points under Equation (4)? Linearizing the system around any arbitrary point $(x_e, y_e, z_e) \in \mathbb{R}^3$ results in the matrix-vector equation.

$$\begin{bmatrix} \dot{x} \\ \dot{y} \\ \dot{z} \end{bmatrix} = \begin{bmatrix} \sigma(y_e - x_e) \\ x_e(\rho - z_e) - y_e \\ x_e y_e - \beta z_e \end{bmatrix} + \begin{bmatrix} -\sigma & \sigma & 0 \\ \rho - z_e & -1 & -x_e \\ y_e & x_e & -\beta \end{bmatrix} \begin{bmatrix} x - x_e \\ y - y_e \\ z - z_e \end{bmatrix} \tag{5}$$

Setting (x_e, y_e, z_e) equal to the first equilibrium point (0, 0, 0), this equation reduces to

$$\begin{bmatrix} \dot{x} \\ \dot{y} \\ \dot{z} \end{bmatrix} = \begin{bmatrix} -10 & 10 & 0 \\ 28 & -1 & 0 \\ 0 & 0 & -8/3 \end{bmatrix} \begin{bmatrix} x \\ y \\ z \end{bmatrix}$$

Therefore the eigenvalues and corresponding eigenvectors of the matrix are

$$\lambda_1 = -8/3 \qquad v_{\lambda_1} = [0, 0, 1]^T$$

$$\lambda_2 = \frac{-11 + \sqrt{1201}}{2} \qquad v_{\lambda_2} = \left[10, \frac{9 + \sqrt{1201}}{2}, 0\right]^T$$

$$\lambda_3 = \frac{-11 - \sqrt{1201}}{2} \qquad v_{\lambda_3} = \left[10, \frac{9 - \sqrt{1201}}{2}, 0\right]^T$$

Thus the origin is a saddle point, with a 2-dimensional stable manifold and a 1-dimensional unstable manifold.

Setting (x_e, y_e, z_e) equal to $(6\sqrt{2}, 6\sqrt{2}, 27)$, Equation (5) reduces to

$$\begin{bmatrix} \dot{x} \\ \dot{y} \\ \dot{z} \end{bmatrix} = \begin{bmatrix} -10 & 10 & 0 \\ 1 & -1 & -6\sqrt{2} \\ 6\sqrt{2} & 6\sqrt{2} & -8/3 \end{bmatrix} \begin{bmatrix} x - 6\sqrt{2} \\ y - 6\sqrt{2} \\ z - 27 \end{bmatrix}$$

The eigenvalues and corresponding eigenvectors of the matrix are

$$\begin{aligned} \lambda_1 &\approx -13.85458 & v_{\lambda_1} &= [60\sqrt{2}, (60 + 6\lambda_1)\sqrt{2}, -\lambda_1(\lambda_1 + 11)]^T \\ \lambda_2 &\approx 0.09396 + 10.19451i & v_{\lambda_2} &= [60\sqrt{2}, (60 + 6\lambda_2)\sqrt{2}, -\lambda_2(\lambda_2 + 11)]^T \\ \lambda_3 &\approx 0.09396 - 10.19451i & v_{\lambda_3} &= [60\sqrt{2}, (60 + 6\lambda_3)\sqrt{2}, -\lambda_3(\lambda_3 + 11)]^T \end{aligned}$$

Similarly, setting (x_e, y_e, z_e) equal to $(-6\sqrt{2}, -6\sqrt{2}, 27)$, Equation (5) reduces to

$$\begin{bmatrix} \dot{x} \\ \dot{y} \\ \dot{z} \end{bmatrix} = \begin{bmatrix} -10 & 10 & 0 \\ 1 & -1 & 6\sqrt{2} \\ -6\sqrt{2} & -6\sqrt{2} & -8/3 \end{bmatrix} \begin{bmatrix} x + 6\sqrt{2} \\ y + 6\sqrt{2} \\ z - 27 \end{bmatrix}$$

The eigenvalues and corresponding eigenvectors of the matrix are again

$$\begin{aligned} \lambda_1 &\approx -13.85458 & v_{\lambda_1} &= [-60\sqrt{2}, -(60 + 6\lambda_1)\sqrt{2}, -\lambda_1(\lambda_1 + 11)]^T \\ \lambda_2 &\approx 0.09396 + 10.19451i & v_{\lambda_2} &= [-60\sqrt{2}, -(60 + 6\lambda_2)\sqrt{2}, -\lambda_2(\lambda_2 + 11)]^T \\ \lambda_3 &\approx 0.09396 - 10.19451i & v_{\lambda_3} &= [-60\sqrt{2}, -(60 + 6\lambda_3)\sqrt{2}, -\lambda_3(\lambda_3 + 11)]^T \end{aligned}$$

Thus, the equilibrium points $(\pm 6\sqrt{2}, \pm 6\sqrt{2}, 27)$ are saddle-focus points, with 2-dimensional unstable manifolds and 1-dimensional stable manifolds.

Now that we understand some of the behavior in the Lorenz System, it is time to visualize the attractor. One of the easiest ways of seeing this fascinating structure is by plotting the unstable manifolds of the origin. The other two equilibrium points simultaneously attract and repel the origin's unstable manifolds; as a result, the unstable manifolds are tossed back and forth between the two saddle-foci in a never-ceasing dance of continuity.

Figure 2 gives a visual representation of the Lorenz Attractor. As one can see, the attractor per definition is invariant under the dynamical system: a trajectory inside the attractor will forever remain inside it. But it is the shape of the attractor that makes it strange. The Lorenz Attractor's structure is much more complicated that a simple attracting point or limit cycle; since the Lorenz Attractor was concretely proven to be a strange attractor in 2002, it can be concluded that the attractor is indeed fractal in nature [34].

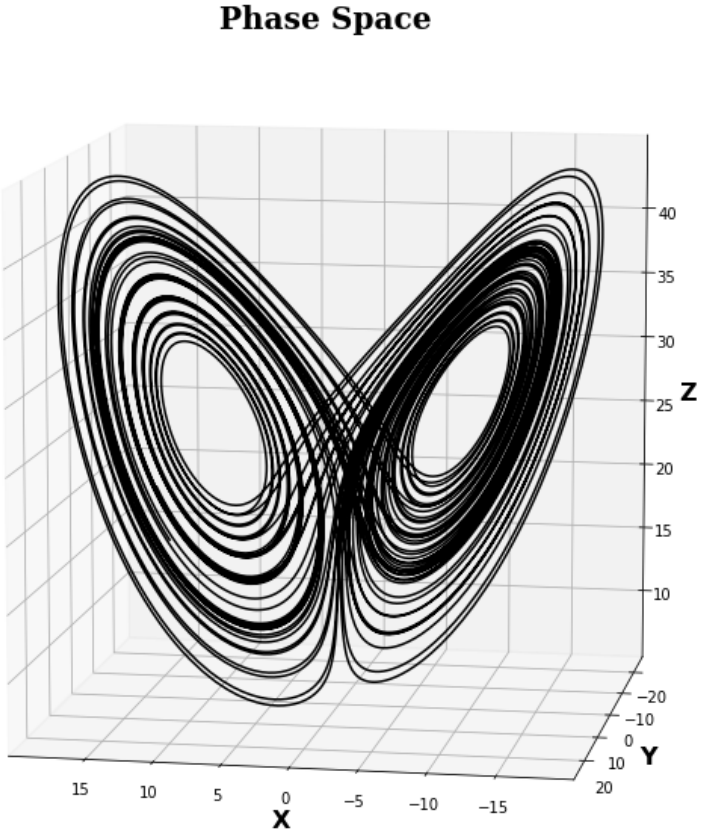

Figure 2: *The Lorenz self-excited Attractor, revolving around two of the three equilibrium points, which in this case are (6$\sqrt{2}$, 6$\sqrt{2}$, 27) and (-6$\sqrt{2}$, -6$\sqrt{2}$, 27). Here $\sigma = 10$, $\rho = 28$, and $\beta = 8/3$. The attractor was approximated using an adaptive explicit RK4 numerical integration technique over a time span of 60 time units using an initial position of (10.383, 16.824, 19.325). See Appendix C for coding details.*

ii. Chua Attractors

Chua's attractors occur in a system of differential equations describing the current and voltage flowing through a simple electronic circuit consisting of two capacitors, one inductor, one nonlinear resistor, and a Chua diode [30]. The system was named after its founder Leon Chua, who introduced the system in the mid 1980's [7][26].

We will simply treat the Chua System as a mathematical one without paying too much attention to the physical interpretation of it. The most common formulation of the Chua System is the one presented in Matsumoto's paper from 1984 [26] and later in Chua, Komuro, and Matsumoto's paper in 1986 [7].

$$\begin{cases} \dot{x} = \alpha(y - x - f(x)) \\ \dot{y} = x - y + z \\ \dot{z} = -\beta y \end{cases} \tag{6}$$

Here, f is a nonlinear function that describes the change in resistance versus current in the Chua diode [26][30]. Mathematically, multiple sources of literature simply define the function as follows [7][21][22][23][26][30].

$$\begin{aligned} f(x) &= m_1 x + \frac{1}{2}(m_0 - m_1)(|x+1| - |x-1|) \\ &= \begin{cases} m_1 x + (m_1 - m_0) & x \in (-\infty, -1) \\ m_0 x & x \in [-1, 1] \\ m_1 x + (m_0 - m_1) & x \in (1, \infty) \end{cases} \end{aligned} \tag{7}$$

Now we define the system's equilibrium points.

Lemma II.3 (**Equilibrium Points of the Chua System**). *The equilibrium points* $\{(x_e, y_e, z_e)\}$ *of the Chua System given in Equation* (6) *with nonlinearity function* f *defined in Equation* (7) *with* $\alpha, \beta \neq 0$ *are*

$$\begin{cases} (0,0,0) & m_0 \neq -1 \\ (\pm\gamma, 0, \mp\gamma) \text{ where } \gamma \in [0,1] & m_0 = -1 \\ \left(\pm\left(\dfrac{m_1 - m_0}{m_1 + 1}\right), 0, \mp\left(\dfrac{m_1 - m_0}{m_1 + 1}\right)\right) & (m_0 + 1)(m_1 + 1) < 0 \\ (\pm\gamma, 0, \mp\gamma) \text{ where } \gamma \in (1, \infty) & m_0, m_1 = -1 \end{cases}$$

Proof. In the first equation, $\dot{x}_e = \alpha(y_e - x_e - f(x_e)) = 0$, meaning that $y_e = x_e + f(x_e)$.
In the second equation, $\dot{y}_e = x_e - y_e + z_e = 0$, meaning that $y_e = x_e + z_e$.
In the third equation, $\dot{z}_e = -\beta y_e = 0$, meaning that $y_e = 0$.

Combining these three equations, we immediately see that any equilibrium point of the Chua System is $(x_e, 0, -x_e)$ where $x_e + f(x_e) = 0$. Therefore, it is crucial to calculate x_e.

We must first prove that the function f as defined in Equation (7) is an odd function; that is, $f(x) = -f(-x)$.

$$\begin{aligned} -f(-x) &= \begin{cases} -m_1(-x) - (m_1 - m_0) & -x \in (-\infty, -1) \\ -m_0(-x) & -x \in [-1, 1] \\ -m_1(-x) - (m_0 - m_1) & -x \in (1, \infty) \end{cases} \\ &= \begin{cases} m_1 x + (m_0 - m_1) & x \in (1, \infty) \\ m_0 x & x \in [-1, 1] \\ m_1 x + (m_1 - m_0) & x \in (-\infty, -1) \end{cases} \\ &= f(x) \end{aligned}$$

In this case, we can keep focus primarily on positive values of x. If there exists some point x_e so that $x_e + f(x_e) = 0$, then $-x_e$ will also be a valid solution. Now we must separate our analysis into a number of cases and investigate them individually.

Suppose $x_e \in [0, 1]$.
Then $f(x_e) = m_0 x_e$. It is trivial to conclude that if $m_0 \neq -1$, then $x_e + f(x_e) = 0$ if and only if $x_e = 0$. If $m_0 = -1$, then x_e can be any value in $[0, 1]$.

Suppose $x_e > 1$.
Then $f(x_e) = m_1 x_e + (m_0 - m_1)$. If $m_1 \neq -1$, then the only possible solution to $x_e + f(x_e) = 0$ is $(m_1 - m_0)/(m_1 + 1)$. The question is whether this value falls in the range $(1, \infty)$.

For ease of analysis, let us define a new function $g : \mathbb{R}^2 \to \mathbb{R}$, defined as

$$g(m_0, m_1) = (m_1 - m_0)/(m_1 + 1)$$

The function g is almost everywhere differentiable, with the exception being when $m_1 = -1$.

$$\frac{\partial g}{\partial m_0} = \frac{-1}{m_1 + 1}, \quad \frac{\partial g}{\partial m_1} = \frac{m_0 + 1}{(m_1 + 1)^2}$$

Suppose $x_e > 1$ and $m_0 < -1$.
Then $\partial g / \partial m_1 < 0$ for all $m_1 \in \mathbb{R} \backslash \{-1\}$. Furthermore, notice the following limit is constant for all values of $m_0 < -1$.

$$\lim_{m_1 \to \infty} g(m_0, m_1) = \lim_{m_1 \to -\infty} g(m_0, m_1) = 1$$

As a result, function g takes on a value less than 1 only for $m_1 < -1$; in the same way, the function g takes on a value greater than 1 only for $m_1 > -1$. We can conclude that the only viable solution to $x_e + f(x_e) = 0$ with $x_e > 1$ is $x_e = g(m_0, m_1) = (m_1 - m_0)/(m_1 + 1)$ when $m_1 > -1$.

And what of $m_1 = -1$? If $m_1 = -1$, then $x_e + f(x_e) = 0$ is equivalent to $m_0 = -1$. However, this is a contradiction to our assumption that $m_0 < -1$.

Suppose $x_e > 1$ and $m_0 > -1$.
Then $\partial g/\partial m_1 > 0$ for all $m_1 \in \mathbb{R}\backslash\{-1\}$. Again, notice the following limit is constant for all values of $m_0 > -1$.

$$\lim_{m_1 \to \infty} g(m_0, m_1) = \lim_{m_1 \to -\infty} g(m_0, m_1) = 1$$

As a result, function g takes on a value greater than 1 only for $m_1 < -1$; in the same way, function g takes on a value less than 1 only for $m_1 > -1$. We can conclude that the only viable solution to $x_e + f(x_e) = 0$ with $x_e > 1$ is $x_e = g(m_0, m_1) = (m_1 - m_0)/(m_1 + 1)$ when $m_1 < -1$.

As before if $m_1 = -1$, the expression $x_e + f(x_e) = 0$ is equivalent to $m_0 = -1$. However, this is a contradiction to our assumption that $m_0 < -1$.

Suppose $x_e > 1$ and $m_0 = -1$
Then $x_e + f(x_e) = 0$ is equivalent to $(m_1 + 1)x_e = (m_1 + 1)$. From this we must conclude that $m_1 = -1$ since $x_e > 1$. However, if $m_1 = -1$ then x_e can be any value in $(1, \infty)$.

In summary, the only solutions for $x_e \geq 0$ are

$$\begin{cases} x_e = 0 & m_0 \neq -1 \\ x_e \in [0, 1] & m_0 = -1 \\ x_e = \left(\dfrac{m_1 - m_0}{m_1 + 1} \right) & (m_0 + 1)(m_1 + 1) < 0 \\ x_e \in (1, \infty) & m_0, m_1 = -1 \end{cases}$$

However, we proved previously that that the function $f(x)$ is odd. Therefore, we can immediately conclude that the only solutions for $x_e \leq 0$ are

$$\begin{cases} x_e = 0 & m_0 \neq -1 \\ x_e \in [-1, 0] & m_0 = -1 \\ x_e = \left(\dfrac{m_0 - m_1}{m_1 + 1} \right) & (m_0 + 1)(m_1 + 1) < 0 \\ x_e \in (-\infty, -1) & m_0, m_1 = -1 \end{cases}$$

In conclusion, the equilibrium points of the Chua System are

$$\begin{cases} (0,0,0) & m_0 \neq -1 \\ (\pm\gamma, 0, \mp\gamma) \text{ where } \gamma \in [0,1] & m_0 = -1 \\ \left(\pm\left(\dfrac{m_1 - m_0}{m_1 + 1}\right), 0, \mp\left(\dfrac{m_1 - m_0}{m_1 + 1}\right)\right) & (m_0 + 1)(m_1 + 1) < 0 \\ (\pm\gamma, 0, \mp\gamma) \text{ where } \gamma \in (1, \infty) & m_0, m_1 = -1 \end{cases}$$

□

The Chua System contains a number of attractors. For example, with parameters $\alpha = 8.4562$, $\beta = 12.08$, $m_0 = -0.1768$, and $m_1 = -1.1468$, the Chua dynamical system contains two hidden attractors pressed against each other [21][23]. Let us first provide a routine analysis of the system with these parameters.

The equilibrium points of the system are approximately (0, 0, 0), (6.607629, 0, -6.607629), and (-6.607629, 0, 6.607629). Linearizing the system around any arbitrary point $(x_e, y_e, z_e) \in \mathbb{R}^3$ with $x_e \neq \pm 1$ results in the matrix-vector equation.

$$\begin{bmatrix} \dot{x} \\ \dot{y} \\ \dot{z} \end{bmatrix} = \begin{bmatrix} \alpha(y_e - x_e - f(x_e)) \\ x_e - y_e + z_e \\ -\beta y_e \end{bmatrix} + \begin{bmatrix} -\alpha\left(1 + \frac{\partial f(x_e)}{\partial x}\right) & \alpha & 0 \\ 1 & -1 & 1 \\ 0 & -\beta & 0 \end{bmatrix} \begin{bmatrix} x - x_e \\ y - y_e \\ z - z_e \end{bmatrix} \tag{8}$$

Linearizing the system about the origin reduces Equation (8) to approximately

$$\begin{bmatrix} \dot{x} \\ \dot{y} \\ \dot{z} \end{bmatrix} = \begin{bmatrix} -6.961144 & 8.4562 & 0 \\ 1 & -1 & 1 \\ 0 & -12.08 & 0 \end{bmatrix} \begin{bmatrix} x \\ y \\ z \end{bmatrix}$$

The eigenvalues and corresponding eigenvectors of the matrix are

$$\begin{aligned} \lambda_1 &\approx -7.958741 & v_{\lambda_1} &= [-\lambda_1(1 + \lambda_1) - 12.08, -\lambda_1, 12.08]^T \\ \lambda_2 &\approx -0.001201 + 3.25051i & v_{\lambda_2} &= [-\lambda_2(1 + \lambda_2) - 12.08, -\lambda_2, 12.08]^T \\ \lambda_3 &\approx -0.001201 - 3.25051i & v_{\lambda_2} &= [-\lambda_3(1 + \lambda_3) - 12.08, -\lambda_3, 12.08]^T \end{aligned}$$

Therefore, the origin is a stable focus-node with a 3-dimensional stable manifold.

Similarly, linearizing the system about the equilibrium points $(\pm 6.607629, 0, \mp 6.607629)$ reduces Equation (8) to approximately

$$\begin{bmatrix} \dot{x} \\ \dot{y} \\ \dot{z} \end{bmatrix} = \begin{bmatrix} 1.24137 & 8.4562 & 0 \\ 1 & -1 & 1 \\ 0 & -12.08 & 0 \end{bmatrix} \begin{bmatrix} x \mp 6.607629 \\ y \\ z \pm 6.607629 \end{bmatrix}$$

The eigenvalues and corresponding eigenvectors of the matrix are

$$\begin{aligned}
\lambda_1 &\approx 2.217218 & v_{\lambda_1} &= [-\lambda_1(1+\lambda_1) - 12.08, -\lambda_1, 12.08]^T \\
\lambda_2 &\approx -0.987924 + 2.405686i & v_{\lambda_2} &= [-\lambda_2(1+\lambda_2) - 12.08, -\lambda_2, 12.08]^T \\
\lambda_3 &\approx -0.987924 - 2.405686i & v_{\lambda_2} &= [-\lambda_3(1+\lambda_3) - 12.08, -\lambda_3, 12.08]^T
\end{aligned}$$

Thus, both equilibrium points $(\pm 6.607629, 0, \mp 6.607629)$ are saddle-foci, with 2-dimensional unstable manifolds and 1-dimensional stable manifolds.

As stated before, the system contains two hidden attractors pressed against each other as shown in Figure 3. These attractors can not be visualized by plotting the unstable manifolds of the equilibrium points. Instead, the attractors simply loop around and around an area centered roughly around the origin. Despite the attractors' much more simple and oscillatory structure, these attractors are indeed strange; numerical evidence of the fact is presented in Section III.

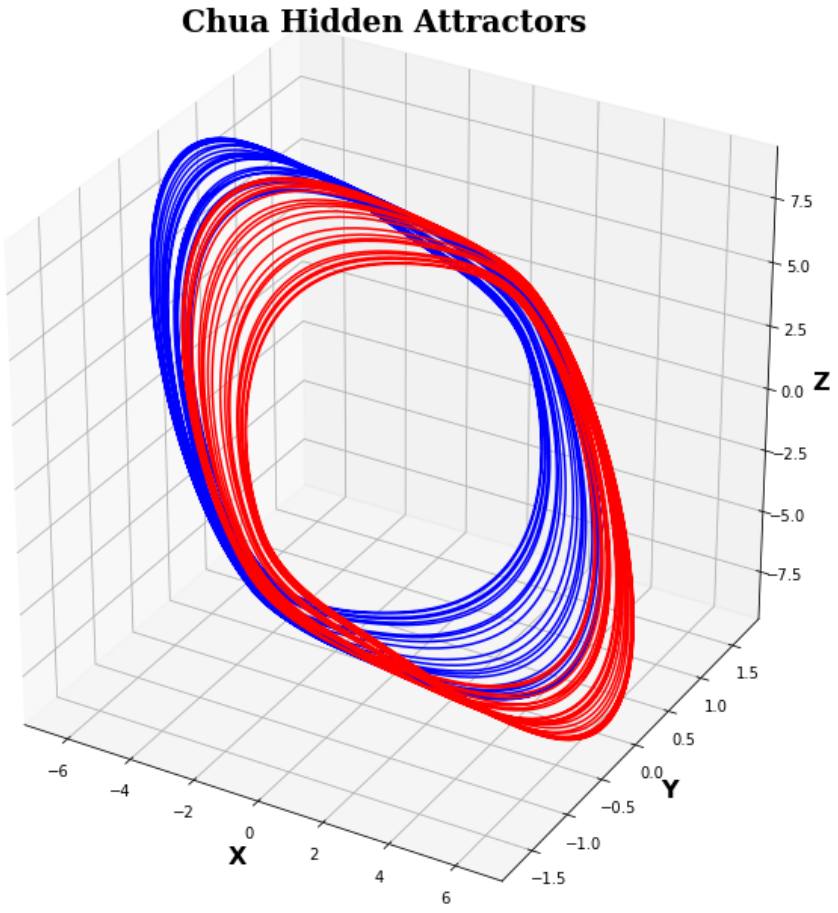

Figure 3: *The Chua Hidden Attractors, revolving in an oscillatory, almost periodic manner. Notice that the first hidden attractor (in red) and the second hidden attractor (in blue) are disjoint. Here* $\alpha = 8.4562$, $\beta = 12.08$, $m_0 = -0.1768$, *and* $m_1 = -1.1468$. *The attractor was approximated using an adaptive explicit RK4 numerical integration technique over a time span of 60 time units using an initial position of (6.230364, 0.331478, -8.772180) for the red attractor, and an initial position of (-6.230364, -0.331478, 8.772180) for the blue attractor. See Appendix C for coding details.*

iii. Wimol-Banlue Attractor

Up till now, this paper has only shown examples of multipolynomial (or piecewise multipolynomial) dynamical systems. Now we focus a somewhat less-known non-multipolynomial system: the Wimol-Banlue Attractor described in [29]. The original Wimol-Banlue System is given by

$$\begin{cases} \dot{x} &= y - x \\ \dot{y} &= -z\tanh(x) \\ \dot{z} &= -\alpha + xy + |y| \end{cases} \tag{9}$$

where $\alpha \in \mathbb{R}$.

Lemma II.4 (**Equilibrium Points of the Wimol-Banlue System**). *The equilibrium points* $\{(x_e, y_e, z_e)\}$ *of the Wimol-Banlue System given by Equation* (9) *is given by*

$$(\pm(1-\sqrt{1+4\alpha})/2, \pm(1-\sqrt{1+4\alpha})/2, 0) \text{ when } \alpha > 0$$

and

$$(0, 0, \gamma) \text{ where } \gamma \in \mathbb{R} \text{ when } \alpha = 0$$

Proof. In the first equation, $\dot{x}_e = y_e - x_e = 0$, meaning that $y_e = x_e$.
In the second equation, $\dot{y}_e = -z_e\tanh(x_e) = 0$, meaning that $z_e = 0$ or $x_e = 0$.
In the third equation, $\dot{z}_e = -\alpha + x_e y_e + |y_e| = 0$.

Let us first combine the equations $\dot{x}_e = 0$ and $\dot{z}_e = 0$. The resulting expression is

$$x_e^2 + |x_e| - \alpha = 0 \tag{10}$$

This is almost a purely quadratic expression. Furthermore, the expression $x_e^2 + |x_e| - \alpha$ is even since $(-x_e)^2 + |-x_e| - \alpha = x_e^2 + |x_e| - \alpha$. As such, if x_e is a solution to Equation (10), then so is $-x_e$. Therefore, we will only be focusing on solutions for Equation (10) for non-negative values of x_e.

If $x_e \geq 0$, then Equation (10) becomes

$$x_e^2 + x_e - \alpha = 0$$

which, according to the quadratic formula, has only one potentially non-negative solution.

$$x_e = \frac{-1 + \sqrt{1+4\alpha}}{2}$$

This solution can only be real and non-negative when $\sqrt{1+4\alpha} \geq 1$ and $1 + 4\alpha \geq 0$. These expressions together are equivalent to $\alpha \geq 0$.

Thus, when $\alpha \geq 0$, $x_e = y_e = \pm(1 - \sqrt{1+4\alpha})/2$. But what about z_e? Recall equation $\dot{y_e} = 0$; since $\tanh(x_e) \neq 0$ for $\alpha > 0$, z_e must be equal to 0. Therefore, for $\alpha > 0$, the only two equilibrium points are $(\pm(1 - \sqrt{1+4\alpha})/2, \pm(1 - \sqrt{1+4\alpha})/2, 0)$.

What about when $\alpha = 0$? Then Equation (10) only has $x_e = 0$ as its solution. If $y_e = x_e = 0$, then equations $\dot{x_e} = 0$, $\dot{y_e} = 0$, $\dot{z_e} = 0$ are already satisfied, meaning that z_e can take on any value it wants. Thus for $\alpha = 0$, the Wimol-Banlue System has the equilibrium points $(0, 0, \gamma)$ where $\gamma \in \mathbb{R}$. □

Because of Lemma II.4, we set parameter $\alpha = 2$ in order to restrict the number of equilibrium points; which in this case are (1, 1, 0) and (-1, -1, 0) [29].

As before, we also wish to analyze the stability of the equilibrium points. Linearizing the system around any arbitrary point $(x_e, y_e, z_e) \in \mathbb{R}^3$ with $y_e \neq 0$ results in the matrix-vector equation.

$$\begin{bmatrix} \dot{x} \\ \dot{y} \\ \dot{z} \end{bmatrix} = \begin{bmatrix} y_e - x_e \\ -z_e \tanh(x_e) \\ -\alpha + x_e y_e + |y_e| \end{bmatrix} + \begin{bmatrix} -1 & 1 & 0 \\ -z_e \operatorname{sech}^2(x_e) & 0 & -\tanh(x_e) \\ y_e & x_e + \frac{\partial}{\partial y}|y_e| & 0 \end{bmatrix} \begin{bmatrix} x - x_e \\ y - y_e \\ z - z_e \end{bmatrix} \tag{11}$$

Setting (x_e, y_e, z_e) equal to equilibrium point $(\pm 1, \pm 1, 0)$ reduces this matrix-vector equation to

$$\begin{bmatrix} \dot{x} \\ \dot{y} \\ \dot{z} \end{bmatrix} = \begin{bmatrix} -1 & 1 & 0 \\ 0 & 0 & \mp\tanh(1) \\ \pm 1 & \pm 2 & 0 \end{bmatrix} \begin{bmatrix} x \mp 1 \\ y \mp 1 \\ z \end{bmatrix}$$

Therefore the eigenvalues and corresponding eigenvectors of the matrix are

$$\begin{aligned} &\lambda_1 \approx -1.247346 && v_{\lambda_1} = [\pm\tanh(1), \pm(\lambda_1 + 1)\tanh(1), -\lambda_1(\lambda_1 + 1)]^T \\ &\lambda_2 \approx 0.123673 + 1.347746i && v_{\lambda_2} = [\pm\tanh(1), \pm(\lambda_2 + 1)\tanh(1), -\lambda_2(\lambda_2 + 1)]^T \\ &\lambda_3 \approx 0.123673 - 1.347746i && v_{\lambda_2} = [\pm\tanh(1), \pm(\lambda_3 + 1)\tanh(1), -\lambda_3(\lambda_3 + 1)]^T \end{aligned}$$

Thus both equilibrium points $(\pm 1, \pm 1, 0)$ are saddle-foci, with a 2-dimensional unstable manifolds and 1-dimensional stable manifolds.

The Wimol-Banlue Attractor is again easy to visualize since it is a self-excited attractor; plotting the unstable manifolds of either eqilibrium point will visualize the attractor. Figure 4 shows that the attractor certainly seems to be very similar to Lorenz's attractor in Figure 2; in fact the authors W. San-Um and B. Srisuchinwong intended for their attractor to be a modification of Lorenz's system. In any case, the authors also numerically proved the attractor is in fact strange [29].

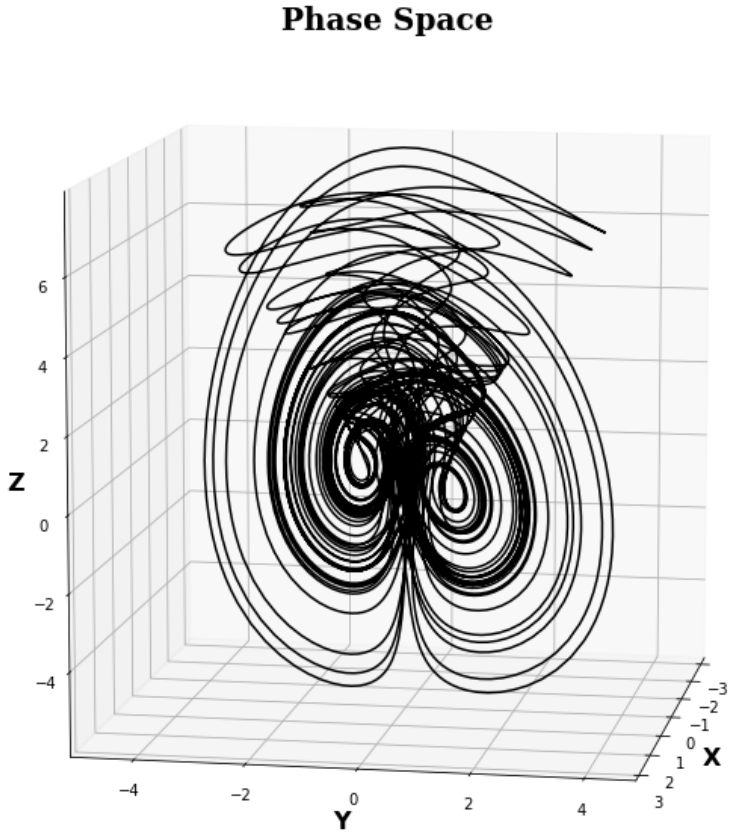

Figure 4: *The Wimol-Banlue self-excited Attractor, revolving around both equilibrium points, which in this case are* $(-1, -1, 0)$ *and* $(1, 1, 0)$*. Here* $\alpha = 2$*. The attractor was approximated using an adaptive explicit RK4 numerical integration technique over a time span of 500 time units using an initial position of (-1.21739, -1.48448, 0.18485). See Appendix C for coding details.*

III. Chaos

All the strange attractors featured in the previous section have been chosen specifically, as they also exhibit a very interesting phenomenon: chaos. Chaos in essence has to do with how microscopic differences in initial conditions can lead to macroscopic differences in the resulting trajectories. There is, in a sense, a separating force between trajectories in a strange attractor, no matter how close these trajectories first were.

The Oseledec Multiplicative Ergodic Theorem

How does one mathematically define this? We will need some material from Probability and Ergodic Theory to define a rigid mathematical background for this.

Definition III.1 (σ-Algebra [35])**.** *A σ-Algebra Σ on a set X is a subset of $\mathcal{P}(X)$ (the power set of X) where*

- $X \in \Sigma$
- $A \in \Sigma \Rightarrow X \backslash A \in \Sigma$
- $A_1, A_2, \cdots A_n \in \Sigma \Rightarrow \bigcup_{i=1}^{n} A_i \in \Sigma$

Definition III.2 (Probability Space [35])**.** *The Probability Space is given by (Ω, Σ, ρ). The sample space Ω is the set of all possible events, and Σ is a σ-algebra on Ω. The probability measure $\rho : \Sigma \to [0, 1]$ on the measurable space (Ω, Σ) is a map that assigns a probability to an event in Σ in such a way that*

- $\rho(\emptyset) = 0$
- $\rho(\Omega) = 1$
- *For $\{E_i \in \Sigma : i \in \mathbb{N}\}$ where $E_i \cap E_j = \emptyset$ for all $i \in \mathbb{N}$ and $j \in \mathbb{N} \backslash \{i\}$,*

$$\rho\left(\bigcup_{i \in \mathbb{N}} E_i\right) = \sum_{i \in \mathbb{N}} \rho(E_i)$$

Now the question arises: how do we apply this to strange attractors? Well, by setting the sample space Ω equivalent to attractor $A \subset \mathbb{R}^n$ and the σ-algebra Σ to $\mathcal{P}(A)$ (the power set of A), we have a measurable space. Can we define a probability measure as well? For this, we will need a theorem.

Theorem III.1. *If the compact set $A \in \mathbb{R}^n$ is invariant under a dynamical system, then there is a probability measure ρ invariant under the dynamical system and with support contained in A. One may choose this ρ to be ergodic; that is, ρ can be chosen to be indecomposible into constituent probability measures [13].*

Why ergodic probability measures are important in dynamical systems becomes clear in the next theorem.

Theorem III.2 (Ergodic Theorem [13]). *Say $A \subset \mathbb{R}^n$ is an attractor a dynamical system $\delta : S \times \mathbb{R} \to \mathbb{R}$. If $\rho : \mathcal{P}(A) \to [0,1]$ is ergodic, then for ρ-almost all initial conditions $\mathbf{x}_0$, the following limit holds.*

$$\rho(a) = \lim_{T\to\infty} \frac{1}{T} \int_0^T \left(\begin{cases} 1 & \delta(\mathbf{x_0}, t) \in a \\ 0 & \delta(\mathbf{x_0}, t) \notin a \end{cases} \right) dt \text{ for } a \in \mathcal{P}(A)$$

With the preliminaries out of the way, we can now finally get to the main theorem used in defining chaos. It would be preferable to define some mathematical structure that would reduce to a simple "Yes" when an attractor is chaotic and a "No" when an attractor is not. The following theorem, though abstract and complex, provides the mathematical rigor for such a structure.

Theorem III.3 (The Multiplicative Ergodic Theorem of Oseledec [13]). *Let ρ be a probability measure on a measurable space (Ω, Σ) and $f : \Omega \to \Omega$ a measure-preserving map (i.e. $\forall a \in \Sigma$, $\rho(f^{-1}(a)) = \rho(a)$) such that ρ is ergodic. Let $T : \Omega \to \mathbb{R}^{n\times n}$ be a measurable map such that*

$$\int_{x\in\Omega} \max(\log(||T(x)||), 0)\rho'(x)dx < \infty$$

If $T_x^m = \prod_{i=m-1}^{0} T(f^i(x))$ and T_x^{m*} is the adjoint of T_x^m, then for ρ-almost all $x \in \Omega$,

$$\lim_{m\to\infty} (T_x^{m*} T_x^m)^{1/2m} = \Lambda_x$$

The logarithm of the eigenvalues of Λ_x are called the Lyapunov or Characteristic Exponents and are ρ-almost everywhere constant. Together, the set of Lyapunov Exponents form what is called the Lyapunov Spectrum.

As a quick summary, the Lyapunov Exponents are the logarithm of the eigenvalues of some matrix Λ_x that can be computed over a specific probability space (Ω, Σ, ρ). Whats more, these Lyapunov Exponents are ρ-almost everywhere constant, meaning there is a one-to-one correspondence between Ω and its Lyapunov Exponents. Calculating these exponents can be done with the following corollary.

Corollary III.4 (Calculation of Lyapunov Exponents [13]). *Suppose ρ and Ω are defined as in Theorem III.3, and $T_x^m, \Lambda_x \in \mathbb{R}^{n\times n}$ are defined for ρ-almost all $x \in \Omega$ as in Theorem III.3. Suppose the eigenvalues $\{\lambda_1, \lambda_2, \cdots, \}$ of Λ_x are sorted in descending order, ignoring multiplicity. Let E_x^i be the subspace of $\mathbb{R}^n$ corresponding to the eigenvalues of Λ_x that are less than or equal to $\exp(\lambda_i)$. Then $\mathbb{R}^n = E_x^1 \supset E_x^2 \supset \cdots$ and for ρ-almost all $x \in \Omega$,*

$$\lim_{m\to\infty} \frac{1}{m} \log\left(||T_x^m u||\right) = \lambda_i \text{ if } u \in E_x^i \backslash E_x^{i+1}$$

Eckmann and Ruelle describes this process as a filtration for the different exponential growth rates between trajectories of the dynamical system [13].

That may be all well and good, but how can we apply this more directly to an attractor in a dynamical system $\delta : S \times \mathbb{R} \to \mathbb{R}$? Since we have defined Ω and Σ, all that is needed is a ergodic probability measure ρ. For this, we need a measure-preserving map $f : \Omega \to \Omega$. We can define f and ρ simultaneously.

$$f(\mathbf{x}) = \delta(\mathbf{x}, \tau) \text{ for } \tau \in \mathbb{R}_{>0}$$
$$\rho(A) = \lim_{T\to\infty} \frac{1}{T} \int_0^T \left(\begin{cases} 1 & \delta(\mathbf{x}_0, t) \in A \\ 0 & \delta(\mathbf{x}_0, t) \notin A \end{cases} \right) dt$$

Eckmann and Ruelle show in their paper that the following probability measure ρ is ergodic and f is a measure-preserving map. This is because in an attractor, ρ is invariant under the flow of the dynamical system δ [13]. As such, we can define matrices T_x^m and Λ_x, and in doing so calculate the Lyapunov Exponents λ_1, λ_2, $\cdots$

$$T_x^m = \begin{bmatrix} \partial\delta(\mathbf{x}_0, m\tau)_1/\partial x_1 & \partial\delta(\mathbf{x}_0, m\tau)_1/\partial x_2 & \cdots & \partial\delta(\mathbf{x}_0, m\tau)_1/\partial x_n \\ \partial\delta(\mathbf{x}_0, m\tau)_2/\partial x_1 & \partial\delta(\mathbf{x}_0, m\tau)_2/\partial x_2 & \cdots & \partial\delta(\mathbf{x}_0, m\tau)_2/\partial x_n \\ \vdots & \vdots & \ddots & \vdots \\ \partial\delta(\mathbf{x}_0, m\tau)_n/\partial x_1 & \partial\delta(\mathbf{x}_0, m\tau)_n/\partial x_2 & \cdots & \partial\delta(\mathbf{x}_0, m\tau)_n/\partial x_n \end{bmatrix}$$
$$\Lambda_x = \lim_{m\to\infty} (T_x^{m*} T_x^m)^{1/2m}$$
$$\lambda_i = \lim_{m\to\infty} \frac{1}{m} \log\left(||T_x^m u||\right) \text{ if } u \in E_x^i \backslash E_x^{i+1}$$

With this all in mind, we can finally define what most mathematicians see as chaos.

Definition III.3 (**Chaos**). *A attractor $A \subset \mathbb{R}^n$ in a dynamical system exhibits chaos if the corresponding maximal Lyapunov Exponent λ_1 is strictly positive [3].*

Now, using the Multiplicative Ergodic Theorem of Oseledec to calculate Lyapunov Exponents is a little like using an elephant gun to shoot a pidgeon. In light of this, the most common algorithm for computing the maximal Lyapunov Exponent of an attractor is by using the following expression [3].

$$\lambda_1 = \lim_{t\to\infty} \lim_{||\mathbf{x}_2 - \mathbf{x}_1||\to 0} \frac{1}{t} \log\left(\frac{||\delta(\mathbf{x}_2, t) - \delta(\mathbf{x}_1, t)||}{||\mathbf{x}_2 - \mathbf{x}_1||} \right)$$

Other, more complicated expressions exist for the computation of the other Lyapunov Exponents, but are not given in this paper. For more information, see [3][13][33].

Using Definition III.3, one can easily provide their own evidence that the Lorenz Attractor, the Chua Attractors, and the Wimol-Banlue Attractor are all chaotic by calculating the Lyapunov Exponents of each system [3][33].

The approximated Lyapunov Spectrum of the Lorenz Attractor using parameters $\sigma = 10$, $\rho = 28$, and $\beta = 8/3$ is given in Figure 5. From this, the maximal Lyapunov Exponent is roughly 0.877648, a positive number. Thus we can safely conclude the Lorenz Attractor is indeed chaotic.

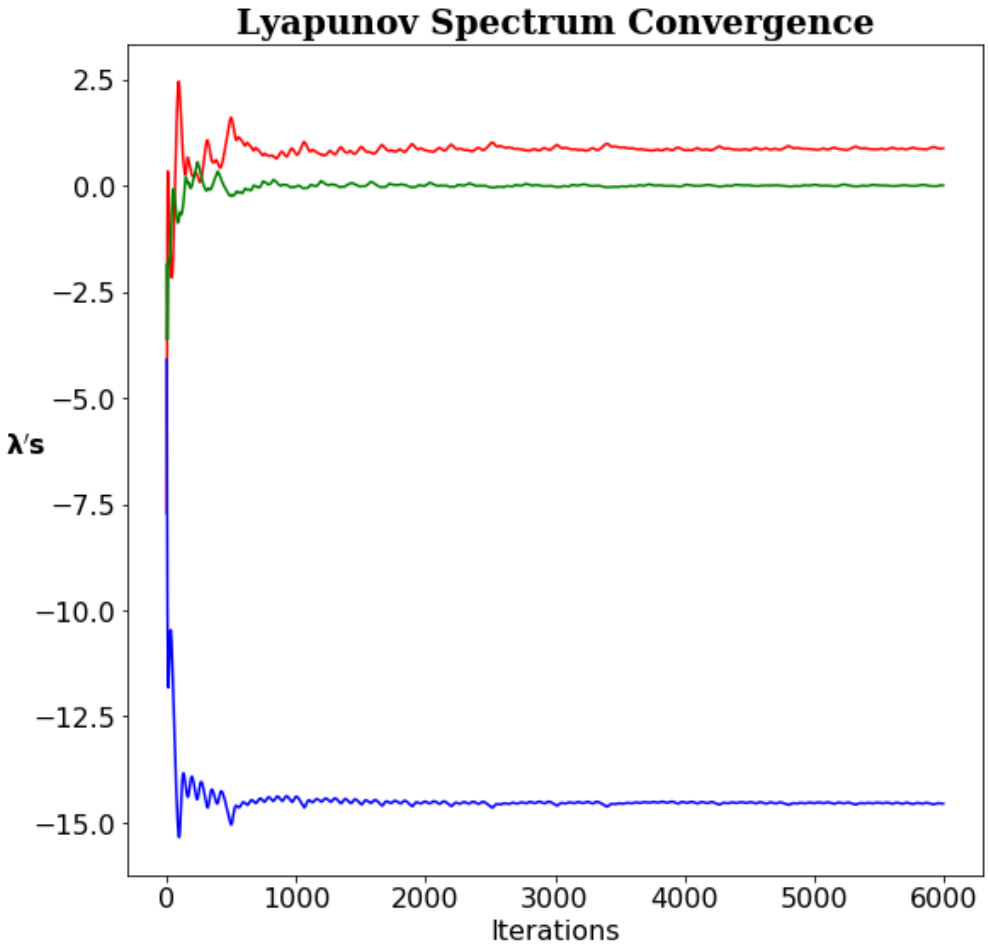

Figure 5: *The convergence of the Lyapunov Spectrum of the Lorenz Attractor using parameters $\sigma = 10$, $\rho = 28$, and $\beta = 8/3$ (the same parameter values as used in Figure 2). According to our calculations, the spectrum is approximately (0.877648, 0.007993, -14.552204). See Appendix C for coding details.*

The same analysis can be provided for the two hidden attractors in Figure 3; their Lyapunov Spectra is shown in Figure 6. The maximal Lyapunov Exponent for both hidden attractors is 0.219717, proving both attractors are indeed chaotic.

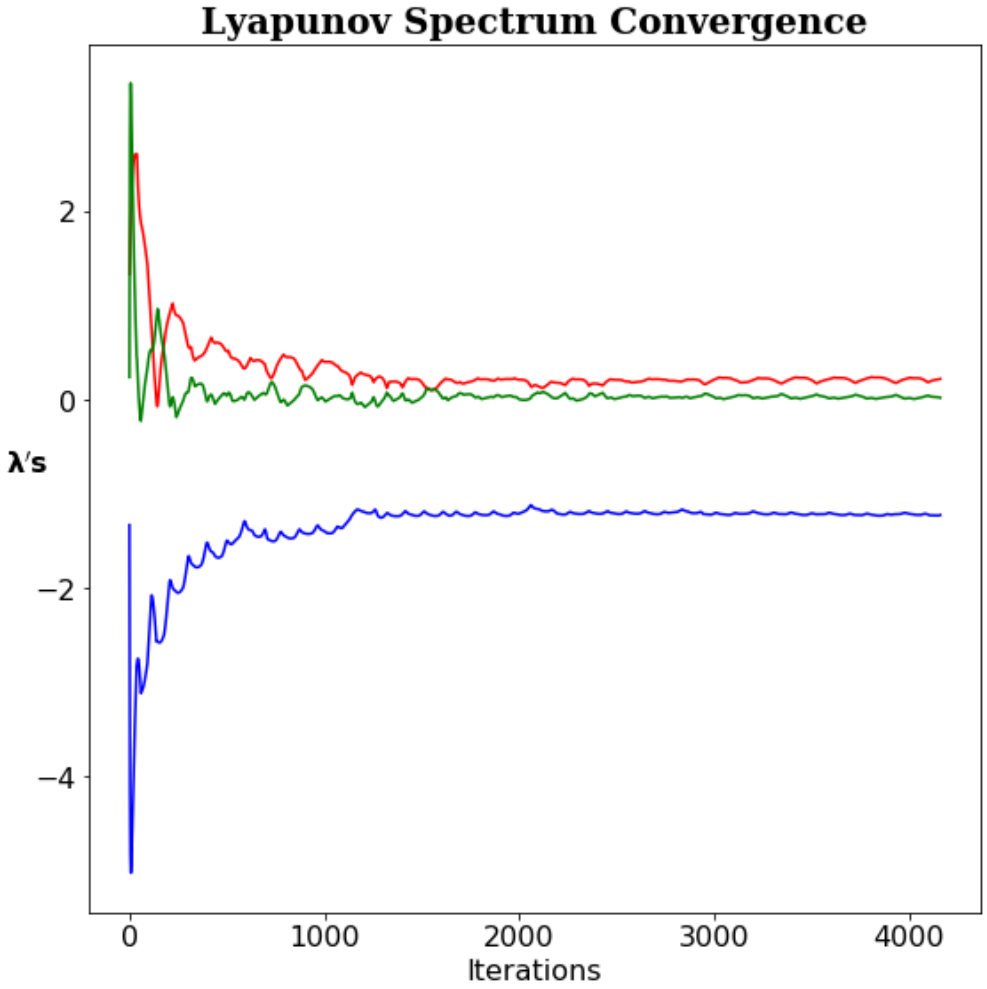

Figure 6: *The convergence of the Lyapunov Spectrum of both hidden Chua Attractors using parameter values* $\alpha = 8.4562$, $\beta = 12.08$, $m_0 = -0.1768$, *and* $m_1 = -1.1468$ *(the same parameter values as used in Figure 3). According to our calculations, both spectra are identically equal to (0.219717, 0.019772, -1.224210). See Appendix C for coding details.*

Finally, we approximate the Lyapunov Spectrum for the Wimol-Banlue Attractor using parameter $\alpha = 10$ in Figure 7. Here maximal Lyapunov Exponent is roughly 0.244054, a positive number. As before, we can safely conclude the Wimol-Banlue Attractor is once again chaotic.

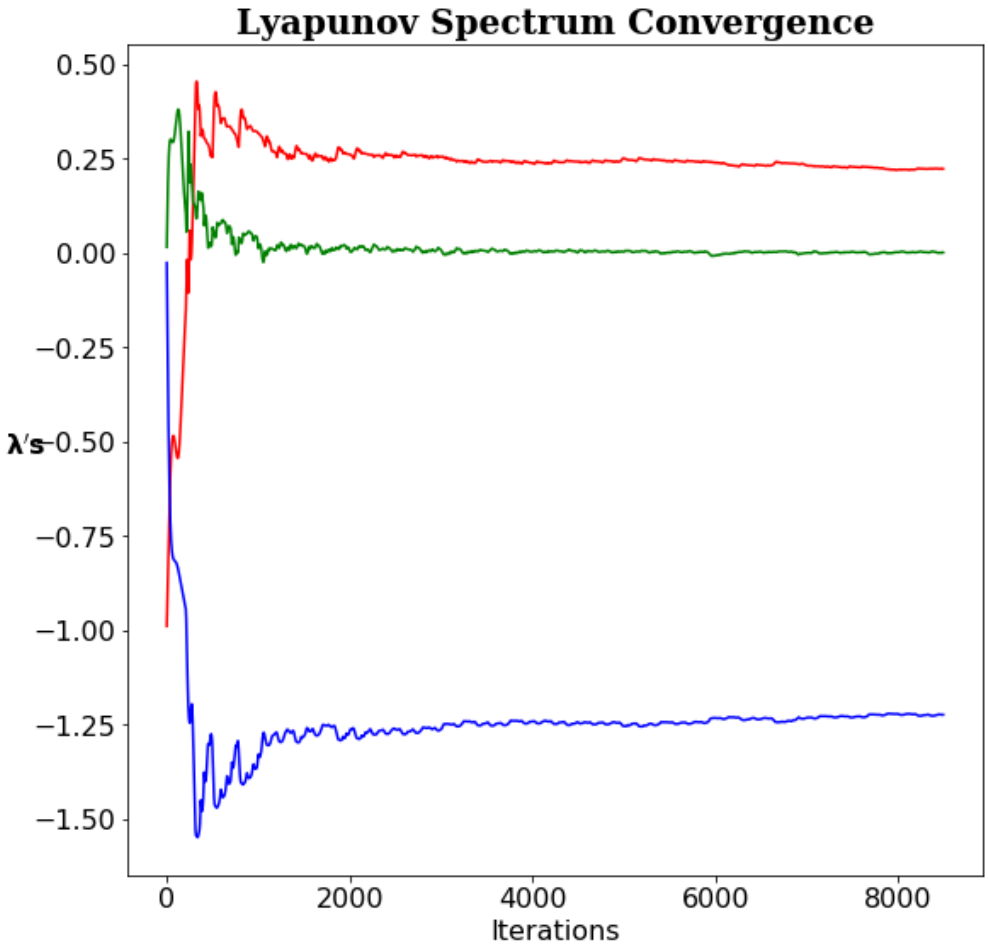

Figure 7: *The convergence of the Lyapunov Spectrum of the Wimol-Banlue Attractor using parameter values $\alpha = 2$. According to our calculations, the spectrum is approximately (0.244054, 0.001476, -1.245531). See Appendix C for coding details.*

Other Formulations of the Definition of Chaos

Some mathematicians define chaos using a different approach, and its worth taking a look at what they say. In doing so, we get a much more in-depth understanding of what chaos is and what it is not. Robert Devaney in his book "An Introduction to Chaotic Dynamical Systems" defined chaos in this way [11].

Definition III.4 (Chaos). *Let Ω be a set. $f : \Omega \to \Omega$ is said to be chaotic on Ω if*

- ***Sensitive Dependence on Initial Conditions**: $\exists \varepsilon > 0$ such that for any $\mathbf{x} \in \Omega$ and any neighborhood $N \subseteq \Omega$ of $\mathbf{x}$, there exists $\mathbf{y} \in N$ and $n \geq 0$ such that $||f^n(\mathbf{x}) - f^n(\mathbf{y})|| > \varepsilon$*
- ***Topological Transitivity**: $\forall U, V \subseteq \Omega$ there exists $n \geq 0$ such that $f^n(U) \cap V \neq \emptyset$*
- ***Periodic points are dense in** Ω: The closure of the set $\{\mathbf{x} \in \Omega : \exists n \geq 0$ such that $f^n(\mathbf{x}) = \mathbf{x}\}$ is equal to Ω*

In this definition, chaos is stronger than just sensitive dependence to initial conditions. As Devaney describes it, there needs to be a sense "unpredictability, indecomposability, and an element of regularity" [11].

Let us take a look at each one of these conditions expressed in the Lorenz System defined in Equation (4) with the same parameters declared in Figure 2, starting with "unpredictability". Say we approximate two trajectories $\mathbf{x}_1(t)$ and $\mathbf{x}_2(t)$, where $||\mathbf{x}_1(0) - \mathbf{x}_2(0)|| = \mathcal{O}(10^{-5})$, using an extremely accurate 14th order RK14(10) numerical integration technique (see Appendix C for details) [16][17]. Figure 8 then shows the dimension-wise progression of $\mathbf{x}_1(t)$ and $\mathbf{x}_2(t)$. One can easily notice the difference between $\mathbf{x}_1(t)$ and $\mathbf{x}_2(t)$ grows as time increases. The difference between the trajectories is the result of the chaotic nature of the Lorenz Attractor.

Devaney's second condition of chaos is "indecomposability", which can also be exemplified the Lorenz Attractor. Suppose 100 points are randomly distributed throughout subset of the phase space near the origin with a volume of $\mathcal{O}(10^{-2})$. Let us denote this subset as $U \subset \mathbb{R}^3$. Suppose each of these points is an initial condition for a trajectory, and that the position of each of these trajectories is recorded at certain intervals of time. Figure 9 shows this exact scenario. As time progresses, the trajectories experience chaos and are pulled and stretched apart, scattering throughout the attractor. Topologically, this means that if $\delta : \mathbb{R}^3 \times \mathbb{R} \to \mathbb{R}$ is the Lorenz dynamical system, then for every subset V of the Lorenz Attractor and every time step $\tau > 0$, there must exist a $n \in \mathbb{N}$ so that $\delta(U, n\tau) \cap V \neq \emptyset$. This is a perfect example of what Devaney described as transitive topology[11]. Any subset of a chaotic attractor, under the influence of the corresponding dynamical system, will at some point intersect every other subset of the attractor.

The third aspect of Devaney's definition is "an element of regularity" and is much more difficult to prove for the Lorenz Attractor, at least numerically. However, Sparrow wrote a

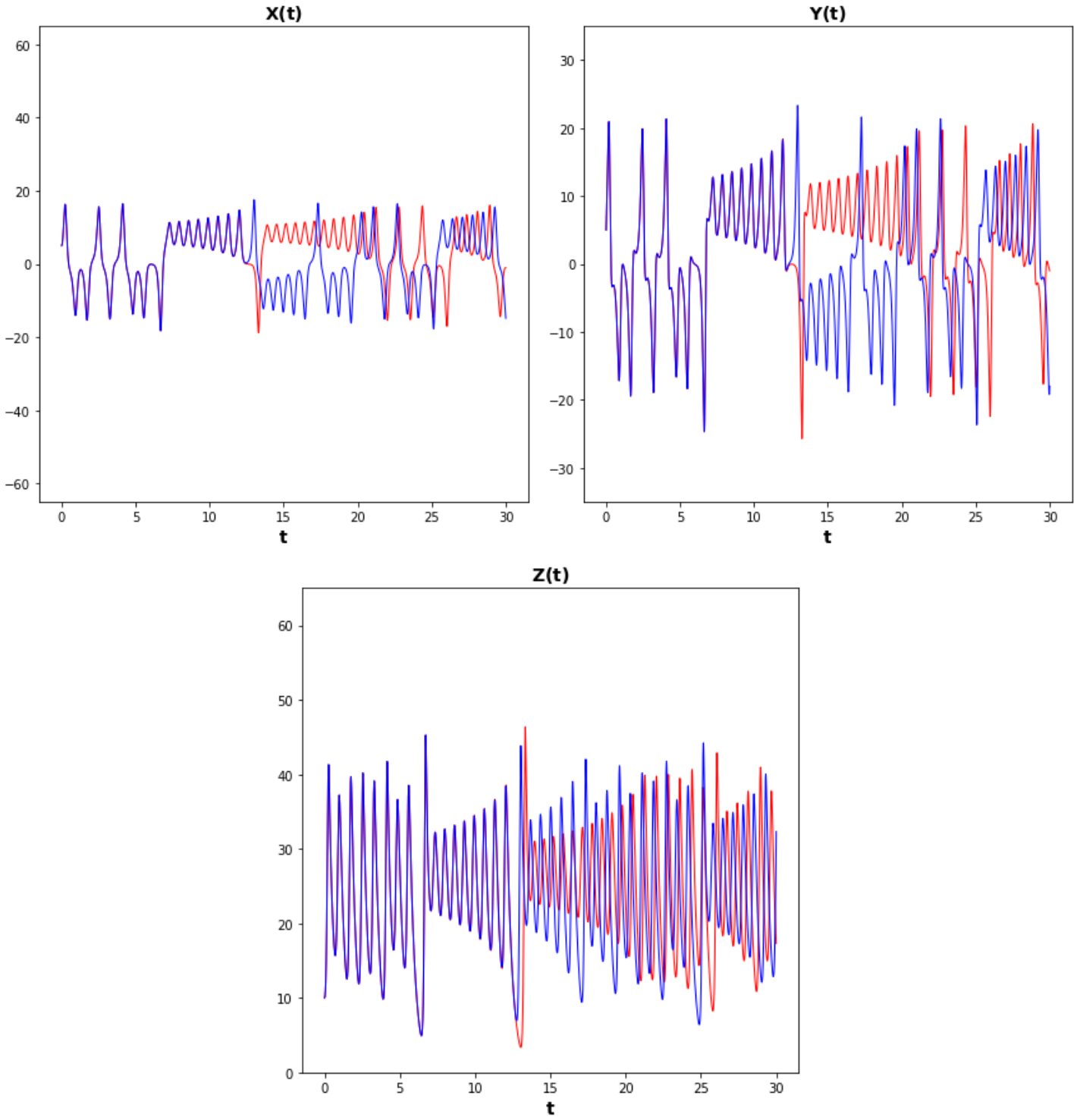

Figure 8: *The component-wise progression of* $\mathbf{x}_1(t)$ *(in red) and* $\mathbf{x}_2(t)$ *(in blue) in the Lorenz system when* $\sigma = 10$*,* $\rho = 28$*, and* $\beta = 8/3$*. These plots were generated with an RK14(10) integration method using a time step of* 0.001 *[16][17]. See Appendix C for details.*

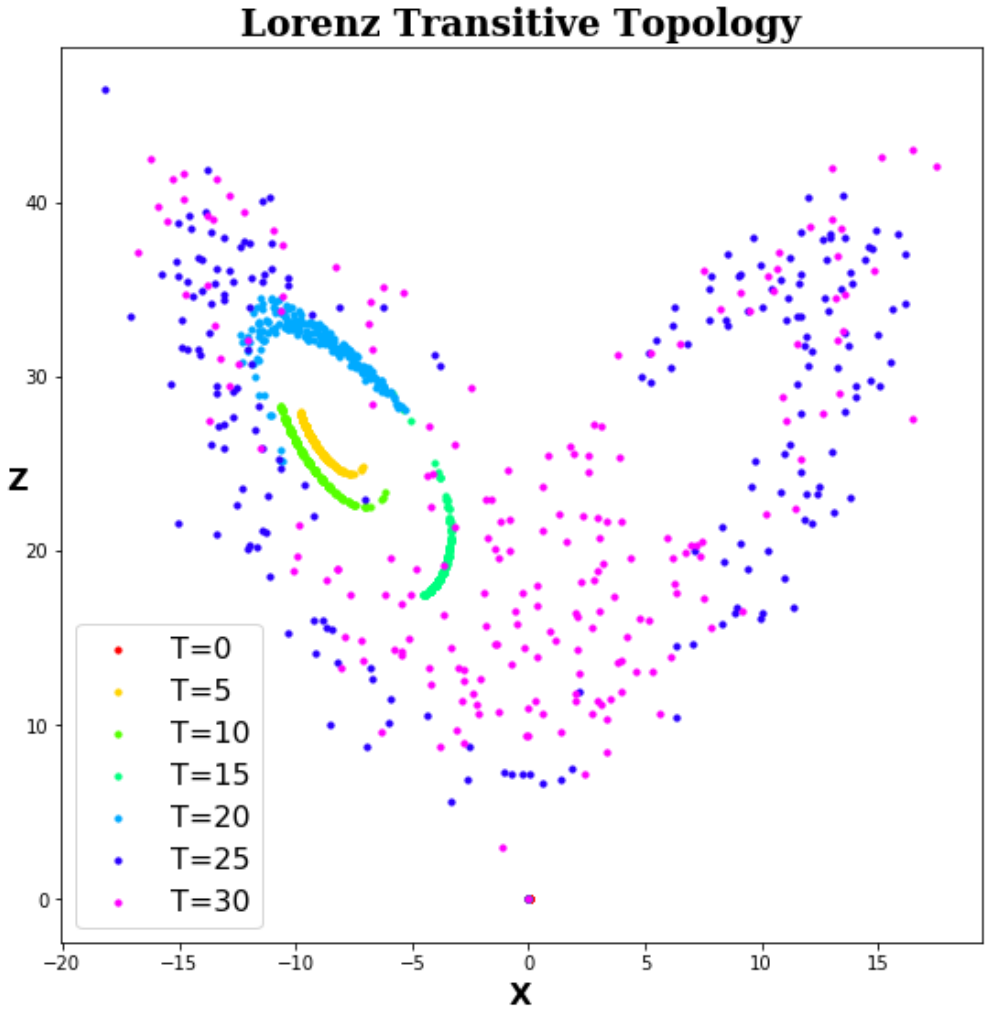

Figure 9: *The transitive topology of the Lorenz Attractor (projected onto the xz-plane), shown through the progression of 100 points moving through the Lorenz dynamical system. The points at time $T = 0$ are at most 1.73205×10^{-2} apparent, but as time T progresses, positions of the points become more and more evenly spread through the attractor.*

collection of papers concerning specifically Lorenz's attractor and provided some fascinating detail on how the periodic orbits of the Lorenz Attractor are born, interact, and behave. For more information, please see [27] and [31].

Lorenz's attractor is a textbook example of chaos emerging from strange attractors. In fact, both the Chua Attractors from Equation (6) and Wimol-Banlue Attractor from Equation (9) have been proven (either algebraically or numerically) to be chaotic [7][29]. The natural question then arises: do all strange attractors exhibit chaos? Are strange attractors synonymous with chaotic attractors? This is unfortunately not the case, as can be proven by a simple counter example: the discrete Feigenbaum Attractor. Research shows that this attractor is a Cantor set, which in itself is a fractal [3]; the Feigenbaum Attractor is therefore a chaotic attractor. However, it can also be shown that the Feigenbaum Attractor does not exhibit chaos [3][13]. For more information, see [18].

Nevertheless, chaos is present in many strange attractors. Because of their intriguing behavior and occurrence in many areas of science, chaotic strange attractors are phenomena that are on the foreground of modern mathematical research. One of the current topics in this field of research is the localization of these attractors: determining which subsets of the phase space could contain an attractor and which sets cannot. In the next section, we will be exploring some current localization techniques currently in use. The reason for this is that localization requires some inherent knowledge of the attractors themselves. Therefore, localizing an attractor may provide insight into some of its properties.

Analyzing localization techniques also provides an appropriate transition into introducing the main theory of this paper: the Competitive Modes Conjecture. Not only is the conjecture a new attempt at understanding chaotic strange attractors, but it also can serve as a more generally applicable localization technique of sorts.

IV. Localization Methods

Localization is the narrowing down of the location of a strange attractor, should it exist [6][28]. The usefulness of localization can be explained with a thought experiment. Say we have a dynamical system and we wish to investigate whether this system under a certain set of parameters contains a strange chaotic attractor. Instead of searching the entire n-dimension phase space, we apply a localization analysis over our dynamical system. In this way, we only need to investigate the regions permitted by the localization analysis to potentially contain a chaotic attractor, and ignore the rest. This can speedup the search for a chaotic attractor significantly. Here we present an overview of a number of localization techniques.

i. Localization through Unstable Manifolds of Equilibrium Points

The easiest method of localizing a chaotic attractor is by simply plotting a trajectory with an initial condition in the basin of attraction of the attractor itself. Chaos may force the trajectory to lose accuracy to the true solution, but for localization this hardly posses a problem; the trajectory will still give a clear picture of the structure and location of the attractor.

The issue then is determining the basins of attraction for each attractor. In general, this is not an easy task. Basins of attraction can be frustratingly small and difficult to find. One could brute-force the issue by plotting a large number of trajectories scattered throughout the phase space, but this is extremely costly; the number of trajectories needed for this approach would be too enormous for this method to be considered viable.

In light of this, remember Definition II.7. A self-excited attractor has a basin of attraction that includes an equilibrium point. Localizing a self-excited attractor therefore only requires plotting the unstable manifolds of an equilibrium point in its basin of attraction; at least one of the manifolds will enter the attractor after a transient period of time, thus showing the location and structure of the attractor.

Of course, this does not guarantee that a self-excited attractor will exist at all; the method is useful only if there is a self-excited attractor to begin with, which is not always known to be the case. Moreover, this method is only efficient for dynamical systems with relatively few equilibrium points. Plotting a large number of unstable manifolds over a (potentially very long) transient period of time can be quite costly.

Unfortunately, this approach does not work at all for locating hidden attractors. These can in theory be located anywhere in the phase space without an equilibrium point to "anchor" them down. Localizing these attractors efficiently requires more complex algorithms. All in all, plotting the unstable manifolds of equilibrium points can be a useful albeit rudimentary localization technique but should not and can not be used in many situations.

ii. Localization of Oscillatory Hidden Attractors

Unlike self-excited attractors, hidden attractors are somewhat more difficult to pin down. Methods have been developed for localizing certain hidden attractors, such as the one presented in this subsection. This method is described entirely in [21] and [23], where the authors of the article apply their technique to differential systems of the form

$$\dot{\mathbf{x}} = P\mathbf{x} + \phi(\mathbf{x}) \tag{12}$$

Here, $\mathbf{x}(t) \in \mathbb{R}^n$, $P \in \mathbb{R}^{n\times n}$ is a constant matrix, and $\phi : \mathbb{R}^{n\times n} \to \mathbb{R}^{n\times n}$ is a continuous vector function with $\phi(\mathbf{0}) = \mathbf{0}$ [21][23].

Now, say there exists some matrix $K \in \mathbb{R}^{n\times n}$ so that $P_0 = P + K$ has two purely imaginary eigenvalues called $\pm i\omega_0$ with $\omega_0 \in \mathbb{R}_{>0}$, and that the rest of the eigenvalues of P_0 all have negative real parts. We can then rewrite Equation (12) into the following form.

$$\begin{aligned} &\dot{\mathbf{x}} = P_0\mathbf{x} + \varepsilon\varphi(\mathbf{x}) \\ &\text{where } \varphi(\mathbf{x}) = \phi(\mathbf{x}) - K\mathbf{x} \end{aligned} \tag{13}$$

For purposes that we shall explain later, we also introduce a new variable $\varepsilon \in [0, 1]$. Notice that if $\varepsilon = 1$, the Equation (12) and Equation (13) are equivalent.

Let us say for $\varepsilon = 0$ that our system contains a periodic attractor, one that we can analytically compute. We can then increase ε by a sufficiently small increment, resulting in a dynamical system that has been slightly augmented. We assume, since this augmentation was small, that the periodic attractor has been slightly augmented as well, resulting in a new (pseudo-) periodic attractor. If the increase to ε was sufficiently small, then it stands to reason that any point $\mathbf{x}_0$ on our original periodic attractor will be in the basin of attraction of this new (pseudo-) periodic attractor. Thus, we can plot a trajectory from $\mathbf{x}_0$ and with it plot our new attractor after a transient period of time [21][23].

Please note that it is very possible that increasing ε beyond a certain value may result in a bifurcation in our dynamical system that destroys our attractor. We have no guarantees that our attractor will stay intact by slowly permuting ε from 0 to 1.

According to the technique, we increase ε over and over, using the attractor found in the previous permutation step to locate the new attractor in the current permutation step. This can be continued until one of two scenarios happens. The first outcome is that any increase in ε augments the system of equations enough to where the (pseudo-) periodic attractor disintegrates entirely. The second outcome occurs when $\varepsilon = 1$. If the latter happens, then we have found an attractor for Equation (12). If this attractor does not contain any equilibrium points in its basin of attraction, then it must be a hidden attractor. Please note that this does not guarantee that this attractor is chaotic or even strange [21][23].

We show this process in more detail with an example taken from [21] and [23]. Suppose we have the following system

$$\begin{cases} \dot{x} = \alpha(y - x - f(x)) \\ \dot{y} = x - y + z \\ \dot{z} = -\beta y - \gamma z \end{cases} \tag{14}$$

where $\alpha = 8.4562$, $\beta = 12.0732$, $\gamma = 0.0052$, and $f(x)$ is defined as in Equation (7) with $m_0 = -0.1768$ and $m_1 = -1.1468$. Notice that this system is very similar to that defined in Equation (6). Therefore, we shall refer to this system as a form of Chua System [21][23].

Following the form presented in Equation (12), we can rewrite our Chua System into the following form [21][23].

$$\begin{aligned} &\dot{\mathbf{x}} = P\mathbf{x} + \mathbf{q}\phi(\mathbf{r}^T\mathbf{x}) \\ &\text{where } \phi(\mathbf{r}^T\mathbf{x}) = (m_0 - m_1)\left(||\mathbf{r}^T\mathbf{x} + 1|| - ||\mathbf{r}^T\mathbf{x} - 1||\right)/2 \\ &P = \begin{bmatrix} -\alpha(m_1+1) & \alpha & 0 \\ 1 & -1 & 1 \\ 0 & -\beta & -\gamma \end{bmatrix}, q = \begin{bmatrix} -\alpha \\ 0 \\ 0 \end{bmatrix}, r = \begin{bmatrix} 1 \\ 0 \\ 0 \end{bmatrix} \end{aligned} \tag{15}$$

Now let us use Equation (15) to define a new system of differential equations following the form represented in Equation (13). For $k \in \mathbb{R}$

$$\begin{aligned} &\dot{\mathbf{x}} = P_0\mathbf{x} + \varepsilon\mathbf{q}\varphi(\mathbf{r}^T\mathbf{x}) \text{ where} \\ &P_0 = P + k\mathbf{q}\mathbf{r}^T = \begin{bmatrix} -\alpha(m_1+1+k) & \alpha & 0 \\ 1 & -1 & 1 \\ 0 & -\beta & -\gamma \end{bmatrix}, \\ &\varphi(\mathbf{r}^T\mathbf{x}) = \phi(\mathbf{r}^T\mathbf{x}) - k\mathbf{r}^T\mathbf{x} \end{aligned} \tag{16}$$

where k is chosen so that the eigenvalues of P_0 are equal to $i\omega_0$, $-i\omega_0$, and $-d$, where $\omega_0 \in \mathbf{R}_{>0}$ and $Re(d) \in \mathbf{R}_{>0}$ [21][23]. Notice that Equation (15) and Equation (16) are equivalent when $\varepsilon = 1$.

In order to compute the variables ω_0, k, and d, we introduce a concept from System and Control Theory: the transfer function[3]. In this case, the transfer function can be defined as

$$W_P(p) = \mathbf{r}^T(P - pI)^{-1}\mathbf{q} \text{ with } p \in \mathbb{C} \tag{17}$$

Then [21] and [23] state that $Im(W_P(\pm i\omega_0)) = 0$ and $k = -Re(W_P(\pm i\omega_0))^{-1}$, giving a method of at least approximating the values of ω_0 and the corresponding values of k. Using some linear algebra, we can conclude that

$$d = \frac{det(P_0)}{-\omega_0^2} = \frac{\alpha(m_1 + k + 1)(\beta + \gamma) - \alpha\gamma}{\omega_0^2}$$

[3]The physical interpretation of this function is not important for this document and therefore is omitted here. For an introduction into transfer functions, see [1]

Now that k, ω_0, and d can be calculated, the next step is to find a periodic trajectory in Equation (16). This can be difficult; therefore, [21] and [23] apply the invertible linear transformation $\mathbf{x} = S\mathbf{y}$, where

$$S = \begin{bmatrix} 1 & 0 & -h \\ m_1 + k + 1 & \frac{-\omega_0}{\alpha} & \frac{h}{\alpha}(d - \alpha(k + m_1 + 1)) \\ m1 + k - \frac{\omega_0^2}{\alpha} & -\omega_0 \left(m_1 + k + 1 + \frac{1}{\alpha} \right) & \frac{h}{\alpha}(\alpha + (d - \alpha(m_1 + k + 1))(1 - d)) \end{bmatrix}$$

where

$$h = \frac{\alpha\left(\alpha^2(m_1 + k + 1)^2 + \alpha + \omega_0^2\right)}{\omega_0^2 + d^2}$$

$$b1 = h - \alpha$$

$$b2 = \frac{dh - \alpha^2(m_1 + k + 1)}{\omega_0}$$

This propagates through Equation (16), transforming it into the following equivalent system of differential equations [21][23].

$$\begin{aligned} &\dot{\mathbf{y}} = A\mathbf{y} + \varepsilon \mathbf{b}\varphi(\mathbf{c}^T\mathbf{y}) \\ &\text{where } \varphi(\mathbf{c}^T\mathbf{y}) = (m_0 - m_1)\left(||\mathbf{c}^T\mathbf{y} + 1|| - ||\mathbf{c}^T\mathbf{y} - 1||\right)/2 - k\mathbf{c}^T\mathbf{y} \\ &A = S^{-1}P_0S = \begin{bmatrix} 0 & -\omega_0 & 0 \\ \omega_0 & 0 & 0 \\ 0 & 0 & -d \end{bmatrix} \\ &b = S^{-1}\mathbf{q} = \begin{bmatrix} b_1 \\ b_2 \\ 1 \end{bmatrix},\ c = \mathbf{r}^T S \begin{bmatrix} 1 \\ 0 \\ h \end{bmatrix} \end{aligned} \tag{18}$$

Then the following theorem can be applied.

Theorem IV.1. *Say we have the system defined in Equation* (16) *with* $\varepsilon = 0$*, and where* ω_0 *and* k *are concretely defined. If there exists an* $a_0 \in \mathbb{R}$ *so that*

$$\Phi(a_0) = \int_0^{2\pi/\omega_0} \varphi(a_0 \cos(\omega_0 t))\left(b_1 \cos(\omega_0 t) + b_2 \sin(\omega_0 t)\right) dt = 0$$

and that $\Phi'(a_0) < 0$*, then there exists a periodic solution in Equation* (16) *with* $\varepsilon = 0$ *with initial condition* $[x(0), y(0), z(0)]^T = S[a_0, 0, 0]^T$ *[23].*

We will use this periodic solution to hopefully construct a hidden attractor in Equation (15), if one exists.

Having completely defined every variable in Equation (18), we can finally try to localize the hidden attractor(s) in Equation (14). The most pivotal step is defining ω_0 and the corresponding value for k using the transfer function given in Equation (17), and then approximating the corresponding value for a_0 from Theorem IV.1 if it exists. There exists one set of appropriate parameters, numerically calculated to be

$$\omega_0 = 2.0392,\ k = 0.2099,\ a_0 = 5.8561$$

Therefore, at most one hidden attractor for Equation (14) can be found using this method.

From Theorem IV.1, we see that the system defined in Equation (16) with $\varepsilon = 0$ has a periodic solution with the initial condition $\mathbf{x}(0) = (5.856145, 0.369332, -8.366536)$. This periodic solution is given in Figure 10.

We can take any point along the periodic orbit shown in Figure 10 and use it as the initial condition of a trajectory in Equation (16), increasing ε incrementally. If ε is increased by a sufficiently small amount, this new trajectory should start somewhere in the basin of attraction of the new (pseudo-) periodic attractor, should it exist. We chose to incrementally increase ε by 0.2. Figure 11 then shows the progression of the periodic attractor (for $\varepsilon = 0$) into the hidden attractor (for $\varepsilon = 1$).

The resulting chaotic attractor when $\varepsilon = 1.0$ is portrayed in in Figure 12. To provide evidence that this is indeed a chaotic attractor, we also quickly analyze its Lyapunov Spectrum, a summary of which is provided in Figure 13. The maximal Lyapunov Exponent is approximately 0.158770, which is positive. According to Definition III.3, this hidden attractor is therefore chaotic.

Notice that this method is generally applicable to all systems that can be described by Equation (12), making this method very generally applicable. However, this method gives no guarantees that an attractor will exist in a particular system, only that if it exists there is the potential of approximating it incrementally. These increments are dependent on ε, and thus great care must be taken in increasing ε during every step of the algorithm. Furthermore, the resulting attractor still needs to be analyzed to confirm that it is indeed strange in nature and chaotic in behavior.

On a different note, we saw that the initial step in this method required a considerable amount of analytic prowess. Our differential system of equations needed to be transformed multiple times, each transformation having its advantages and disadvantages. Perhaps it would be better to use a different method that is not as academically taxing.

In conclusion, this method of localizing potential chaotic strange attractors can be very generally applicable, but as a trade-off is academically dense and does not always conclude

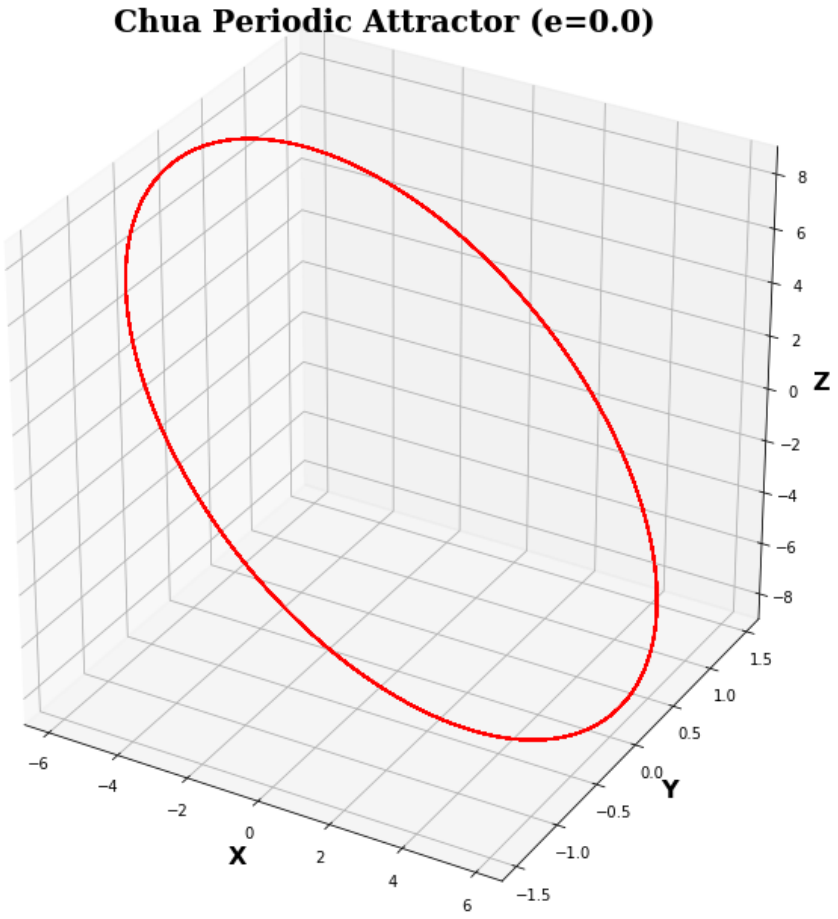

Figure 10: *A periodic solution of the system described in Equation* (16) *using parameters* $\alpha = 8.4562$, $\beta = 12.0732$, $\gamma = 0.0052$, $m_0 = -0.1768$, $m_1 = -1.1468$, *and* $\varepsilon = 0$. *The attractor was approximated using an adaptive explicit RK4 numerical integration technique over a time span of 100 time units using an initial position of (5.856145, 0.369332, -8.366536). See Appendix C for coding details.*

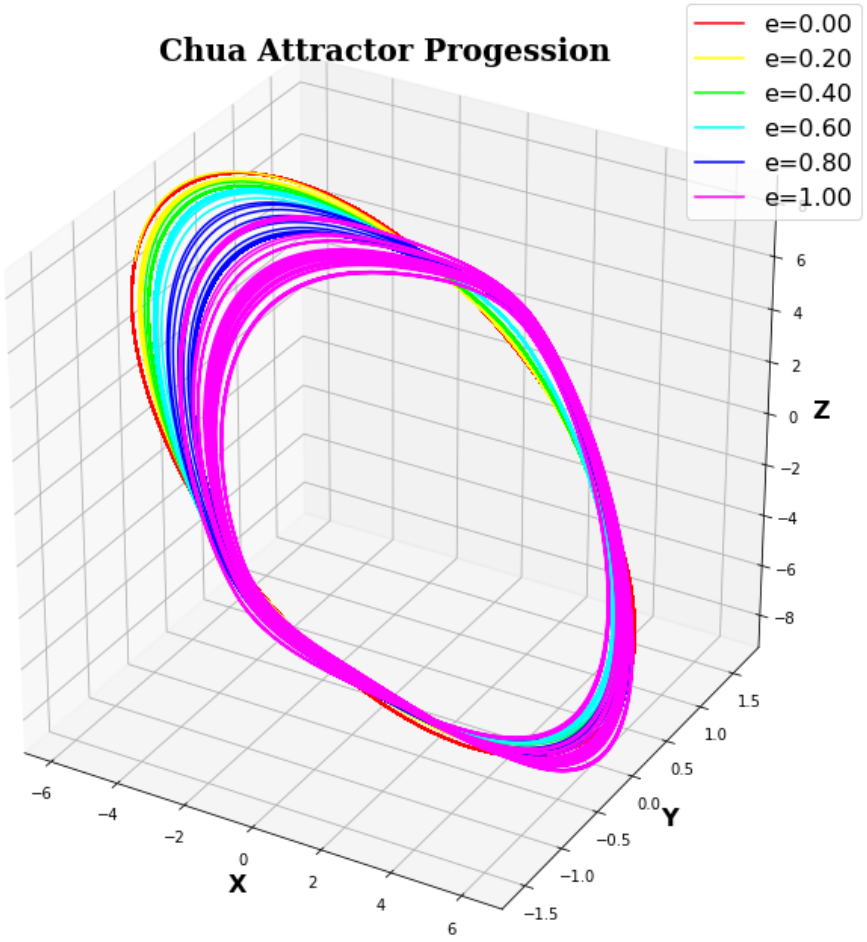

Figure 11: *The progression of the periodic attractor into chaotic hidden attractor by incrementally increasing ε from 0.0 to 1.0. The attractors were approximated using an adaptive explicit RK4 numerical integration technique over a time span of 100 time units each. See Appendix C for coding details.*

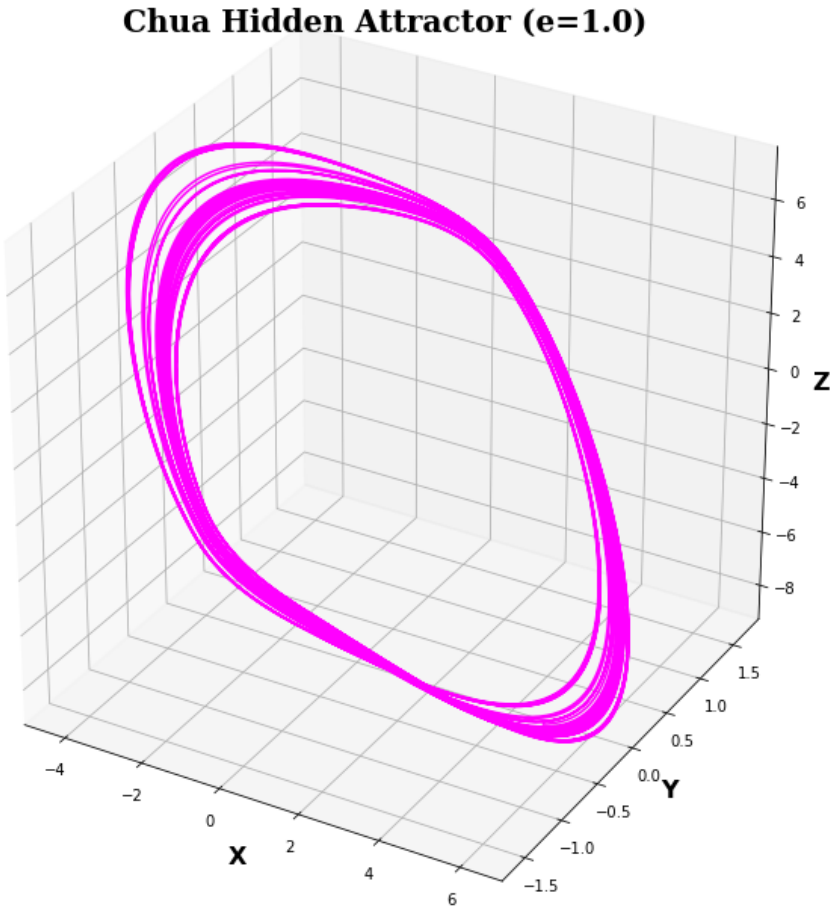

Figure 12: *An attractor of the Chua System described in Equation* (14) *using parameters* $\alpha = 8.4562$, $\beta = 12.0732$, $\gamma = 0.0052$, $m_0 = -0.1768$, *and* $m_1 = -1.1468$. *The attractor was approximated using an adaptive explicit RK4 numerical integration technique over a time span of 100 time units using an initial position of (5.389790, -0.341422, -8.255775). See Appendix C for coding details.*

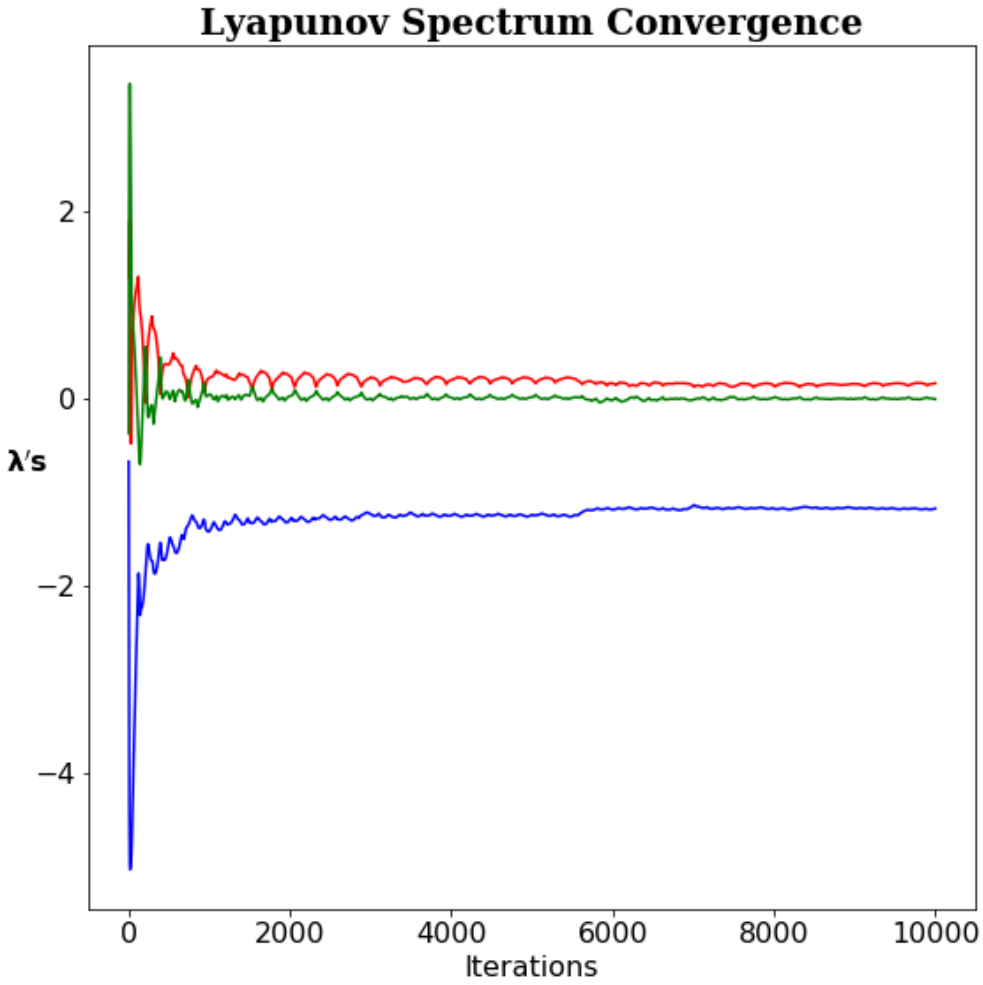

Figure 13: *The convergence of the Lyapunov Spectrum of the hidden Chua Attractor from Equation* (14) *using parameters* $\alpha = 8.4562$, $\beta = 12.0732$, $\gamma = 0.0052$, $m_0 = -0.1768$, *and* $m_1 = -1.1468$. *According to our calculations, the spectrum is approximately (0.158770, -0.010016, -1.178385). See Appendix C for coding details.*

in desirable results. One can now begin to understand the gravity of finding a generally-applicable, numerically-light, and user-friendly algorithm for attractor localization; doing so is not an easy task.

iii. Localization through Nambu Hamiltonians

Instead of using individual trajectories of the dynamical system, this method uses Nambu mechanics, a generalization of Hamiltonian mechanics which are commonplace in mechanical physics. We first give the definition for a Hamiltonian System. Then we expand upon it using the Nambu formalism, but only focusing on the 3-dimensional case for simplicity's sake; for a more complete definition, see [32].

Definition IV.1. ***Hamiltonian System***
Say $A, B \subseteq \mathbb{R}^n$ so that $\mathbf{x}(t) \in A$ and $\mathbf{y}(t) \in B$ are differentiable for $t \in T \subseteq \mathbb{R}$, where T is open. Suppose there exists a function $H : A \times B \to \mathbb{R}$ with $H \in \mathcal{C}^1(A, B)$ so that the following $2n$-dimensional system of equations holds.

$$\begin{cases} \dot{\mathbf{x}} = \dfrac{\partial H}{\partial \mathbf{y}} = \left(\dfrac{\partial H}{\partial y_1}, \cdots, \dfrac{\partial H}{\partial y_n} \right)^T \\ \dot{\mathbf{y}} = -\dfrac{\partial H}{\partial \mathbf{x}} = -\left(\dfrac{\partial H}{\partial x_1}, \cdots, \dfrac{\partial H}{\partial x_n} \right)^T \end{cases}$$

This is known as a Hamiltonian System with n-degrees of freedom, where H is the Hamiltonian of the system [27].

Notice that in a Hamiltonian System,

$$\dot{H} = \frac{\partial H}{\partial \mathbf{x}} \cdot \dot{\mathbf{x}} + \frac{\partial H}{\partial \mathbf{y}} \cdot \dot{\mathbf{y}} = -\dot{\mathbf{y}} \cdot \dot{\mathbf{x}} + \dot{\mathbf{x}} \cdot \dot{\mathbf{y}} = 0$$

We can conclude that $H(\mathbf{x}(t), \mathbf{y}(t)) = H(\mathbf{x}(0), \mathbf{y}(0))$ for all $t \in T$. This means that for any trajectory in a continuous dynamical system, the value of H remains constant.

This can also be seen it a different way. The equation $H(\mathbf{x}(t), \mathbf{y}(t)) = H(\mathbf{x}(0), \mathbf{y}(0))$ generally defines a (n-1)-dimensional surface in the n-dimensional phase plane. If a trajectory of the corresponding dynamical system were to have the initial condition $(\mathbf{x}(0), \mathbf{y}(0))$, then the trajectory would have to remain on this surface for all $t \in \mathbf{R}$.

As one can see, using the Hamiltonian is an incredibly efficient way to localize the trajectories of a system. However, it is not always possible to find a Hamiltonian function. Even when it is possible, calculating a suitable Hamiltonian is usually a very difficult task.

We now expand on the concept of a Hamiltonian System by introducing what is called a Nambu System. For simplicity, we only focus on 3-dimensional Nambu Systems; for a more complete definition, see [32].

Definition IV.2. ***Nambu System for 3 Dimensions***
Suppose $A \subseteq \mathbb{R}^3$ so that $(\mathrm{x}(t), \mathrm{y}(t), \mathrm{z}(t)) \in A$ is differentiable for all $t \in T \subseteq \mathbb{R}$. Suppose there exist functions $H_1, H_2 : A \to \mathbb{R}$ with $H_1, H_2 \in \mathcal{C}^1(A)$ so that the following 3-dimensional system of equations holds.

$$\begin{cases} \dot{x} = \dfrac{\partial H_1}{\partial y}\dfrac{\partial H_2}{\partial z} - \dfrac{\partial H_1}{\partial z}\dfrac{\partial H_2}{\partial y} \\ \dot{y} = \dfrac{\partial H_1}{\partial z}\dfrac{\partial H_2}{\partial x} - \dfrac{\partial H_1}{\partial x}\dfrac{\partial H_2}{\partial z} \\ \dot{z} = \dfrac{\partial H_1}{\partial x}\dfrac{\partial H_2}{\partial y} - \dfrac{\partial H_1}{\partial y}\dfrac{\partial H_2}{\partial x} \end{cases}$$

We call this a 3-dimensional Nambu System, where H_1 and H_2 are the "Nambunians" of the system (this naming is a personal choice by the authors and is not reflected in other literature). Notice that we can reduce this definition significantly into the equation $\dot{\mathbf{x}} = \nabla H_1 \times \nabla H_2$, where "$\times$" signifies the cross-product [28][32].

We now introduce and prove a few lemmas for 3-dimensional Nambu Systems.

Lemma IV.2. *Suppose we have a Nambu System as described in Definition IV.2. Then $\dot{H}_1 = \dot{H}_2 = 0$ [28][32]*

Proof. We prove this for H_1 only. The proof for H_2 is extremely similar.

$$\begin{aligned} \dot{H}_1 &= \nabla H_1 \cdot \dot{\mathbf{x}} \\ &= \frac{\partial H_1}{\partial x}\left(\frac{\partial H_1}{\partial y}\frac{\partial H_2}{\partial z} - \frac{\partial H_1}{\partial z}\frac{\partial H_2}{\partial y}\right) \\ &\quad + \frac{\partial H_1}{\partial y}\left(\frac{\partial H_1}{\partial z}\frac{\partial H_2}{\partial x} - \frac{\partial H_1}{\partial x}\frac{\partial H_2}{\partial z}\right) \\ &\quad + \frac{\partial H_1}{\partial z}\left(\frac{\partial H_1}{\partial x}\frac{\partial H_2}{\partial y} - \frac{\partial H_1}{\partial y}\frac{\partial H_2}{\partial x}\right) \\ &= \frac{\partial H_1}{\partial x}\frac{\partial H_1}{\partial y}\frac{\partial H_2}{\partial z} - \frac{\partial H_1}{\partial x}\frac{\partial H_1}{\partial z}\frac{\partial H_2}{\partial y} \\ &\quad + \frac{\partial H_1}{\partial y}\frac{\partial H_1}{\partial z}\frac{\partial H_2}{\partial x} - \frac{\partial H_1}{\partial x}\frac{\partial H_1}{\partial y}\frac{\partial H_2}{\partial z} \\ &\quad + \frac{\partial H_1}{\partial x}\frac{\partial H_1}{\partial z}\frac{\partial H_2}{\partial y} - \frac{\partial H_1}{\partial y}\frac{\partial H_1}{\partial z}\frac{\partial H_2}{\partial x} \\ &= 0 \end{aligned}$$

□

Just as before with Hamiltonian Systems, we can use Lemma IV.2 to conclude that

$$H_1(x(t), y(t), z(t)) = H_1(x(0), y(0), z(0))$$
$$H_2(x(t), y(t), z(t)) = H_2(x(0), y(0), z(0))$$

Generally, both equations describe 2-dimensional surfaces in the 3-dimensional phase space. As a result, if H_1 and H_2 are distinct sets, the trajectory with initial condition $(x(0), y(0), z(0))$ must lie in the intersection of these two surfaces. Therefore, if one knows the Nambunians of a Nambu System, they are able to very accurately predict where any trajectory will be in the phase space [28].
In order to show the power of Nambu Systems and provide a concrete example as to how they can be used to localize strange attractors, we focus yet again on the Lorenz System as described in Equation (4) with $\sigma = 10$, $\rho = 28$, and $\beta = 8/3$. This example is handled in far greater detail in [28]. We simplify the mathematics here, focusing on understandability.

First of all, the Lorenz System cannot be written as a 3-dimensional Nambu System; the reason for this is that only divergence-free systems have the possibility of being a Nambu System [28]. However, the divergence of the Lorenz System is $\nabla \cdot \dot{\mathbf{x}} = -(\sigma + \beta + 1)$. Therefore, we must split the system into a "dissipative" (meaning "divergence-containing") part (x_d, y_d, z_d) and a "non-dissipative" (meaning "divergence-free") part (x_{nd}, y_{nd}, z_{nd}) [28].

$$\begin{cases} \dot{x} = \sigma(y - x) \\ \dot{y} = x(\rho - z) - y \\ \dot{z} = xy - \beta z \end{cases} = \begin{cases} \dot{x}_{nd} = \sigma y_{nd} \\ \dot{y}_{nd} = x_{nd}(\rho - z_{nd}) \\ \dot{z}_{nd} = x_{nd} y_{nd} \end{cases} + \begin{cases} \dot{x}_d = -\sigma x_d \\ \dot{y}_d = -y_d \\ \dot{z}_d = \beta z_d \end{cases} \tag{19}$$

We will focus on the non-dissipative part for now, later reconnecting it with the dissipative part and drawing conclusions from that.

For the non-dissipative part of the Lorenz System, the Nambunians are calculated to be the following [28].

$$H_1(x, y, z) = \frac{1}{2}y^2 + \frac{1}{2}(z - \rho)^2 - \frac{1}{2}\rho^2, \; H_2(x, y, z) = -\frac{1}{2}x^2 + \sigma z \tag{20}$$

From Lemma IV.2, we are able to conclude that a trajectory starting at $(x_{nd}(0), y_{nd}(0), z_{nd}(0))$ will always lie in the intersection of

$$\begin{aligned} H_1(x_{nd}(t), y_{nd}(t), z_{nd}(t)) &= H_1(x_{nd}(0), y_{nd}(0), z_{nd}(0)) \\ H_2(x_{nd}(t), y_{nd}(t), z_{nd}(t)) &= H_2(x_{nd}(0), y_{nd}(0), z_{nd}(0)) \end{aligned} \tag{21}$$

This phenomenon is shown in Figure 14 by setting the initial condition arbitrarily to $(x_{nd}(0), y_{nd}(0), z_{nd}(0)) = (1, 5, -1)$ and plotting the corresponding non-dissipative trajectory along with the surfaces from Equation (21).

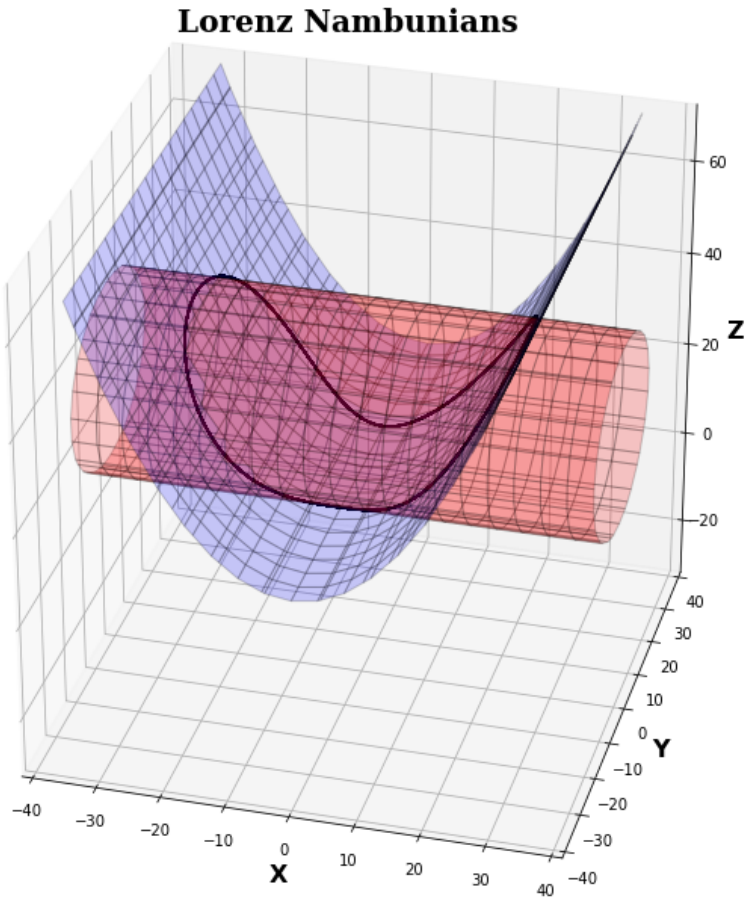

Figure 14: *The non-dissipative part of the Lorenz System as the intersection between the surfaces defined in Equation* (21)*. The parameters here are* $\sigma = 10$*,* $\rho = 28$*, and* $\beta = 8/3$*. The trajectory was approximated using an adaptive explicit RK4 numerical integration technique over a time span of 10 time units using an initial position of (10.383, 16.824, 19.325). The 3-dimensional surfaces were approximated using an adaptive Marching Cube Algorithm. See Appendix C for coding details.*

How does these Nambunians impact the original Lorenz System? Let us recombine the dissipative and non-dissipative parts and see what conclusions we can make. The following analysis is based on [28], which we refer to for a more complete overview. We start by focusing on the Nambunian H_1.

The Nambunian H_1

The formula for the Nambunian H_1 found in Equation (20) can be rewritten.

$$\begin{aligned} H_1(x,y,z) &= \frac{1}{2}y^2 + \frac{1}{2}(z-\rho)^2 - \frac{1}{2}\rho^2 \\ &\Leftrightarrow \\ y^2 + (z-\rho)^2 &= 2H_1(x,y,z) + \rho^2 \end{aligned}$$

If $H_1(x,y,z)$ is set to some value $k \in \mathbb{R}$, then this expression describes some sort of surface in the phase space; in the case of $k > -\rho^2/2$, a cylinder with radius $\sqrt{2k+\rho^2}$ is formed around the x-axis.

Let us say there exists some trajectory $\delta(\mathbf{x}_0, t) \in \mathbb{R}^3$ of the Lorenz System. For any $t \in \mathbb{R}$, the surface

$$S_1(\mathbf{x}_0, t) = \left\{(x,y,z) \in \mathbb{R}^3 : y^2 + (z-\rho)^2 = 2H_1(\delta(\mathbf{x}_0,t)) + \rho^2\right\} \tag{22}$$

must contain the point $\delta(\mathbf{x}_0, t)$ per construction.

Things get interesting when analyzing the derivative of H_1 with respect to t.

$$\dot{H}_1(x,y,z) = -y^2 - \beta(z-\rho/2)^2 + \beta\rho^2/4$$

Notice that $\dot{H}_1(x,y,z) \leq 0$ for all points in the phase space where $y^2 + \beta(z-\rho/2)^2 \geq \beta\rho^2/4$. This result has some very interesting implications. Suppose there exists some $k > -\rho^2/2$ so that $\dot{H}_1(x,y,z) < 0$ for all points in the phase space outside the cylinder

$$S_k = \left\{(x,y,z) \in \mathbb{R}^3 : y^2 + (z-\rho)^2 = 2k + \rho^2\right\}$$

Proving that such a k exists is relatively straight-forward. The only impact k has on S_k is the size of its radius: any increase in k will increase radius $\sqrt{2k+\rho^2}$. As a result, there must exist some k sufficiently large so that every point in S_k is completely outside the cylinder $y^2 + \beta(z-\rho/2)^2 = \beta\rho^2/4$. Thus, there must exist some k sufficiently large so that $\dot{H}_1(x,y,z) < 0$ for every point in S_k.

We can conclude that if trajectory $\delta(\mathbf{x}_0, t)$ has its initial condition outside of S_k, then there must exist a $\tau \in \mathbb{R}_{>0} \cup \{\infty\}$ so that $\dot{H}_1(\delta(\mathbf{x}_0,t)) < 0$ for all $0 \leq t < \tau$[4]. This means that

[4]It is to be noted that τ is specific for each trajectory.

for all $0 \leq t < \tau$, $S_1(\mathbf{x}_0, t)$ will shrink in radius. However, since $\delta(\mathbf{x}_0, t)$ is always found on $S_1(\mathbf{x}_0, t)$ per construction, this is equivalent to saying that for all $0 \leq t < \tau$, $\delta(\mathbf{x}_0, t)$ will get closer and closer to some subset inside or on the cylinder S_k.

Assume without loss of generality that $\dot{H}_1(\delta(\mathbf{x}_0, \tau)) = 0$. Then $\delta(\mathbf{x}_0, \tau)$ must be inside or on the cylinder S_k. However, we know then that $\delta(\mathbf{x}_0, t)$ cannot return back to the exterior of S_k since we just saw that any trajectory with any initial condition outside of S_k must be unequivocally drawn towards S_k. Therefore, $\delta(\mathbf{x}_0, t)$ will stay inside or on S_k for all $t \geq \tau$. In conclusion, we have proven that $\delta(\mathbf{x}_0, t)$ will be attracted to some subset of the surface or interior of S_k. Since we have not specified the trajectory $\delta(\mathbf{x}_0, t)$, we can conclude that all attractors, global or otherwise, are found inside or on S_k, including the Lorenz Attractor itself.

Therefore, the Lorenz Attractor must be found inside the set of the phase space where

$$\left\{(x, y, z) \in \mathbb{R}^3 : y^2 + (z - \rho)^2 \leq 2k + \rho^2,\ k > -\rho^2/2,\ \dot{H}_1(x, y, z) \leq 0\right\}$$

However, we now hope to find the optimal k in order to localize the Lorenz Attractor as efficiently as possible. In essence, we wish to find

$$k_{min} = \min\left\{k > -\frac{1}{2}\rho^2 : \dot{H}_1(x, y, z) \leq 0 \quad \forall (x, y, z) \text{ where } y^2 + (z - \rho)^2 \geq 2k + \rho^2\right\}$$

This is a constrained optimization problem that can be solved using the Lagrange's Multiplier Method (see [10]). Sparing the extraneous details, we see that the Lorenz Attractor must be found somewhere in the set

$$\begin{aligned} &S_{k_{min}} = \left\{(x, y, z) \in \mathbb{R}^3 : y^2 + (z - \rho)^2 \leq 2k_{min} + \rho^2\right\} \\ &\text{where} \\ &k_{min} = H_1\left(0, \frac{\pm\,\beta\rho}{2 - 2\beta}\sqrt{\beta - 2}, \frac{\rho(2 - \beta)}{2 - 2\beta}\right) = \frac{\rho^2}{2}\,\frac{(\beta - 2)^2}{4(\beta - 1)} \end{aligned} \tag{23}$$

It is trivial to conclude that $k_{min} > -\rho^2/2$ when $\beta > 1$.

Figure 15 plots the Lorenz Attractor along with boundary of the localizing set defined in Equation (23).

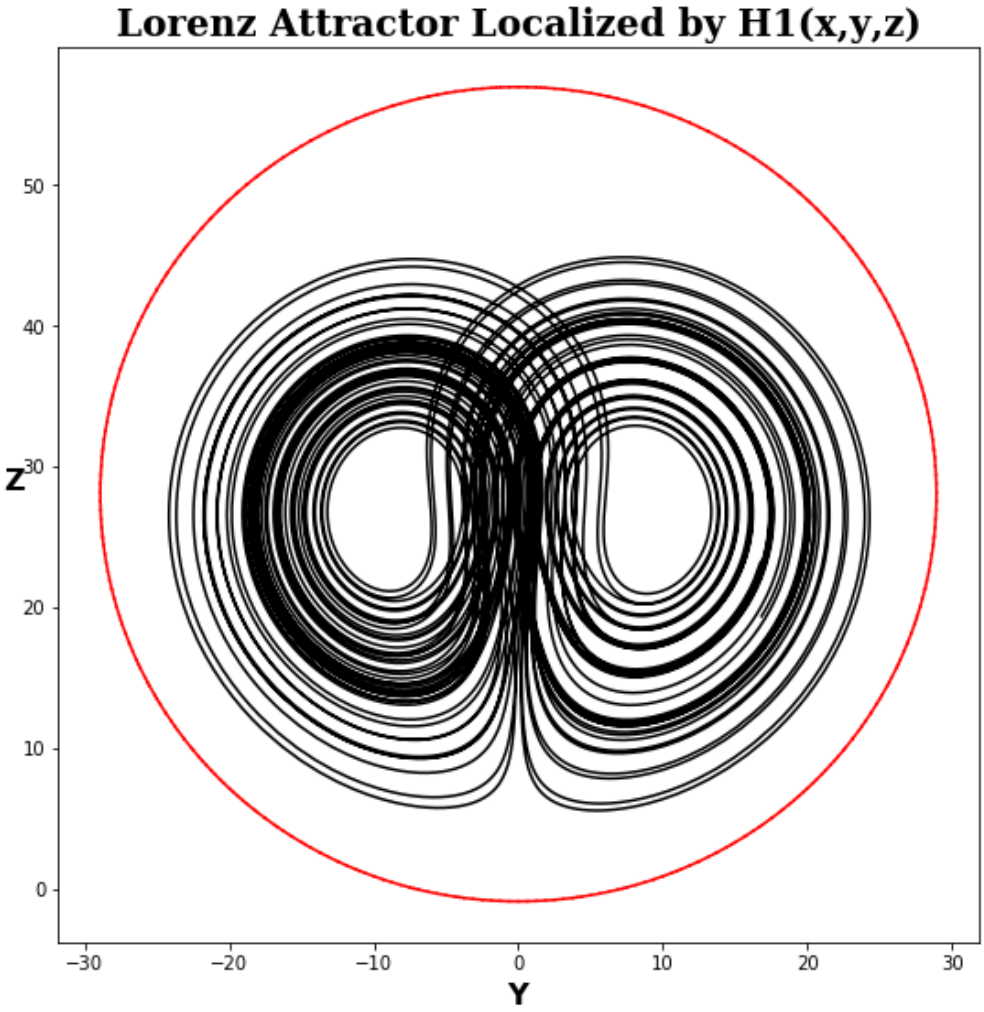

Figure 15: *The Lorenz Attractor, nestled comfortably within the localizing set defined in Equation* (23) *(projected onto to the yz-plane). The parameters here are* $\sigma = 10$, $\rho = 28$, *and* $\beta = 8/3$. *The 2-dimensional projection of the set defined in Equation* (23) *was approximated using an adaptive Marching Square Algorithm. See Appendix C for details.*

The Nambunian H_2

Just as with H_1, the formula for the Nambunian H_2 from Equation (20) can be rewritten.

$$H_2(x,y,z) = -\frac{1}{2}x^2 + \sigma z$$
$$\Leftrightarrow$$
$$2\sigma z = x^2 + 2H_2(x,y,z)$$

If $H_2(x,y,z)$ is set to some vale of $k \in \mathbb{R}$, then this expression describes a paraboloid.

Let us say there exists some trajectory $\delta(\mathbf{x}_0, t) \in \mathbb{R}^3$ of the Lorenz System. Like for $S_1(\mathbf{x}_0, t)$, for any $t \in \mathbb{R}$, the surface

$$S_2(\mathbf{x}_0, t) = \left\{(x,y,z) \in \mathbb{R}^3 : 2\sigma z = x^2 + 2H_2(\delta(\mathbf{x}_0, t))\right\} \tag{24}$$

must contain the point $\delta(\mathbf{x}_0, t)$.

The derivative is again of great importance.

$$\dot{H}_2(x,y,z) = \sigma(x^2 - \beta z)$$

Notice that $\dot{H}_2(x,y,z) \geq 0$ for all points in the phase space where $\sigma x^2 \geq \beta\sigma z$. Again, suppose there exists some $k \in \mathbb{R}$ so that $\dot{H}_2(x,y,z) > 0$ for all points in the phase space "below" the paraboloid

$$S_k = \left\{(x,y,z) \in \mathbb{R}^3 : 2\sigma z = x^2 + 2k\right\}$$

Proving such a k exists is simple. Under the assumption that $2\sigma \geq \beta > 0$ and $k < 0$, the following inequality always holds.

$$\sigma x^2 \geq \sigma x^2 + 2\sigma k = 2\sigma^2 z \geq \beta\sigma z$$

Thus, every point in S_k is completely "underneath" the paraboloid $\sigma x^2 \geq \beta\sigma z$. Thus, for $2\sigma \geq \beta > 0$ there must exist a k so that $\dot{H}_2(x,y,z) > 0$ for every point in S_k.

Similar to our analysis with the Nambunian H_1, we can conclude that if trajectory $\delta(\mathbf{x}_0, t)$ has its initial condition below S_k, then there must exist a $\tau \in \mathbb{R}_{>0} \cup \{\infty\}$ so that $\forall 0 \leq t < \tau$, $\dot{H}_2(\delta(\mathbf{x}_0, t)) > 0$[5]. This means that for all $0 \leq t < \tau$, $S_2(\mathbf{x}_0, t)$ will shift upwards in the positive z-direction. However, since $\delta(\mathbf{x}_0, t)$ is always found on $S_2(\mathbf{x}_0, t)$ per construction, this is equivalent to saying that $\delta(\mathbf{x}_0, t)$ will get closer and closer to some subset above or on the paraboloid S_k $\forall 0 \leq t < \tau$.

[5]It is to be noted that τ is specific for each trajectory.

Again assume without loss of generality that $\dot{H}_2(\delta(\mathbf{x}_0, \tau)) = 0$. Then $\delta(\mathbf{x}_0, \tau)$ must be "above" or on the paraboloid S_k. However, we know then that $\delta(\mathbf{x}_0, t)$ cannot return to the area underneath S_k since we just saw that any trajectory with any initial condition underneath S_k must be unequivocally drawn towards S_k. Therefore, $\delta(\mathbf{x}_0, t)$ will stay above or on S_k for all $t \geq \tau$. In conclusion, we have proven that $\delta(\mathbf{x}_0, t)$ will be attracted to some subset of the surface or area above S_k. Since we have not specified $\delta(\mathbf{x}_0, t)$, we can conclude that all attractors, global or otherwise, are found above or on S_k, including the Lorenz Attractor.

Thus, the Lorenz Attractor must be found inside the set of the phase space

$$\left\{(x, y, z) \in \mathbb{R}^3 : 2\sigma z \geq x^2 + 2k,\ k \in \mathbb{R},\ \dot{H}_2(x, y, z) \geq 0\right\}$$

However, we now hope to once again find the optimal k in order to localize the Lorenz Attractor as efficiently as possible. In essence, we wish to find

$$k_{max} = \max\left\{k \in \mathbb{R} : \dot{H}_2(x, y, z) \geq 0 \quad \forall (x, y, z) \text{ where } 2\sigma z \leq x^2 + 2k\right\}$$

Once again, this is a constrained optimization problem that can be solved using Lagrange's Multiplier Method (see [10]). Sparing the extraneous details and under the assumption that $2\sigma \geq \beta > 0$, we see that the Lorenz Attractor must be found somewhere in the set

$$\begin{aligned} &S_{k_{max}} = \left\{(x, y, z) \in \mathbb{R}^3 : 2\sigma z \geq x^2 + 2k_{max}\right\} \\ &\text{where} \\ &k_{max} = H_2(0, 0, 0) = 0 \end{aligned} \tag{25}$$

Figure 16 plots the Lorenz Attractor along with boundary of the localizing set defined in Equation (25).

Using both Nambunians H_1 and H_2, the Lorenz Attractor can be localized very efficiently. We represent these results in Figure 17 by plotting the Lorenz Attractor along with boundary of the localizing sets defined in Equations (23) and (25).

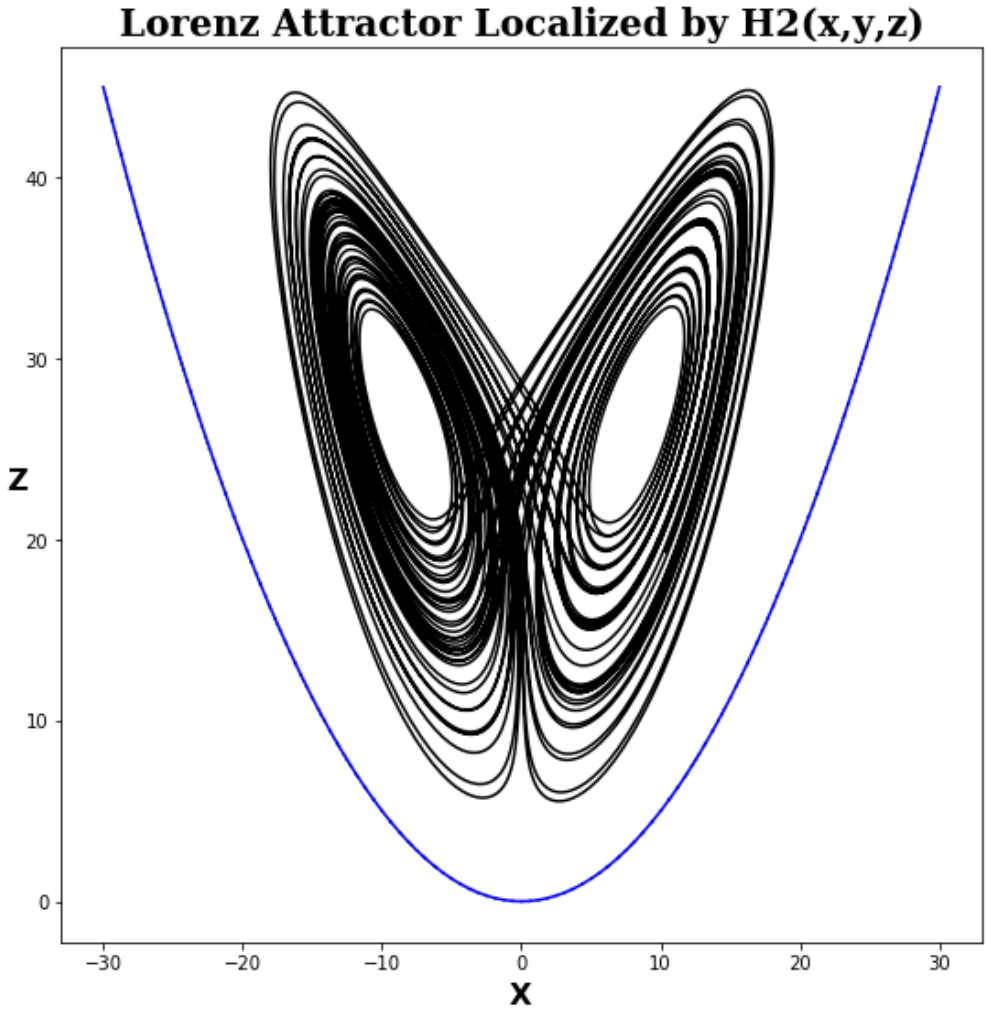

Figure 16: *The Lorenz Attractor, nestled comfortably within the localizing set defined in Equation* (25) *(projected onto to the xz-plane). The parameters here are $\sigma = 10$, $\rho = 28$, and $\beta = 8/3$. The 2-dimensional projection of the set defined in Equation* (25) *was approximated using an adaptive Marching Square Algorithm. See Appendix C for details.*

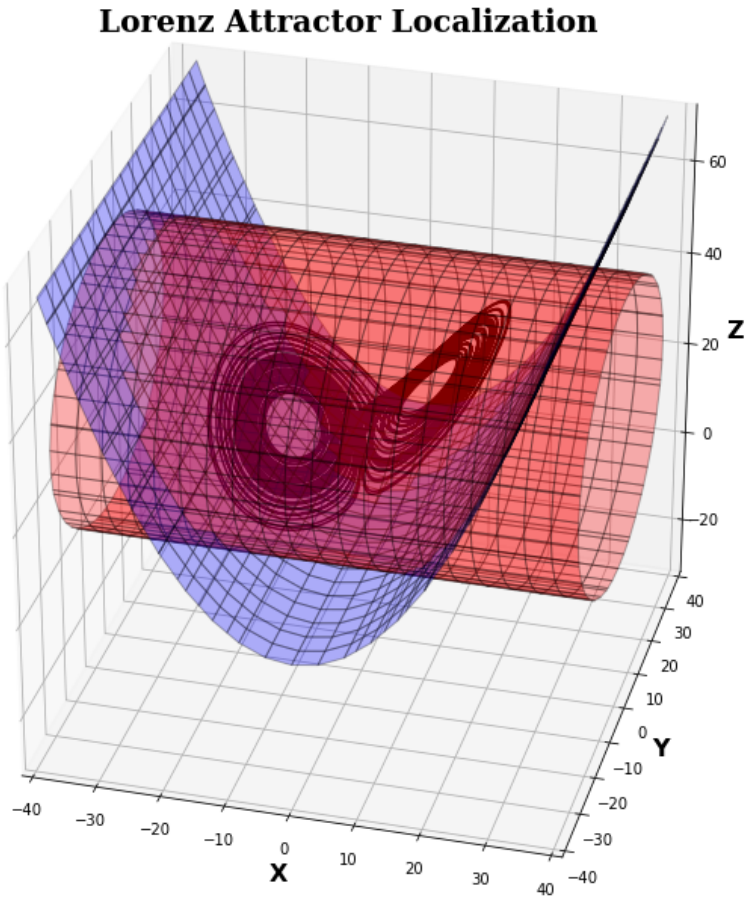

Figure 17: *The Lorenz Attractor, nestled comfortably within the localizing sets defined in Equations* (23) *and* (25)*. The parameters here are* $\sigma = 10$*,* $\rho = 28$*, and* $\beta = 8/3$*. The surfaces were approximated using an adaptive Marching Cube Algorithm. See Appendix C for details.*

As a concluding note, we introduce a useful lemma.

Lemma IV.3. *Suppose we have a Nambu System as described in Definition IV.2. Suppose* $\mathcal{H}_1$ *and* $\mathcal{H}_2$ *are continuously differentiable functions of* H_1 *and* H_2*, where the corresponding Jacobian has a determinant of 1. Then* $\mathcal{H}_1$ *and* $\mathcal{H}_2$ *can be used instead of* H_1 *and* H_2 *in Definition IV.2 [28][32].*

Proving this lemma only requires a basic understanding of linear algebra and thus will not be presented here. For more details, see [28] and [32].

Using this lemma, an infinite number of Nambunian pairs H_1 and H_2 can be constructed, and in-so-doing an infinite number of different localizing sets just like those constructed in Equations (23) and (25). Therefore, a more intensive analysis using multiple pairs of localizing sets could lead to a very efficient localization of the Lorenz Attractor indeed.

Of course, this method is only applicable to systems of differential equations that have a non-zero non-dissipative part, for which the Nambunians can be found (which is a difficult task in and of itself). The analysis that follows is also rather lengthy and may not even be possible. It all depends on how the Nambunians behave and interact with the system, which can make analysis difficult if not impossible. In conclusion, this method can be very efficient in localizing strange attractors, but can only be applied effectively to a limited number of dynamical systems due to the cost of finding the appropriate Nambunian functions.

V. The Competitive Modes Conjecture

The previous sections' focus has been to understand chaotic strange attractors and the properties thereof. Even the localization methodologies presented in the section beforehand attempt to make use of special properties found among certain sets of dynamical systems, with varying success. This section will introduce a somewhat new methodology, one that may provide great insight into the very nature of chaos itself. All knowledge presented in this section comes from sources [4], [5], [6], [9], [14], and [37].

Given is a general n-dimensional autonomous system of differential equations $\dot{\mathbf{x}} = \mathbf{F}(\mathbf{x})$ with $\mathbf{x} : \mathbb{R} \to \mathbb{R}^n$. We can easily transform this system into a system of second-order differential equations as follows

$$\begin{aligned} \ddot{\mathrm{x}}_i &= \dot{F}_i(\mathbf{x}) \\ &= \nabla F_i(\mathbf{x}) \cdot \dot{\mathbf{x}} \\ &= \sum_{j=1}^{n} \frac{\partial F_i}{\partial \mathrm{x}_j}(\mathbf{x}) F_j(\mathbf{x}) \\ &\equiv f_i(\mathbf{x}) \end{aligned} \tag{26}$$

This of course only works if F_i is x_j-differentiable for all $i, j \in \{1, 2, \cdots, n\}$.

Definition V.1 (Splitting of a Function)**.** *In previous literature, function $f_i : \mathbb{R}^n \to \mathbb{R}$ can be split with respect to x_i if it can be rewritten as*

$$f_i(\mathbf{x}) = h_i(\mathrm{x}_1, \cdots, \mathrm{x}_{i-1}, \mathrm{x}_{i+1}, \cdots, \mathrm{x}_n) - \mathrm{x}_i g_i(\mathbf{x}) \tag{27}$$

We name function $h_i : \mathbb{R}^{n-1} \to \mathbb{R}$ the i^{th} forcing function. We name function $g_i : \mathbb{R}^n \to \mathbb{R}$ the i^{th} squared frequency function.

For simplicity, let us establish the notation of a particular operator function that we will use often. Say we have $\mathbf{x} \in \mathbb{R}^n$. Then function $\mathfrak{p}_i : \mathbb{R}^n \to \mathbb{R}^{n-1}$ is defined as follows.

$$\mathfrak{p}_i(\mathbf{x}) = [\mathrm{x}_1, \cdots \mathrm{x}_{i-1}, \mathrm{x}_{i+1}, \cdots \mathrm{x}_n]^T \tag{28}$$

If Equation (26) holds and the resulting functions f_i can all be split, then we can rewrite our original system of differential equations into the form

$$\begin{cases} \ddot{\mathrm{x}}_1 + g_1(\mathbf{x})\mathrm{x}_1 = h_1(\mathfrak{p}_1(\mathbf{x})) \\ \ddot{\mathrm{x}}_2 + g_2(\mathbf{x})\mathrm{x}_2 = h_2(\mathfrak{p}_2(\mathbf{x})) \\ \cdots \\ \ddot{\mathrm{x}}_i + g_i(\mathbf{x})\mathrm{x}_i = h_i(\mathfrak{p}_i(\mathbf{x})) \\ \cdots \\ \ddot{\mathrm{x}}_n + g_n(\mathbf{x})\mathrm{x}_n = h_n(\mathfrak{p}_n(\mathbf{x})) \end{cases} \tag{29}$$

In a sense, we have turned our system of differential equations into a system of interconnected, nonlinear "oscillators".

Definition V.2 (Competitive Modes)**.** *Say we have the n-dimensional autonomous system of differential equations* $\dot{\mathbf{x}} = \mathbf{F}(\mathbf{x})$*. If Equation* (26) *holds for this system and the resulting functions* f_i *can all be split, then the system can be transformed as shown into Equation* (29)*. The solutions* x_i *for Equation* (29) *are then known as the competitive modes of the system, with* g_i *and* h_i *being the corresponding squared frequency functions and forcing functions, respectively.*

Currently, there is an open conjecture connecting chaos and competitive modes together, and it is presented as follows.

Conjecture V.1 (Competitive Modes Conjecture)**.** *The necessary conditions for a dynamical system to exhibit chaotic are given below (assuming Equation* (26) *holds and the resulting functions* f_i *can all be split):*

- *the dimension n of the dynamical system is greater than 2;*
- *at least two distinct squared frequency functions* g_i *and* g_j *are competitive or nearly competitive; that is, there exists* $t \in \mathbb{R}$ *so that* $g_i(t) \approx g_j(t)$ *and* $g_i(t), g_j(t) > 0$*;*
- *at least one squared frequency function* g_i *is not constant with respect to time;*
- *at least one forcing function* h_i *is not constant with respect to some system variable* x_j*.*

Notice that the conjecture specifically states necessary conditions, not sufficient ones. That is, if an attractor exhibits chaos, then the stated conditions are met, not the other way around. It describes what properties a chaotic system will have; it does not describe a guaranteed approach for constructing them. The authors find the particular wording of the conjecture to be a bit confusing and difficult to understand, and therefore wanted to place specific emphasis on explaining exactly how the conjecture works.

The conjecture gets its name from its most important condition: two competitive modes must compete with each other, which is equivalent to saying that the corresponding squared frequency functions must intersect. We can group these intersections into sets: say we have squared frequency function g_i and g_j where $i \neq j$. We can then define intersection set G_{ij} as

$$G_{ij} = \{\mathbf{x} \in \mathbb{R}^n : g_i(\mathbf{x}) = g_j(\mathbf{x})\} \tag{30}$$

Furthermore,

$$G_{ij}^{+} = \{\mathbf{x} \in \mathbb{R}^n : g_i(\mathbf{x}) = g_j(\mathbf{x}) > 0\} \tag{31}$$

This then means that if the conjecture is correct, for a chaotic attractor $A \subset \mathbb{R}^n$ there must exist some $i, j \in \{1, 2, \cdots, n\}$ where $i \neq j$ so that $A \cap G_{i,j}^{+} \neq \emptyset$. This phenomenon is the focus of Reference [6] and serves to localize chaotic attractors.

As in [6], let us exemplify this localization technique using the Lorenz Attractor (Equation 4 from Section II). Differentiating the Lorenz System with respect to time and then splitting each of the equations into their respective forcing and squared frequency functions, we obtain the following [6][6].

$$\begin{aligned} h_x(y,z) &= -\sigma(\sigma+1)y \\ g_x(x,y,z) &= \sigma(z-\sigma-\rho) \\ h_y(x,z) &= (\sigma+\beta+1)xz - \rho(\sigma+1)x \\ g_y(x,y,z) &= x^2 + \sigma z - \sigma\rho - 1 \\ h_z(x,y) &= \rho x^2 - (\sigma+\beta+1)xy + \sigma y^2 \\ g_z(x,y,z) &= x^2 - \beta^2 \end{aligned}$$

Let us go through each of the conjecture's necessary conditions individually before going forward[6].

- The dimension of the Lorenz System is 3, which is greater than 2.
- As least one squared frequency function (for example $g_x(x(t), y(t), z(t))$ is not constant with respect to time t.
- As least one of the forcing functions (for example $h_y(x(t), z(t))$ is not constant with respect to both x and z.

The only condition left to be verified is whether at least two squared frequency functions intersect for some point $(x(t^*), y(t^*), z(t^*))$ in the Lorenz Attractor. Plotting a random trajectory inside of the Lorenz Attractor (with the correct set of parameters) does reveal this to be indeed true; verification can be found in Figure 18 [6]. As a result, the Lorenz Attractor is an example of where the Competitive Modes Conjecture predict accurate results about chaos, meaning that the conjecture could be true [31][34].

In fact, the subsets of the phase space where the three squared frequency functions intersect each other form the continuous 2-dimensional surfaces G_{xy}, G_{xz}, and G_{yz}. These surfaces are plotted in Figure 19. As one can see, the attractor concretely intersects G_{yz}. Figure 18 provides evidence that not only does the attractor intersects G_{yz}, it specifically intersects G^+_{yz}. Thus, the Competitive Modes Conjecture can be used as a localization technique of chaotic attractors: if the conjecture is true, it indicates if a chaotic attractor could exist and where it would reside in the phase space [6].

Unfortunately, the Competitive Modes Conjecture is surprisingly vague in how to mathematically define forcing functions and squared frequency functions. For multipolynomial systems, previous literature seems to indicate an unspoken rule: splitting a multipolynomial function in terms of variable x_i results in the forcing function being equal the sum of all terms that do not include x_i [4][5][6][9][14][37]. However, this relatively straightforward

[6]Calculations are performed in detail in Section VII

"definition" is only applicable to functions that are at least polynomial in x_i. As far as the authors know, no research has been done on an actual mathematically rigorous counterpart to Definition V.1. The latter half of this paper is aimed towards rectifying this oversight.

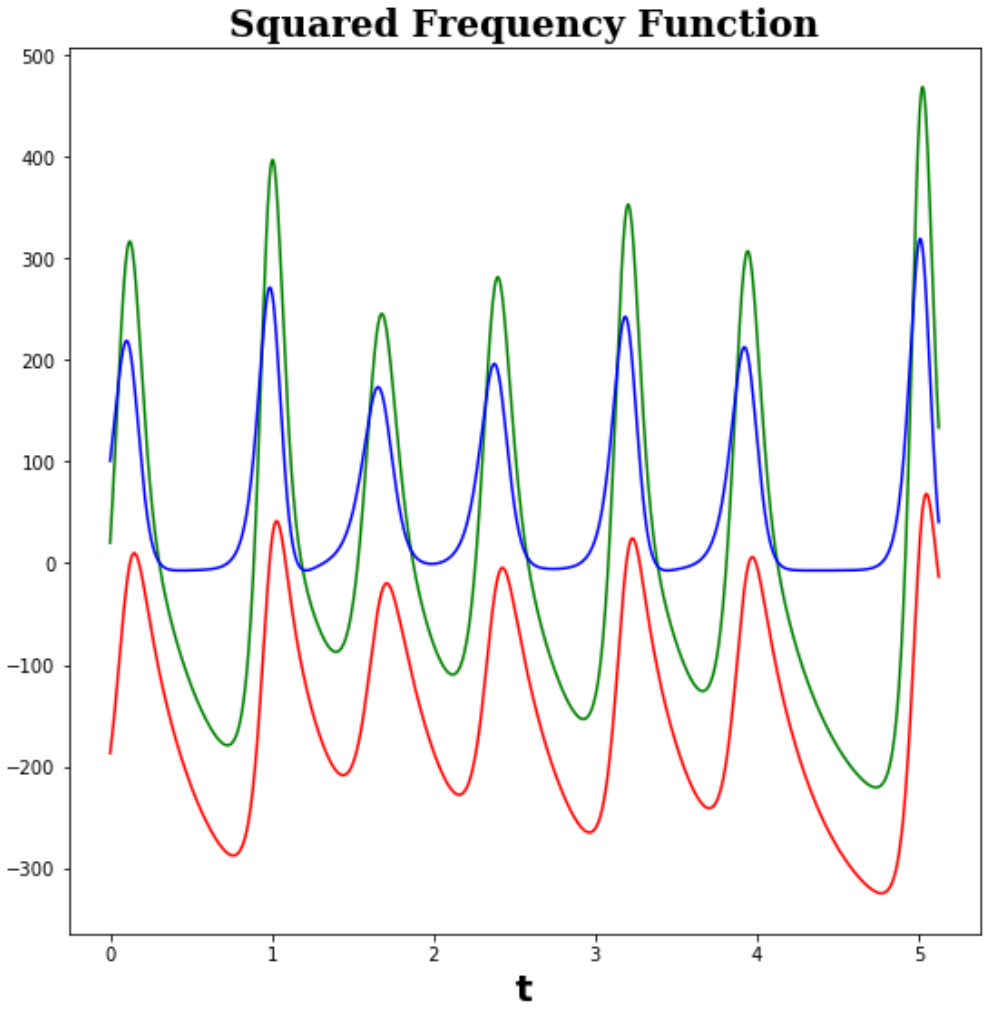

Figure 18: *The squared frequency functions g_x (in red), g_y (in green), and g_z (in blue) applied to a random trajectory in the Lorenz Attractor, where $\sigma = 10$, $\rho = 28$, and $\beta = 8/3$. Notice that g_y and g_z intersect on a regular basis, and that all intersections occur when g_y and g_z take on positive values.*

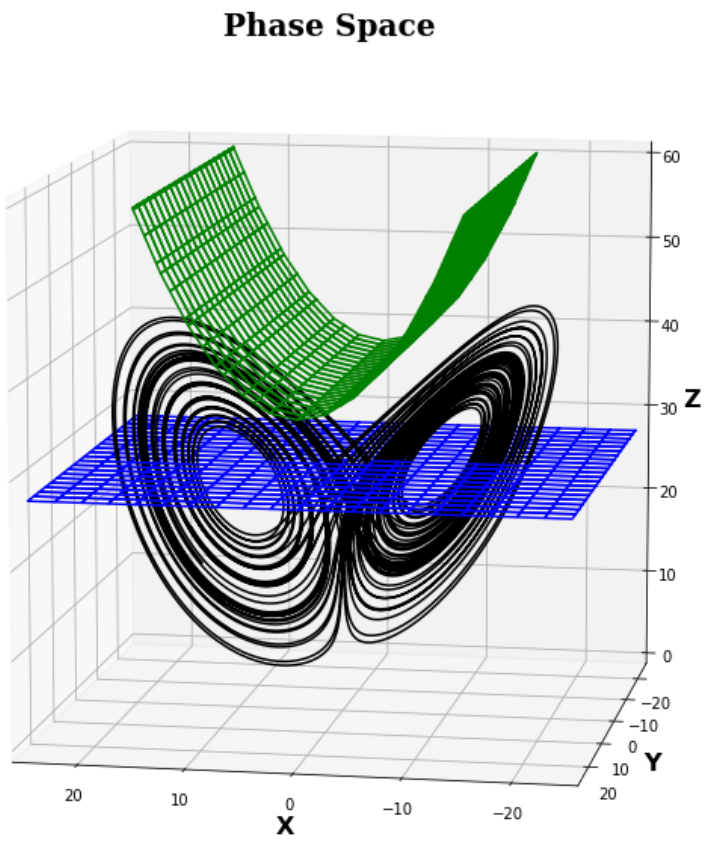

Figure 19: *The visualization of the intersection set G_{xy} (an empty set), the intersection set G_{xz} (in green), and the intersection set G_{yz} (in blue). The surfaces were approximated using an adaptive Marching Cube Algorithm. See Appendix C for coding details.*

VI. Splitting of Functions

This section is devoted to providing a new definition for the splitting of a function. Throughout this paper, we shall refer to domain $D_i^n(\mathbf{v}, r_1, r_2)$, which is the n-dimensional region of space dependent on center $\mathbf{v} \in \mathbb{R}^n$ and radii $r_1, r_2 \in \mathbb{R}_{>0} \cup \{\infty\}$ defined as

$$D_i^n(\mathbf{v}, r_1, r_2) \equiv \left\{ \mathbf{x} \in \mathbb{R}^n : \sum_{j \neq i} (\mathrm{x}_j - \mathrm{v}_j)^2 < r_1^2,\ |\mathrm{x}_i - \mathrm{v}_i| < r_2 \right\} \tag{32}$$

It is important to see that $D_i^n(\mathbf{v}, r_1, r_2)$ is a nonempty set that resembles an open cylinder-like object. In the i-th dimension, $D_i^n(\mathbf{v}, r_1, r_2)$ is restricted between $\mathrm{v}_i - r_2$ and $\mathrm{v}_i + r_2$, while in the other dimensions it is restricted to a $(n-1)$-dimensional ball of radius r_1. If for example n is 3, $D_1^3(\mathbf{v}, r_1, r_2)$, $D_2^3(\mathbf{v}, r_1, r_2)$, and $D_3^3(\mathbf{v}, r_1, r_2)$ are all exactly open cylinders, each with a different axis. As a note of special interest, $D_i^n(\mathbf{v}, \infty, \infty) \equiv \mathbb{R}^n$ for all $\mathbf{v} \in \mathbb{R}^n$. For reading ease, we often denote $D_i^n(\mathbf{v}, r_1, r_2)$ simply as D_i^n since center $\mathbf{v}$ and radii $r_1,\ r_2$ are presumed to be suitably chosen for each situation.

Definition VI.1 (Splitting of a Function)**.** *We now say that for some $\mathbf{v} \in \mathbb{R}^n$ and $r_1, r_2 \in \mathbb{R}_{>0} \cup \{\infty\}$, function $f : D_i^n(\mathbf{v}, r_1, r_2) \to \mathbb{R}$ can be split with respect to the i-th dimension and splitting parameter $c \in (\mathrm{v}_i - r_2, \mathrm{v}_i + r_2)$ if over D_i^n, f can be rewritten as*

$$f(\mathbf{x}) = h(\mathfrak{p}_i(\mathbf{x}); c) - (\mathrm{x}_i - c) g(\mathbf{x}; c) \tag{33}$$

where

- *$i \in \{1, 2, \cdots n\}$;*
- *f is continuous in x_i for all $\mathbf{x} \in D_i^n$;*
- *the subset $\{\mathbf{x} \in D_i^n : \mathrm{x}_i = c\}$ is not empty;*
- *h is constant and finite in x_i, given $\mathrm{x}_1, \cdots, \mathrm{x}_{i-1}, \mathrm{x}_{i+1}, \cdots, \mathrm{x}_n$;*
- *g is continuous with respect to x_i in $\mathbb{R}$, given $\mathrm{x}_1, \cdots, \mathrm{x}_{i-1}, \mathrm{x}_{i+1}, \cdots, \mathrm{x}_n$*

Here, h is the forcing function and g is the squared frequency function as before.

The necessity of the first requisite in this new definition is obvious: index i refers to a specific dimension in vector $\mathbf{x} \in \mathbb{R}^n$ and therefore must be a natural number between 1 and n. The second requisite is simply to ensure we are dealing with well-behaved functions. The third requisite is to guarantee that forcing function h is well-defined (this will be discussed in greater detail in Section VIII). The fourth requisite is an assumption carried over from previous literature on the subject and involves somewhat abstract oscillatory dynamical system theory. The last requisite from Definition VI.1 is to ensure that the squared frequency functions are well-behaved.

As a result, the following lemma is possibly the simplest lemma in this entire paper, but also arguably the most crucial.

Lemma VI.1. *Say function $f : D_i^n \to \mathbb{R}$ can be split with respect to the i-th dimension and splitting parameter $c \in \mathbb{R}$ into forcing function h and squared frequency function g. Then $h(\mathfrak{p}_i(\mathbf{x}); c) = f(\mathbf{x})|_{\mathrm{x}_i=c}$.*

Proof. Say function $f : D_i^n \to \mathbb{R}$ can be split with respect to the i-th dimension and splitting parameter $c \in \mathbb{R}$ into forcing function h and squared frequency function g. Then for all $\mathbf{x} \in D_i^n$, since g is continuous in x_i,

$$g(\mathbf{x})|_{\mathrm{x}_i=c} = \lim_{\mathrm{x}_i \to c} \left(\frac{h(\mathfrak{p}_i(\mathbf{x}); c) - f(\mathbf{x})}{\mathrm{x}_i - c} \right) \in \mathbb{R}$$

Because of this, $\lim_{\mathrm{x}_i \to c} (h(\mathfrak{p}_i(\mathbf{x}); c) - f(\mathbf{x})) = 0$. Otherwise, $\lim_{\mathrm{x}_i \to c} g(\mathbf{x})$ would surely be infinite or undefined. Thus, we can conclude that, since f is continuous in x_i,

$$0 = \lim_{\mathrm{x}_i \to c} (h(\mathfrak{p}_i(\mathbf{x}); c) - f(\mathbf{x})) = h(\mathfrak{p}_i(\mathbf{x}); c) - \lim_{\mathrm{x}_i \to c} f(\mathbf{x}) = h(\mathfrak{p}_i(\mathbf{x}); c) - f(\mathbf{x})|_{\mathrm{x}_i=c}$$

□

This lemma is important, as it symbolizes the ideology behind Definition VI.1. Our research started by trying to rigorously define the forcing function h, and then defining the squared frequency function g as a direct result. The realization came that in multipolynomial systems, Lemma VI.1 was always true. In fact, it seemed that previous literature had specifically defined h so that the lemma would always hold for $c = 0$ [4][5][6], [9][14][37]. We decided to expand this idea to general continuous functions and build the rest of our theory on this principle.

Lemma VI.2 (Uniqueness Lemma)**.** *Say function $f : D_i^n \to \mathbb{R}$ can be split with respect to the i-th dimension and splitting parameter $c \in \mathbb{R}$ into forcing function h and squared frequency function g. Then h and g are uniquely defined over D_i^n.*

Proof. Say function $f : D_i^n \to \mathbb{R}$ can be split with respect to the i-th dimension and splitting parameter $c \in \mathbb{R}$ into forcing function h_1 and squared frequency function g_1, and also into forcing function h_2 and squared frequency function g_2. Then for all $\mathbf{x} \in D_i^n$,

$$f(\mathbf{x}) = h_1(\mathfrak{p}_i(\mathbf{x}); c) - (\mathrm{x}_i - c) g_1(\mathbf{x}; c) = h_2(\mathfrak{p}_i(\mathbf{x}); c) - (\mathrm{x}_i - c) g_2(\mathbf{x}; c)$$

Using Lemma VI.1, we can immediately conclude that $h_1 \equiv h_2$ over D_i^n.
As a result, for all $\mathbf{x} \in D_i^n$,

$$(\mathrm{x}_i - c)(g_1(\mathbf{x}; c) - g_2(\mathbf{x}; c)) = h_1(\mathfrak{p}_i(\mathbf{x}); c) - h_2(\mathfrak{p}_i(\mathbf{x}); c) = 0$$

We can conclude for all $\mathbf{x} \in D_i^n$ with $\mathrm{x}_i \neq c$, $g_1(\mathbf{x}; c) = g_2(\mathbf{x}; c)$.
Furthermore, since g_1 and g_2 are both continuous in D_i^n,

$$g_1(\mathbf{x}; c)|_{\mathrm{x}_i=c} = \lim_{\mathrm{x}_i \to c} g_1(\mathbf{x}; c) = \lim_{\mathrm{x}_i \to c} g_2(\mathbf{x}; c) = g_2(\mathbf{x}; c)|_{\mathrm{x}_i=c}$$

Thus, we have proven that $g_1 \equiv g_2$ over D_i^n. □

Lemma VI.3 (Combination Lemma)**.** *Say function $f_1 : D_i^n \to \mathbb{R}$ can be split with respect to the i-th dimension and splitting parameter $c \in \mathbb{R}$ into forcing function h_1 and squared frequency function g_1. Say function $f_2 : D_i^n \to \mathbb{R}$ can be split with respect to the i-th dimension and c into forcing function h_2 and squared frequency function g_2.*

- *For arbitrary $\alpha, \beta \in \mathbb{R}$, the sum $(\alpha f_1 + \beta f_2) : D_i^n \to \mathbb{R}$ can be split with respect to i-th dimension and c into forcing function $(\alpha h_1 + \beta h_2)$ and squared frequency function $(\alpha g_1 + \beta g_2)$.*
- *The product $(f_1 f_2) : D_i^n \to \mathbb{R}$ can be split with respect to the i-th dimension and c into forcing function $(h_1 h_2)$ and squared frequency function $(h_1 g_2 + h_2 g_1 - (\mathrm{x}_i - c) g_1 g_2)$.*
- *The quotient $(f_1/f_2) : D_i^n \to \mathbb{R}$ can be split with respect to the i-th dimension and c into forcing function (h_1/h_2) and squared frequency function $((h_2 g_1 - h_1 g_2)/(h_2 f_2))$, provided both $f_2(\mathbf{x})$ and $h_2(\mathfrak{p}_i(\mathbf{x}))$ are nonzero for all $\mathbf{x} \in D_i^n$ and for c*

Proof. Say function $f_1 : D_i^n \to \mathbb{R}$ can be split with respect to i-th dimension and c into forcing function h_1 and squared frequency function g_1. Then for all $\mathbf{x} \in D_i^n$,

$$f_1(\mathbf{x}) = h_1(\mathfrak{p}_i(\mathbf{x}); c) - (\mathrm{x}_i - c) g_1(\mathbf{x}; c)$$

Say function $f_2 : D_i^n \to \mathbb{R}$ can also be split with respect to i-th dimension and c into forcing function h_2 and squared frequency function g_2. Then for all $\mathbf{x} \in D_i^n$,

$$f_2(\mathbf{x}) = h_2(\mathfrak{p}_i(\mathbf{x}); c) - (\mathrm{x}_i - c) g_2(\mathbf{x}; c)$$

Notice that since both f_1 and f_2 are splittable in D_i^n, $i \in \{1, 2, \cdots n\}$ and the subset $\{\mathbf{x} \in D_i^n : \mathrm{x}_i = c\}$ is not empty.

Take $\alpha, \beta \in \mathbb{R}$ arbitrarily. Then

$$\begin{aligned} \alpha f_1(\mathbf{x}) + \beta f_2(\mathbf{x}) &= \alpha\big(h_1(\mathfrak{p}_i(\mathbf{x}); c) - (\mathrm{x}_i - c) g_1(\mathbf{x}; c)\big) + \beta\big(h_2(\mathfrak{p}_i(\mathbf{x}); c) - (\mathrm{x}_i - c) g_2(\mathbf{x}; c)\big) \\ &= \big(\alpha h_1(\mathfrak{p}_i(\mathbf{x}); c) + \beta h_2(\mathfrak{p}_i(\mathbf{x}); c)\big) - (\mathrm{x}_i - c)\big(\alpha g_1(\mathbf{x}; c) + \beta g_2(\mathbf{x}; c)\big) \end{aligned}$$

Notice that

- the linear combination $\alpha f_1 + \beta f_2$ is continuous over D_i^n in x_i since f_1 and f_2 are continuous over D_i^n in x_i;
- the linear combination $\alpha h_1 + \beta h_2$ is constant and finite over D_i^n in x_i since h_1 and h_2 are constant and finite over D_i^n in x_i;
- the linear combination $\alpha g_1 + \beta g_2$ is continuous over D_i^n in x_i since g_1 and g_2 are continuous over D_i^n in x_i

Thus we constructed the splitting of $(\alpha f_1 + \beta f_2)$ with respect to the i-th dimension and splitting parameter c.

We can also split the product of f_1 and f_2.

$$\begin{aligned} f_1(\mathbf{x})f_2(\mathbf{x}) &= \big(h_1(\mathfrak{p}_i(\mathbf{x});c) - (\mathrm{x}_i - c)g_1(\mathbf{x};c)\big)\big(h_2(\mathfrak{p}_i(\mathbf{x});c) - (\mathrm{x}_i - c)g_2(\mathbf{x};c)\big) \\ &= h_1(\mathfrak{p}_i(\mathbf{x});c)h_2(\mathfrak{p}_i(\mathbf{x});c) - (\mathrm{x}_i - c)\big(h_1(\mathfrak{p}_i(\mathbf{x});c)g_2(\mathbf{x};c) + h_2(\mathfrak{p}_i(\mathbf{x});c)g_1(\mathbf{x};c)\big) \\ &\qquad + (\mathrm{x}_i - c)^2 g_1(\mathbf{x};c)g_2(\mathbf{x};c) \end{aligned}$$

Notice that

- the product $f_1 f_2$ is continuous over D_i^n in x_i since f_1 and f_2 are continuous over D_i^n in x_i;
- the product $h_1 h_2$ is constant and finite over D_i^n in x_i since h_1 and h_2 are constant and finite over D_i^n in x_i;
- the function $h_1 g_2 + h_2 g_1 - (\mathrm{x}_i - c)g_1 g_2$ is continuous over D_i^n in x_i since g_1 and g_2 are continuous and h_1 and h_2 are constant and finite over D_i^n in x_i

Thus we constructed the splitting of $f_1 f_2$ with respect to the i-th dimension and splitting parameter c.

We can also split the quotient of f_1 and f_2, provided $h_2(\mathfrak{p}_i(\mathbf{x});c) \neq 0$ and $f_2(\mathbf{x}) \neq 0$ for all $\mathbf{x} \in D_i^n$ and for c.

$$\begin{aligned} \frac{f_1(\mathbf{x})}{f_2(\mathbf{x})} &= \frac{h_1(\mathfrak{p}_i(\mathbf{x});c) - (\mathrm{x}_i - c)g_1(\mathbf{x};c)}{f_2(\mathbf{x})} \\ &= \frac{h_2(\mathfrak{p}_i(\mathbf{x});c)\big(h_1(\mathfrak{p}_i(\mathbf{x});c) - (\mathrm{x}_i - c)g_1(\mathbf{x};c)\big)}{h_2(\mathfrak{p}_i(\mathbf{x});c)f_2(\mathbf{x})} \\ &\qquad + \frac{(\mathrm{x}_i - c)h_1(\mathfrak{p}_i(\mathbf{x});c)g_2(\mathbf{x};c) - (\mathrm{x}_i - c)h_1(\mathfrak{p}_i(\mathbf{x});c)g_2(\mathbf{x};c)}{h_2(\mathfrak{p}_i(\mathbf{x});c)f_2(\mathbf{x})} \\ &= \left(\frac{h_1(\mathfrak{p}_i(\mathbf{x});c)}{h_2(\mathfrak{p}_i(\mathbf{x});c)}\right) - (\mathrm{x}_i - c)\left(\frac{h_2(\mathfrak{p}_i(\mathbf{x});c)g_1(\mathbf{x};c) - h_1(\mathfrak{p}_i(\mathbf{x});c)g_2(\mathbf{x};c)}{h_2(\mathfrak{p}_i(\mathbf{x});c)f_2(\mathbf{x})}\right) \end{aligned}$$

Notice that

- the quotient f_1/f_2 is continuous over D_i^n in x_i since f_1 and f_2 are continuous over D_i^n in x_i, and $f_2(\mathbf{x}) \neq 0$ for all $\mathbf{x} \in D_i^n$ and for c;
- the quotient h_1/h_2 is constant and finite over D_i^n in x_i since h_1 and h_2 are constant and finite over D_i^n in x_i, and $h_2(\mathfrak{p}_i(\mathbf{x});c) \neq 0$ for all $\mathbf{x} \in D_i^n$ and for c;
- the function $(h_2 g_1 - h_1 g_2)\,/\,(h_2 f_2)$ is continuous over D_i^n in x_i since g_1 and g_2 are continuous over D_i^n in x_i, h_1 and h_2 are constant and finite over D_i^n in x_i, and $h_2(\mathfrak{p}_i(\mathbf{x});c)$, $f_2(\mathbf{x}) \neq 0$ for all $\mathbf{x} \in D_i^n$ and for c

Thus we have constructed the splitting of f_1/f_2 with respect to the i-th dimension and splitting parameter c. □

Using Lemma VI.3, functions that may seem difficult to split can be broken into smaller constituent pieces. As a result, the Competitive Modes Conjecture can analyze systems of differential equations using a "divide-and-conquer" methodology on each of the competitive modes.

The question still remains: when is a function splittable? When does the splitting of a function according to Definition VI.1 exist? The following theorem is perhaps the most useful theorem concerning these questions.

Theorem VI.4 (Splittings for Differentiable Functions)**.** *Say function $f : D_i^n \to \mathbb{R}$ is differentiable over D_i^n with respect to the ith dimension. If for parameter $c \in \mathbb{R}$ the partial derivative $\partial f/\partial \mathrm{x}_i$ is continuous over some open neighborhood of $\{\mathbf{x} \in D_i^n : \mathrm{x}_i = c\}$ with respect to x_i, then f can be split with respect to the i-th dimension and splitting parameter c into forcing function h and squared frequency function g, defined as*

$$h(\mathfrak{p}_i(\mathbf{x}); c) = f(\mathbf{x})|_{\mathrm{x}_i=c}$$

$$g(\mathbf{x}; c) = \begin{cases} \dfrac{f(\mathbf{x})|_{\mathrm{x}_i=c} - f(\mathbf{x})}{\mathrm{x}_i - c} & \mathrm{x}_i \neq c \\ -\dfrac{\partial f(\mathbf{x})}{\partial \mathrm{x}_i}\Big|_{\mathrm{x}_i=c} & \mathrm{x}_i = c \end{cases}$$

Proof. Say function $f : D_i^n \to \mathbb{R}$ is differentiable over D_i^n with respect to x_i. Notice that by definition, f must be continuous over D_i^n with respect to x_i. Furthermore, let us define functions h and g as above.

We can see immediately that h is constant with respect to x_i. Furthermore, since f is continuous over D_i^n with respect to x_i, h is finite with respect to x_i given $\mathrm{x}_1, ...\mathrm{x}_{i-1}, \mathrm{x}_{i+1}, ...\mathrm{x}_n$ and c.

Investigating the properties of g takes a bit more work. Let us take $\mathrm{x}_i \neq c$, then g is continuous over D_i^n in x_i since f is continuous over D_i^n in x_i.

Let us take $\mathrm{x}_i = c$, then we can conclude the following, using L'Hopital's Theorem and the prerequisite that the partial derivative $\partial f/\partial \mathrm{x}_i$ must be continuous over some open neighborhood of $\{\mathbf{x} \in D_i^n : \mathrm{x}_i = \mathrm{c_i}\}$ with respect to x_i.

$$\begin{aligned} \lim_{\mathrm{x}_i \to c} g(\mathbf{x}; c) &= \lim_{\mathrm{x}_i \to c} \left(\frac{f(\mathbf{x})|_{\mathrm{x}_i=c} - f(\mathbf{x})}{\mathrm{x}_i - c} \right) \\ &= -\lim_{\mathrm{x}_i \to c} \frac{\partial f(\mathbf{x})}{\partial \mathrm{x}_i} \\ &= -\frac{\partial f(\mathbf{x})}{\partial \mathrm{x}_i}\Big|_{\mathrm{x}_i=c} \\ &= g(\mathbf{x}; c)|_{\mathrm{x}_i=c} \in \mathbb{R} \end{aligned}$$

Thus, we have proven that g is continuous in D_i^n with respect to x_i.

Finally, we must prove that

$$h(\mathfrak{p}_i(\mathbf{x})) - (\mathrm{x}_i - c)g(\mathbf{x}) = f(\mathbf{x}) \ \forall \mathbf{x} \in D_i^n$$

Take $\mathbf{x} \in D_i^n$ arbitrarily. We then have to consider two mutually exclusive cases.
Say $\mathrm{x}_i \neq c$. Then

$$\begin{aligned} h(\mathfrak{p}_i(\mathbf{x}); c) - (\mathrm{x}_i - c)g(\mathbf{x}; c) &= f(\mathbf{x})|_{\mathrm{x}_i=c} - (\mathrm{x}_i - c)\left(\frac{f(\mathbf{x})|_{\mathrm{x}_i=c} - f(\mathbf{x})}{\mathrm{x}_i - c}\right) \\ &= f(\mathbf{x})|_{\mathrm{x}_i=c} - \big(f(\mathbf{x})|_{\mathrm{x}_i=c} - f(\mathbf{x})\big) \\ &= f(\mathbf{x}) \end{aligned}$$

Say instead $\mathrm{x}_i = c$. Then we know that $(\mathrm{x}_i - c)g(\mathbf{x}; c)|_{\mathrm{x}_i=c} = 0$ since $g(\mathbf{x}; c)|_{\mathrm{x}_i=c}$ is continuous and therefore finite in D_i^n with respect to x_i. Thus

$$\begin{aligned} h(\mathfrak{p}_i(\mathbf{x})) - (\mathrm{x}_i - c)g(\mathbf{x}; c) &= f(\mathbf{x})|_{\mathrm{x}_i=c} - 0 \\ &= f(\mathbf{x}) \end{aligned}$$

Thus, for any $\mathbf{x} \in D_i^n$, $h(\mathfrak{p}_i(\mathbf{x}); c) - (\mathrm{x}_i - c)g(\mathbf{x}; c) = f(\mathbf{x})$. Therefore, f can be split with respect to the i-th dimension and splitting parameter c into forcing function h is the forcing function and the squared frequency function g. □

The following corollary connects Definition V.1 to Definition VI.1.

Corollary VI.5 (Splitting of a Polynomial)**.** *Say function $f : D_i^n \to \mathbb{R}$ is a polynomial of degree m with respect to x_i. Then f can be defined as*

$$f(\mathbf{x}) = \sum_{j=0}^{m} A_j(\mathfrak{p}_i(\mathbf{x}))\mathrm{x}_i^j$$

where $A_1, A_2, \cdots A_n : \mathbb{R}^{n-1} \to \mathbb{R}$ are the coefficient functions of f. Function f can then be split with respect to the i-th dimension and splitting parameter $c = 0$ into forcing function h and squared frequency function g, defined as

$$\begin{aligned} h(\mathfrak{p}_i(\mathbf{x}); 0) &= A_0(\mathfrak{p}_i(\mathbf{x})) \\ g(\mathbf{x}; 0) &= -\sum_{j=1}^{m} A_j(\mathfrak{p}_i(\mathbf{x}))\mathrm{x}_i^{j-1} \end{aligned}$$

Proof. Function $f : D_i^n \to \mathbb{R}$ can be defined as

$$f(\mathbf{x}) = \sum_{j=0}^{m} A_j(\mathfrak{p}_i(\mathbf{x}))\mathrm{x}_i^j$$

where $A_1, A_2, \cdots A_n : \mathbb{R}^{n-1} \to \mathbb{R}$ are the coefficient functions of f.

Via Theorem VI.4, f can be split with respect to the i-th dimension and splitting parameter $c = 0$ into forcing function h and squared frequency function g, defined as

$$h(\mathfrak{p}_i(\mathbf{x}); 0) = f(\mathbf{x})|_{\mathrm{x}_i=0} = A_0(\mathfrak{p}_i(\mathbf{x}))$$

$$g(\mathbf{x}; 0) = \begin{cases} \dfrac{f(\mathbf{x})|_{\mathrm{x}_i=0} - f(\mathbf{x})}{\mathrm{x}_i} & \mathrm{x}_i \neq 0 \\ -\dfrac{\partial f(\mathbf{x})}{\partial \mathrm{x}_i}\Big|_{\mathrm{x}_i=0} & \mathrm{x}_i = 0 \end{cases}$$

Suppose $\mathrm{x}_i \neq 0$.

$$g(\mathbf{x}; 0) = \frac{f(\mathbf{x})|_{\mathrm{x}_i=0} - f(\mathbf{x})}{\mathrm{x}_i} = -\frac{\sum_{j=1}^{m} A_j(\mathfrak{p}_i(\mathbf{x}))\mathrm{x}_i^j}{\mathrm{x}_i} = -\sum_{j=1}^{m} A_j(\mathfrak{p}_i(\mathbf{x}))\mathrm{x}_i^{j-1}$$

Let us say that $\mathrm{x}_i = 0$.

$$\begin{aligned} g(\mathbf{x}; 0) &= -\frac{\partial f(\mathbf{x})}{\partial \mathrm{x}_i}\Big|_{\mathrm{x}_i=0} \\ &= -\left(\sum_{j=1}^{m} A_j(\mathfrak{p}_i(\mathbf{x}))j\mathrm{x}_i^{j-1}\right)\Big|_{\mathrm{x}_i=0} \\ &= -A_1(\mathfrak{p}_i(\mathbf{x})) \end{aligned}$$

Thus, the squared frequency function can be simplified to

$$g(\mathbf{x}; 0) = -\sum_{j=1}^{m} A_j(\mathfrak{p}_i(\mathbf{x}))\mathrm{x}_i^{j-1}$$

□

Using this corollary, we can see that the splitting of a multi-polynomial always exists, and that the resulting forcing function and squared frequency function are defined identically to the forcing functions and squared frequency functions defined in previous literature when the splitting parameter is zero. [4][5][6][9][14][37]. As a result, the theory of splittings presented in Definition VI.1 is a direct expansion of Definition V.1.

In fact, due to this expansion, we can use Theorem VI.4 to split a large number of basic mathematical functions, as denoted in Table 1. Obviously, each function is defined only over its respective domain. Furthermore, because of Lemma VI.3, we can split combinations of these basic functions, expanding our knowledge even further.

	$f(\mathbf{x})$	$h(\mathfrak{p}_i(\mathbf{x}); c)$	$g(\mathbf{x}; c)$	Notes
1	x_i^m	c^m	$-\sum_{j=1}^{m}(c^{m-j}\mathrm{x}_i^{j-1})$	$m > 0$
2	x_i^{-m}	c^{-m}	$\left(\sum_{j=1}^{m}(c^{m-j}\mathrm{x}_i^{j-1})\right)/(c^m\mathrm{x}_i^m)$	$m > 0$; $\mathrm{x}_i, c \neq 0$
3	$\mathrm{x}_i^{a/b}$	$c^{a/b}$	$\begin{cases}\left(c^{a/b} - \mathrm{x}_i^{a/b}\right)/(\mathrm{x}_i - c) & \mathrm{x}_i \neq c \\ -\frac{a}{b}c^{a/b-1} & \mathrm{x}_i = c\end{cases}$	$b > 0$
4	$\sin(\mathrm{x}_i)$	$\sin(c)$	$\begin{cases}(\sin(c) - \sin(\mathrm{x}_i))/(\mathrm{x}_i - c) & \mathrm{x}_i \neq c \\ -\cos(c) & \mathrm{x}_i = c\end{cases}$	
5	$\cos(\mathrm{x}_i)$	$\cos(c)$	$\begin{cases}(\cos(c) - \cos(\mathrm{x}_i))/(\mathrm{x}_i - c) & \mathrm{x}_i \neq c \\ \sin(c) & \mathrm{x}_i = c\end{cases}$	
6	$\tan(\mathrm{x}_i)$	$\tan(c)$	$\begin{cases}(\tan(c) - \tan(\mathrm{x}_i))/(\mathrm{x}_i - c) & \mathrm{x}_i \neq c \\ -\sec^2(c) & \mathrm{x}_i = c\end{cases}$	$\mathrm{x}_i, c \notin \pi\mathbb{Z} + \frac{\pi}{2}$
7	α^{x_i}	α^c	$\begin{cases}(\alpha^c - \alpha^{\mathrm{x}_i})/(\mathrm{x}_i - c) & \mathrm{x}_i \neq c \\ -\log(\alpha)\alpha^c & \mathrm{x}_i = c\end{cases}$	$\alpha > 0$
8	$\log(\mathrm{x}_i)$	$\log(c)$	$\begin{cases}-\log(\mathrm{x}_i/c)/(\mathrm{x}_i - c) & \mathrm{x}_i \neq c \\ -c^{-1} & \mathrm{x}_i = c\end{cases}$	$\mathrm{x}_i, c > 0$
9	$\sinh(\mathrm{x}_i)$	$\sinh(c)$	$\begin{cases}(\sinh(c) - \sinh(\mathrm{x}_i))/(\mathrm{x}_i - c) & \mathrm{x}_i \neq c \\ -\cosh(c) & \mathrm{x}_i = c\end{cases}$	
10	$\cosh(\mathrm{x}_i)$	$\cosh(c)$	$\begin{cases}(\cosh(c) - \cosh(\mathrm{x}_i))/(\mathrm{x}_i - c) & \mathrm{x}_i \neq c \\ \sinh(c) & \mathrm{x}_i = c\end{cases}$	
11	$\tanh(\mathrm{x}_i)$	$\tanh(c)$	$\begin{cases}(\tanh(c) - \tanh(\mathrm{x}_i))/(\mathrm{x}_i - c) & \mathrm{x}_i \neq c \\ -\operatorname{sech}^2(c) & \mathrm{x}_i = c\end{cases}$	

Table 1: *Basic Functions and their Splittings. Notice that all functions $f : D_i^n \to \mathbb{R}$ are split with respect to the i-th dimension and splitting parameter c*

VII. Examples of Splitting Dynamical Systems

In order to "get a feel" for how to split dynamical systems and they can apply evidence of the validity of the Competitive Modes Conjecture, we revisit the three examples portrayed in Section II.

i. Lorenz Attractor

As described in Equation (4), the Lorenz dynamical system is a multilinear system capable of producing a chaotic attractor for certain values of its parameters. For consistency's sake, the parameters are set to the ever-reoccurring $\sigma = 10$, $\rho = 28$, $\beta = 8/3$.

Let us again apply the Lorenz System to the Competitive Modes Conjecture. This has been done before in previous literature [4][5][6][9][14][37] and in Section V, but we will now apply our new definition, lemmas, and theorems outlined in Section VI. The first step is to differentiate the system in terms of time.

$$\begin{cases} \ddot{x} = -\sigma(\sigma+1)y - \sigma(z-\sigma-\rho)x \\ \ddot{y} = (\sigma+\beta+1)xz - \rho(\sigma+1)x - (x^2+\sigma z - \sigma\rho - 1)y \\ \ddot{z} = \rho x^2 - (\sigma+\beta+1)xy + \sigma y^2 - (x^2-\beta^2)z \end{cases}$$

Then we can calculate the proper partial derivatives as follows.

$$\begin{cases} \partial\ddot{x}/\partial x = \sigma(\sigma+\rho-z) \\ \partial\ddot{y}/\partial y = \sigma\rho + 1 - x^2 - \sigma z \\ \partial\ddot{z}/\partial z = \beta^2 - x^2 \end{cases}$$

Since $\partial\ddot{x}/\partial x$, $\partial\ddot{y}/\partial y$, and $\partial\ddot{z}/\partial z$ are continuous over all of $\mathbb{R}^3$, we can use Theorem VI.4 and Lemma VI.5 to split function $\ddot{x} : D_x^3(\mathbf{0}, \infty, \infty) \to \mathbb{R}$ with respect to variable x and splitting parameter c_x, function $\ddot{y} : D_y^3(\mathbf{0}, \infty, \infty) \to \mathbb{R}$ with respect to variable y and splitting parameter c_y, and function $\ddot{z} : D_z^3(\mathbf{0}, \infty, \infty) \to \mathbb{R}$ with respect to variable z and splitting parameter c_z. As a result,

$$\begin{aligned} h_x(y,z;c_x) &= -\sigma(\sigma+1)y - \sigma(z-\sigma-\rho)c_x \\ g_x(x,y,z:c_x) &= \sigma(z-\sigma-\rho) \\ h_y(x,z;c_y) &= (\sigma+\beta+1)xz - \rho(\sigma+1)x - (x^2+\sigma z-\sigma\rho-1)c_y \\ g_y(x,y,z:c_y) &= x^2+\sigma z-\sigma\rho-1 \\ h_z(x,y;c_z) &= \rho x^2 - (\sigma+\beta+1)xy + \sigma y^2 - (x^2-\beta^2)c_z \\ g_z(x,y,z:c_z) &= x^2-\beta^2 \end{aligned} \tag{34}$$

Proving the first, third, and fourth necessary conditions of the Competitive Modes Conjecture (Conjecture V.1) are trivial for this example. The difficulty in proving the second

necessary condition: that at least two of the competitive modes compete.

So far so good. Notice that g_x, g_y, and g_z do not depend on splitting parameters c_x, c_y, and c_z at all. Therefore, the intersection surfaces G_{xy}, G_{xy}, and G_{xy} (Equation 30 from Section V) are independent of splitting parameter selection. Now the next question is: are there regions in the phase space where the squared frequency functions g_x, g_y, g_z intersect each other?

First off, we set g_x and g_y equal to each other. The result is a simple equation.

$$G_{x,y} \equiv \{(x, y, z) \in \mathbb{R}^3 : x = \pm\sqrt{1 - \sigma^2}\}$$

Of course, when $|\sigma| \geq 1$, this equation has no real solutions. Perhaps something could be said about analyzing the complex solutions for this equation, but the authors do not believe this would result in anything useful. As such, since $\sigma = 10$, we conclude that $G_{xy} = \emptyset$ and thus g_x and g_y do not intersect in the phase space.

Next, we analyze the intersection between g_x and g_z. The resulting equation is slightly more complicated than the previous.

$$G_{xz} \equiv \{(x, y, z) \in \mathbb{R}^3 : \sigma z = x^2 + \sigma(\sigma + \rho) - \beta^2\} \tag{35}$$

Solutions to this equation describe a real surface. Later sections will prove that this surface is a 2-dimensional manifold (see Section IX and Lemma IX.1), but the important detail is that the surface is path-continuous and 2-dimensional in the 3-dimensional phase space.

Finally, the intersection between g_y and g_z results in the equation

$$G_{yz} = \{(x, y, z) \in \mathbb{R}^3 : \sigma z = \sigma\rho + 1 - \beta^2\} \tag{36}$$

Again, this equation describes a real, path-continuous, 2-dimensional surface in the 3-dimensional phase space. Both this surface and the one previously described are portrayed in Figure 20, along with the Lorenz Attractor. Notice that the attractor does in fact intersect at least one of these surfaces, indicating that at least two of the competitive modes could compete on a regular basis.

To prove the additional requirement that these squared frequency functions intersect positively, we take a single trajectory in the strange attractor and calculate the squared frequency functions of the Lorenz System over this trajectory, like Figure 18 in Section V. For emphasis and the reader's convenience, here we give that figure again in Figure 21. As one can see, most if not all intersections between each of the three g functions happens when these g functions take on positive values, thus proving that at least two of the competitive modes do compete.

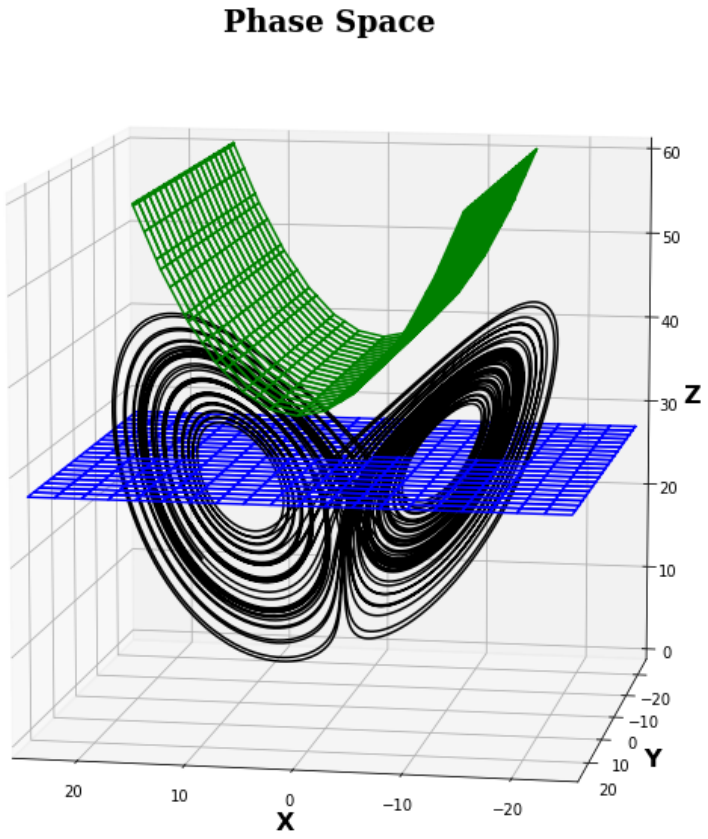

Figure 20: *The Lorenz Attractor along with the surfaces G_{xz} described in Equation* (35) *(in green) and G_{yz} in Equation* (36) *(in blue). The surfaces were approximated using an adaptive Marching Cube Algorithm. See Appendix C for coding details.*

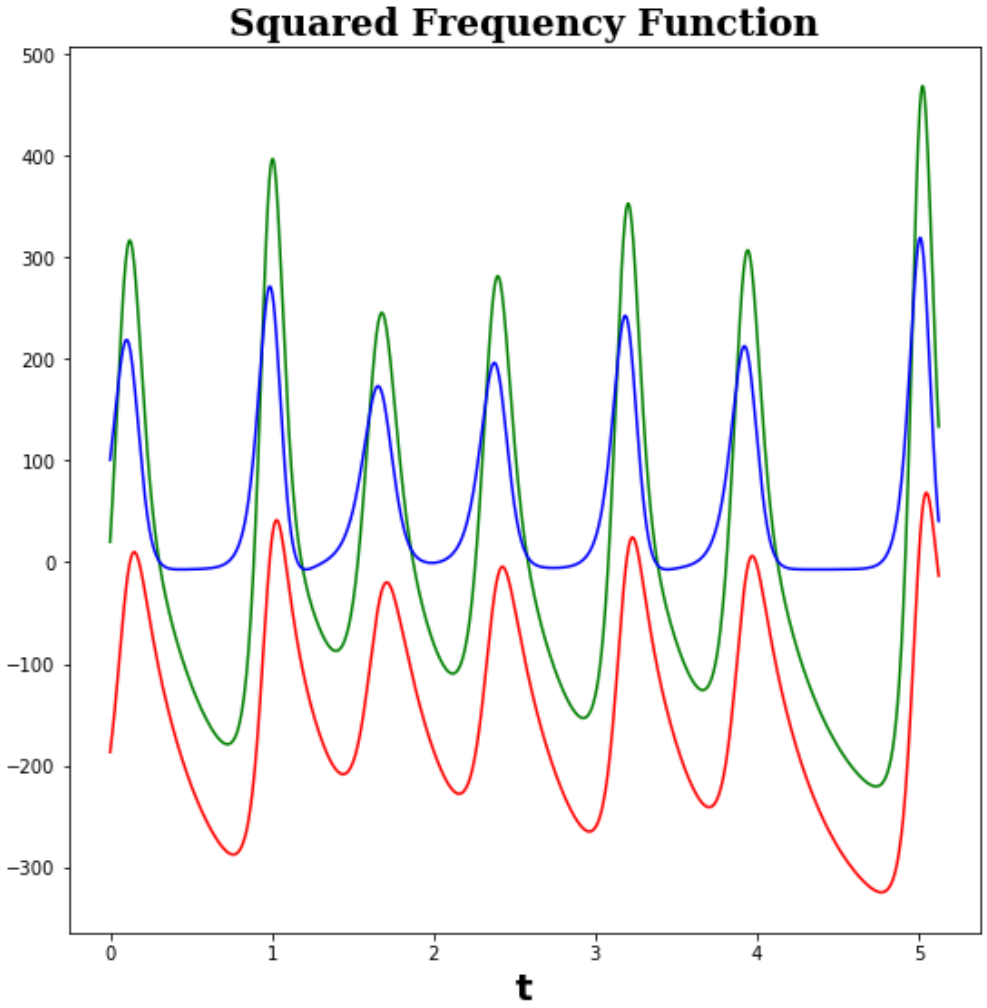

Figure 21: *The squared frequency functions g_x (in red), g_y (in green), and g_z (in blue) applied to a random trajectory in the Lorenz Attractor, where $\sigma = 10$, $\rho = 28$, and $\beta = 8/3$. The splitting parameters inn this situation are $c_x, c_y, c_z = 0$. Notice that g_y and g_z intersect on a regular basis, and that all intersections occur when g_y and g_z take on positive values. This means that the Lorenz Attractor consistently intersects the intersection set G_{yz}^{+} as defined in Equation 31 from Section V.*

In conclusion, the Competitive Modes Conjecture again accurately predicts the properties of the chaotic Lorenz Attractor, thereby providing further evidence that the conjecture may indeed be correct and the formulation of Definition VI.1 is a valid, mathematically rigorous expansion of Definition V.1.

ii. Chua Attractors

The Chua System, already described in Equation (6), is a little different from the Lorenz System in that $\dot{x}$ can not be differentiated with respect to time. This is because function f (defined in Equation (7)) is not differentiable in $x = \pm 1$ if $m_0 \neq m_1$. For this, we will need to introduce a differentiable approximation of f.

For now, let us say $f_{appr} : \mathbb{R} \to \mathbb{R}$ is a $\mathcal{C}^2(x)$ approximation of f. Then the adjusted Chua System as detailed in Equation (6) can be differentiated with respect to time as follows.

$$\begin{cases} \ddot{x} = \alpha(x - y + z) - \alpha^2(y - x - f_{appr}(x))(1 + f'_{appr}(x)) \\ \ddot{y} = -(1 + \alpha)x + (\alpha - \beta + 1)y - z - \alpha f_{appr}(x) \\ \ddot{z} = -\beta(x - y + z) \end{cases}$$

Then we can calculate the proper partial derivatives as follows.

$$\begin{cases} \partial\ddot{x}/\partial x = \alpha - \alpha^2(y - x - f_{appr}(x))f''_{appr}(x) + \alpha^2(1 + f'_{appr}(x))^2 \\ \partial\ddot{y}/\partial y = \alpha - \beta + 1 \\ \partial\ddot{z}/\partial z = -\beta \end{cases}$$

Since $\partial\ddot{x}/\partial x$, $\partial\ddot{y}/\partial y$, and $\partial\ddot{z}/\partial z$ are continuous over all of $\mathbb{R}^3$, we can use Theorem VI.4 and Lemma VI.5 to split the function $\ddot{x} : D^3_x(\mathbf{0}, \infty, \infty) \to \mathbb{R}$ with respect to variable x and splitting parameter c_x, $\ddot{y} : D^3_y(\mathbf{0}, \infty, \infty) \to \mathbb{R}$ with respect to variable y and splitting parameter c_y, and $\ddot{z} : D^3_z(\mathbf{0}, \infty, \infty) \to \mathbb{R}$ with respect to variable z and splitting parameter c_z.

$$\begin{aligned} h_x(y, z; c_x) &= \alpha(c_x - y + z) - \alpha^2(y - c_x - f_{appr}(c_x))(1 + f'_{appr}(c_x)) \\ g_x(x, y, z : c_x) &= \begin{cases} -\alpha(1 + \alpha) - \alpha^2 \left(\dfrac{f_{appr}(x) - f_{appr}(c_x)}{x - c_x} \right) \\ \quad +\alpha^2 \left(\dfrac{(y - x - f_{appr}(x))f'_{appr}(x) - (y - c_x - f_{appr}(c_x))f'_{appr}(c_x))}{x - c_x} \right) & x \neq c_x \\ -\alpha - \alpha^2(1 + f'_{appr}(c_x))^2 + \alpha^2(y - c_x - f_{appr}(c_x))f''_{appr}(c_x) & x = c_x \end{cases} \\ h_y(x, z; c_y) &= -(1 + \alpha)x + (\alpha - \beta + 1)c_y - z - \alpha f_{appr}(x) \\ g_y(x, y, z : c_y) &= \beta - \alpha - 1 \\ h_z(x, y; c_z) &= -\beta(x - y + c_z) \\ g_z(x, y, z : c_z) &= \beta \end{aligned} \tag{37}$$

Proving the first, third, and fourth necessary conditions of the Competitive Modes Conjecture (Conjecture V.1) are trivial for this example. The difficulty in proving the second

necessary condition: that at least two of the competitive modes compete.

Now we ask the same question as before: are there regions in the phase space where the squared frequency functions g_x, g_y, and g_z intersect each other?

Like before, we first set g_x and g_y equal to each other. The result is then split into two cases. When $x \neq c_x$, then

$$\begin{aligned}\alpha^2(f'_{appr}(x) - f'_{appr}(c_x))y =&(\alpha^2+\beta-1)(x-c_x) + \alpha^2(f_{appr}(x) - f_{appr}(c_x)) \\ &+ \alpha^2(x + f_{appr}(x))f'_{appr}(x) - \alpha^2(c_x + f_{appr}(c_x))f'_{appr}(c_x)\end{aligned} \tag{38}$$

and when $x = c_x$, then

$$\alpha^2 f''_{appr}(c_x)y = \beta - 1 + \alpha^2(c_x + f_{appr}(c_x))f''_{appr}(c_x) + \alpha^2(1 + f'_{appr}(c_x))^2 \tag{39}$$

As such, the intersection g_x and g_y describes a 2-dimensional real surface in the 3-dimensional phase space, which we call G_{xy}. The continuity of this surface depends on f_{appr}, f'_{appr}, and f''_{appr}, specifically when $x = c_x$.

Next, we set g_x and g_z equal to each other, the result again being split into two situations. When $x \neq c_x$, then

$$\begin{aligned}\alpha^2(f'_{appr}(x) - f'_{appr}(c_x))y =&(\alpha^2+\alpha+\beta)(x-c_x) + \alpha^2(f_{appr}(x) - f_{appr}(c_x)) \\ &+ \alpha^2(x + f_{appr}(x))f'_{appr}(x) - \alpha^2(c_x + f_{appr}(c_x))f'_{appr}(c_x)\end{aligned} \tag{40}$$

and when $x = c_x$, then

$$\alpha^2 f''_{appr}(c_x)y = \alpha + \beta + \alpha^2(c_x + f_{appr}(c_x))f''_{appr}(c_x) + \alpha^2(1 + f'_{appr}(c_x))^2 \tag{41}$$

As a result, the intersection between g_x and g_z describes a 2-dimensional real surface in the 3-dimensional phase space, which we call G_{xz}. Again, the continuity of this surface depends on f_{appr}, f'_{appr}, and f''_{appr}, specifically when $x = c_x$.

And finally, we set g_y and g_z equal to each other, resulting in the simple requisite

$$\alpha = 1$$

Generally, α will not meet this requisite. As a result, generally there is no intersection of g_y and g_z in the phase space and $G_{yz} = \emptyset$.

Before the surfaces described above can be plotted, f_{appr} needs to be properly defined, specifically with the requisite that $f_{appr} \in \mathcal{C}^2(x)$. As such, one option is to define f_{appr} as follows.

$$f_{appr}(x) = \begin{cases} m_1 x + (m_1 - m_0) & x < -2 \\ \dfrac{(m_1-m_0)x^7}{1024} + \dfrac{3(m_0-m_1)x^5}{128} + \dfrac{13(m_1-m_0)x^3}{64} + m_0 x & x \in [-2,2] \\ m_1 x + (m_0 - m_1) & x > 2 \end{cases} \tag{42}$$

This is a $\mathcal{C}^2(x)$ function with first derivative

$$f'_{appr}(x) = \begin{cases} m_1 & x < -2 \\ \dfrac{7(m_1 - m_0)x^6}{1024} + \dfrac{15(m_0 - m_1)x^4}{128} + \dfrac{39(m_1 - m_0)x^2}{64} + m_0 & x \in [-2, 2] \\ m_1 & x > 2 \end{cases} \tag{43}$$

and second derivative

$$f''_{appr}(x) = \begin{cases} 0 & x < -2 \\ \dfrac{21(m_1 - m_0)x^5}{512} + \dfrac{30(m_0 - m_1)x^3}{64} + \dfrac{39(m_1 - m_0)x}{32} & x \in [-2, 2] \\ 0 & x > 2 \end{cases} \tag{44}$$

Notice that (calculations not shown)

$$\forall x \in (-\infty, -2] \cup \{0\} \cup [2, \infty);\ f_{appr}(x) = f(x),\ f'_{appr}(x) = f'(x),\ f''_{appr}(x) = f''(x)$$

Hence, f_{appr} is an excellent approximation of f defined in Equation (7) in Section II.

Now that f_{approx} has been defined, one still needs to confirm that this modification to the Chua System still allows for chaotic attractors to be present. The two hidden attractors from the original system shown in Figure 3 now merge into a single hidden attractor as shown in Figure 22. The Lyapunov Spectrum of this attractor is represented in Figure 23, showing that the maximal Lyapunov Exponent is approximately 0.280920. This attractor is therefore still chaotic.

The intersection surfaces G_{xy} and G_{xz} between the now completely-defined squared frequency functions can now be plotted. It is easier to understand the behavior of these intersections from a top-down aerial view (a projection of the 3-dimensional phase space onto the 2-dimensional $x-y$ plane). This is because Equations (38), (39), (40), and (41) do not include the variable z. The projected intersections are plotted in Figure 24. The splitting parameters in this situation are $c_x, c_y, c_z = 0$.

From Figure 24, we see that the attractor intersects both of the intersection surfaces G_{xy} and G_{xz}. This indicates that at least two of the competitive modes could compete on a regular basis. To prove the additional requirement that these squared frequency functions intersect positively, we take a single trajectory in the strange attractor and calculate the squared frequency functions of the Chua System over this trajectory. The results are given in Figure 25. As one can see, all intersections between each of the three g functions happens when these g functions take on positive values, proving that at least two of the competitive modes do compete on a regular basis.

In conclusion, the Competitive Modes Conjecture again accurately predicts the properties of a chaotic attractor, this time focusing on the hidden Chua Attractor through the new splitting definition (Definition VI.1). This provides evidence that the conjecture may indeed be correct not only for self-excited attractors, but also for hidden attractors.

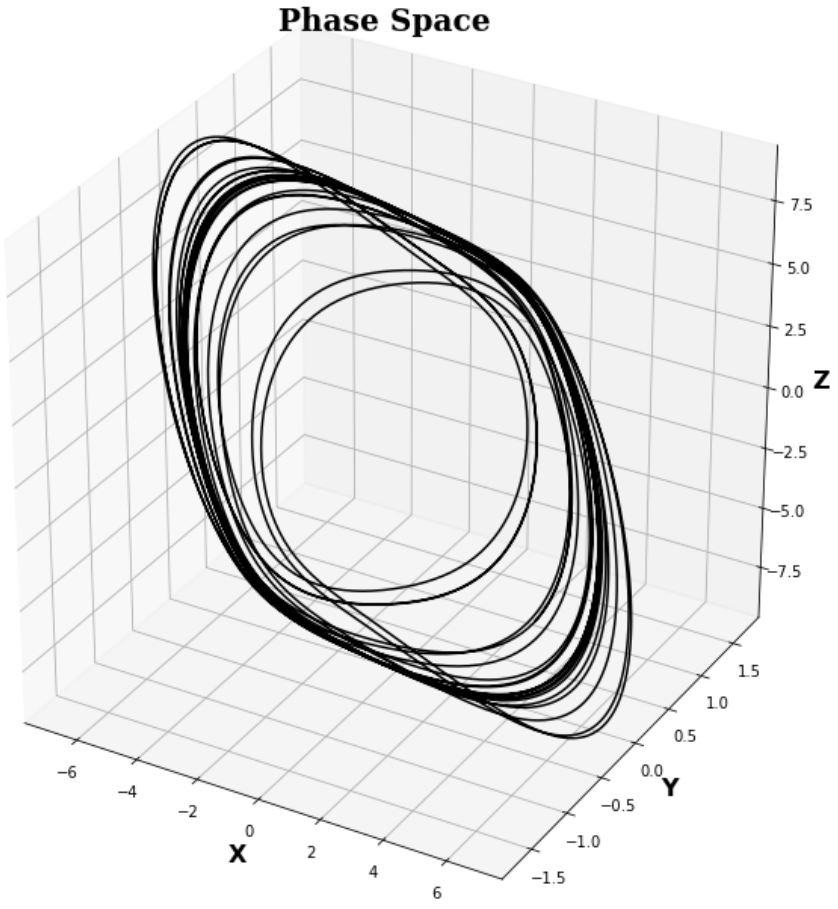

Figure 22: *The modified hidden Chua Attractor, approximating f with f_{appr} as described in Equation* (42)*. Parameter values are $\alpha = 8.4562$, $\beta = 12.08$, $m_0 = -0.1768$, and $m_1 = -1.1468$. The attractor was approximated using an adaptive explicit RK4 numerical integration technique over a time span of 60 time units using an initial position of (-2.617933, -1.635851, 1.751381). See Appendix C for coding details.*

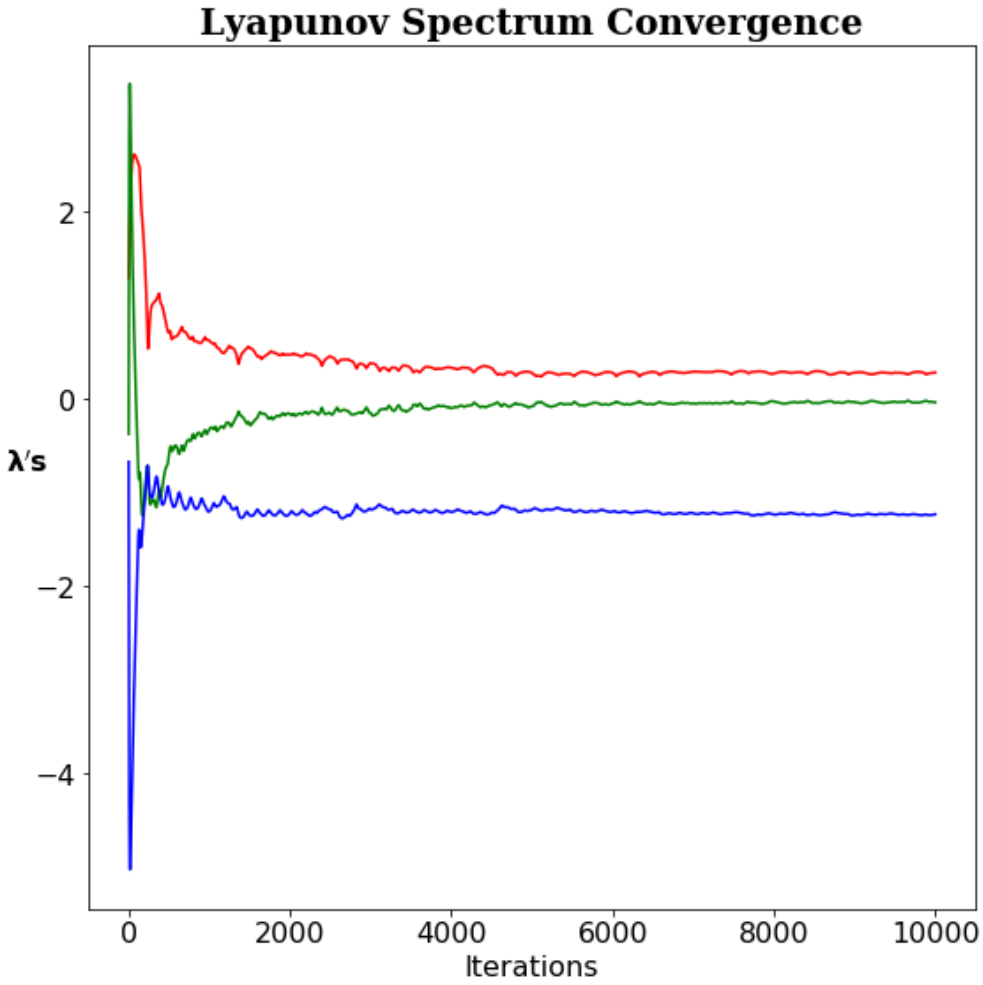

Figure 23: *The convergence of the Lyapunov Spectrum of the modified hidden Chua Attractor, approximating f with f_{appr} as described in Equation* (42)*. According to our calculations, the spectrum is approximately (0.280920, -0.037423, -1.231454). See Appendix C for coding details.*

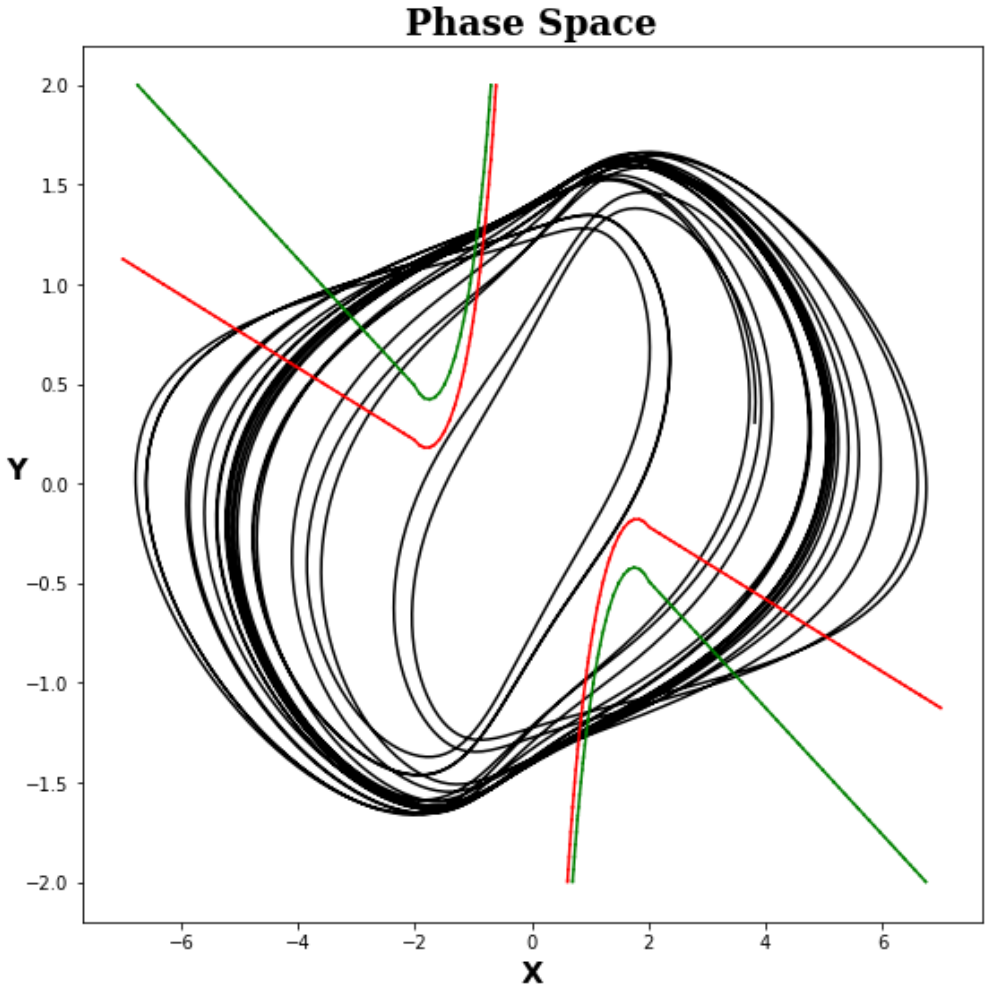

Figure 24: *The modified hidden Chua Attractor, along with the projected intersection surfaces G_{xy} (in red) and G_{xz} (in green). The splitting parameters in this situation are $c_x, c_y, c_z = 0$. The surfaces were approximated using an adaptive Marching Square Algorithm. See Appendix C for coding details.*

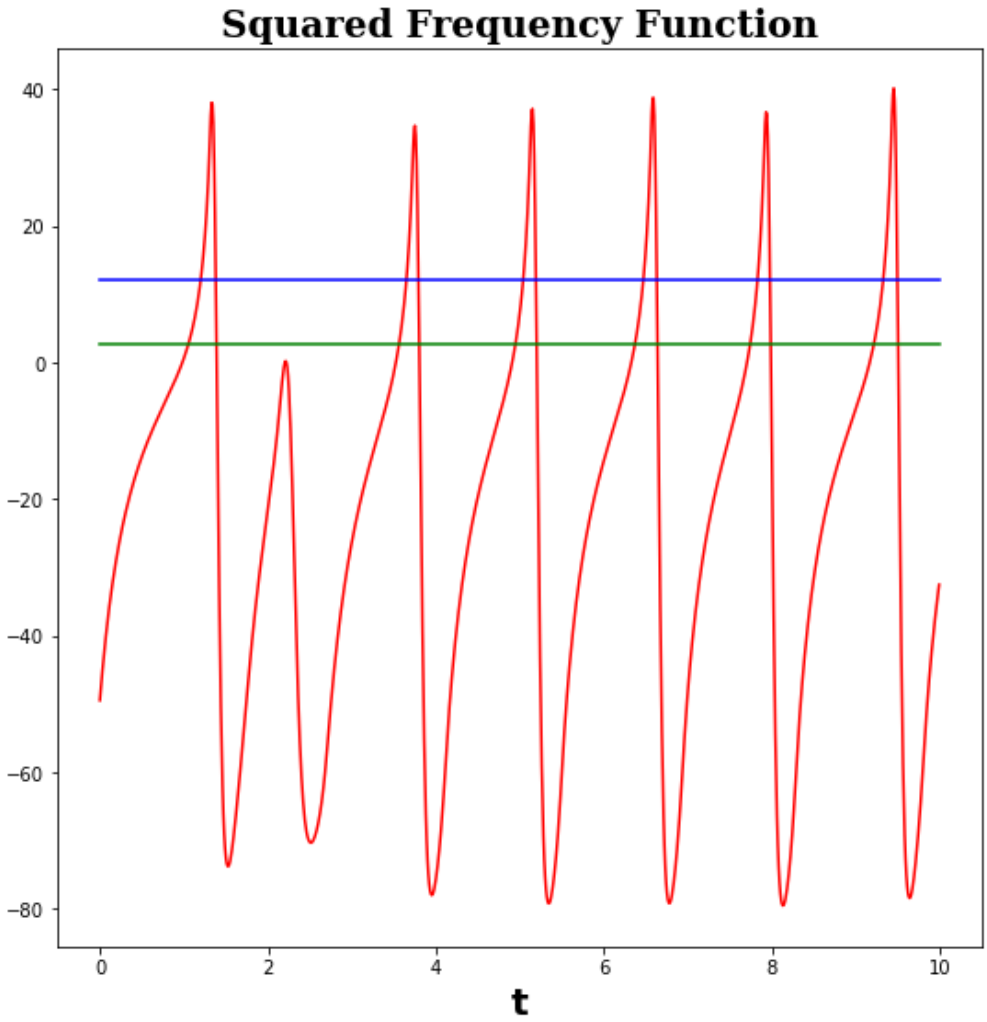

Figure 25: *The squared frequency functions g_x (in red), g_y (in green), and g_z (in blue) applied to a random trajectory in the Chua Attractor, where $\alpha = 8.4562$, $\beta = 12.08$, $m_0 = -0.1768$, and $m_1 = -1.1468$. The splitting parameters in this situation are $c_x, c_y, c_z = 0$. Notice that g_x intersects g_y and g_z on a regular basis, and that all intersections occur when g_x, g_y, and g_z take on positive values. This means that the modified Chua Hidden Attractor consistently intersects the intersection sets G^+_{xy} and G^+_{xz} as defined in Equation 31 from Section V.*

iii. Wimol-Banlue Attractor

Equation (9) from Section II describes the lesser-known Wimol-Banlue Attractor. W. San-Um and B. Srisuchinwong present a simple yet non-multipolynomial and not even differentiable dynamical system able to produce chaotic attractors [29]. Like before, we must first differentiate the system in terms of time, and that will require a differentiable approximation of the absolute value function.

In order to really put Theorem VI.4 to the test, let us introduce a somewhat strange approximation of the absolute value function:

$$\begin{aligned} \phi(y;\beta) &= \frac{1}{\beta}\ln(2\cosh(\beta y)) = \frac{1}{\beta}\ln\left(e^{\beta y}+e^{-\beta y}\right) \\ \phi'(y;\beta) &= \tanh(\beta y) \end{aligned} \tag{45}$$

where $\beta > 0$. The parameter β will allow ϕ to get as close to the absolute value function as possible. To prove this, first notice that ϕ is even in variable y. That is, $\phi(y;\beta) = \phi(-y;\beta)$. This will simplify the analysis considerably.

Let us calculate the difference between $\phi(y;\beta)$ and $|y|$ (calculations not show).

$$\phi(y;\beta) - |y| = \begin{cases} \dfrac{1}{\beta}\ln\left(1+e^{-2\beta y}\right) & y \geq 0 \\ \dfrac{1}{\beta}\ln\left(1+e^{2\beta y}\right) & y < 0 \end{cases}$$

Using this, we can make the following conclusions.

$$\begin{aligned} &\phi(y;\beta) - |y| > 0 \ \forall y \in \mathbb{R} \\ &\lim_{y\to\infty} \phi(y;\beta) - |y| = \frac{1}{\beta}\lim_{y\to\infty} \ln\left(1+e^{-2\beta y}\right) = 0 \\ &\lim_{y\to-\infty} \phi(y;\beta) - |y| = \frac{1}{\beta}\lim_{y\to-\infty} \ln\left(1+e^{2\beta y}\right) = 0 \end{aligned}$$

Moreover, the difference between $\phi(y;\beta)$ and $|y|$ is also almost-everywhere differentiable.

$$\frac{\partial}{\partial y}\Big(\phi(y;\beta) - |y|\Big) = \begin{cases} \dfrac{-2e^{-2\beta y}}{1+e^{-2\beta y}} & y > 0 \\ \dfrac{2e^{2\beta y}}{1+e^{2\beta y}} & y < 0 \end{cases}$$

As a result, the difference $\phi(y;\beta) - |y|$ is strictly decreasing over positive values of y, and strictly increasing over negative values of y. Hence, the following equation is true.

$$\max\left\{\left|\phi(y;\beta) - |y|\right| : y \in \mathbb{R}, \beta > 0\right\} = \phi(0;\beta) - |0| = \ln(2)/\beta$$

Therefore ϕ is a differentiable approximation of the absolute value function, where the quality of the approximation can be determined completely by the parameter β.

Now that the validity of ϕ has been proven, let us modify the original Wimol-Banlue dynamical system to include our approximation.

$$\begin{cases} \dot{x} &= y - x \\ \dot{y} &= -z\tanh(x) \\ \dot{z} &= -\alpha + xy + \frac{1}{\beta}\ln(2\cosh(\beta y)) \end{cases} \tag{46}$$

where $\alpha > 0$ and $\beta = 10$. Just like with our modification of the Chua System, we must first prove that our modified Wimol-Banlue System is still able to produce chaotic attractors. To this end, Figure 26 shows a trajectory through the phase space, highlighting the attractor still being present. Furthermore, analysis of the Lyapunov Spectrum of this attractor in Figure 27 approximates the maximal Lyapunov Exponent at about 0.240112. Thus, this evidence concludes there is still a chaotic attractor present in our modified Wimol-Banlue dynamical system.

Differentiating System (46) with respect to time leads to

$$\begin{cases} \ddot{x} &= x - y - z\tanh(x) \\ \ddot{y} &= \operatorname{sech}^2(x)(x-y)z + \tanh(x)\left(\alpha - xy - \frac{1}{\beta}\ln(2\cosh(\beta y))\right) \\ \ddot{z} &= y^2 - xy - (x + \tanh(\beta y))\tanh(x)z \end{cases}$$

Then we can calculate the proper partial derivatives as follows.

$$\begin{cases} \partial\ddot{x}/\partial x = 1 - z\operatorname{sech}^2(x) \\ \partial\ddot{y}/\partial y = -\operatorname{sech}^2(x)z - \tanh(x)\left(x + \tanh(\beta y)\right) \\ \partial\ddot{z}/\partial z = -(x + \tanh(\beta y))\tanh(x) \end{cases}$$

Since $\partial\ddot{x}/\partial x$, $\partial\ddot{y}/\partial y$, and $\partial\ddot{z}/\partial z$ are continuous over all of $\mathbb{R}^3$, we can use Theorem VI.4 to split $\ddot{x}$, $\ddot{y}$, and $\ddot{z}$ using splitting parameters c_x, c_y, and c_z, respectively.

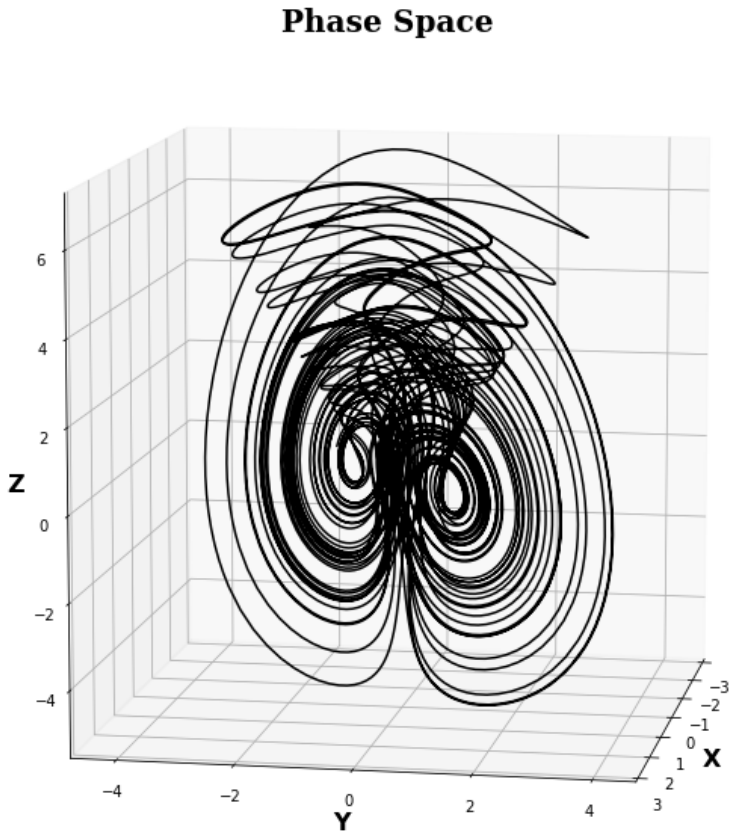

Figure 26: *The Modified Wimol-Banlue Attractor, using a parameter values* $\alpha = 2$ *and* $\beta = 10$*. The attractor was approximated using an adaptive explicit RK4 numerical integration technique over a time span of 250 time units using an initial position of (-1.21739, -1.48448, 0.18485). See Appendix C for coding details.*

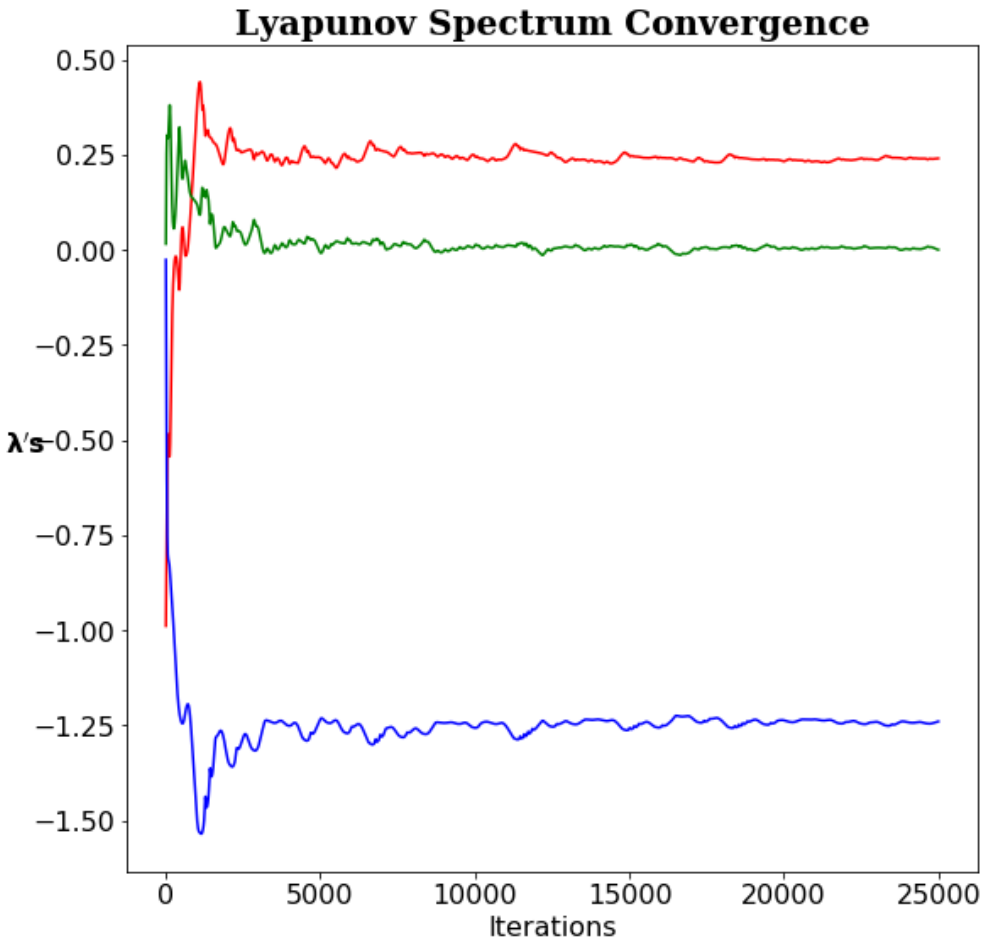

Figure 27: *The convergence of the Lyapunov Spectrum of the modified self-excited Wimol-Banlue Attractor. According to our calculations, the spectrum is approximately (0.240112, 0.000093, -1.240206). See Appendix C for coding details.*

$$
\begin{aligned}
h_x(y,z;c_x) &= c_x - y - z\tanh(c_x) \\
g_x(x,y,z;c_x) &= \begin{cases} -1 + z\left(\dfrac{\tanh(x)-\tanh(c_x)}{x-c_x}\right) & x \neq c_x \\ -1+\operatorname{sech}^2(c_x)z & x = c_x \end{cases} \\
h_y(x,z;c_y) &= \operatorname{sech}^2(x)(x-c_y)z + \tanh(x)\left(\alpha - xc_y - \frac{1}{\beta}\ln(2\cosh(\beta c_y))\right) \\
g_y(x,y,z;c_y) &= \begin{cases} \tanh(x)x + \operatorname{sech}^2(x)z + \dfrac{\tanh(x)}{\beta(y-c_y)}\ln\left(\dfrac{\cosh(\beta y)}{\cosh(\beta c_y)}\right) & y \neq c_y \\ \tanh(x)x + \operatorname{sech}^2(x)z + \tanh(x)\tanh(\beta c_y) & y = c_y \end{cases} \\
h_z(x,y;c_z) &= y^2 - xy - (x+\tanh(\beta y))\tanh(x)c_z \\
g_z(x,y,z;c_z) &= (x+\tanh(\beta y))\tanh(x)
\end{aligned}
\tag{47}
$$

Proving the first, third, and fourth necessary conditions of the Competitive Modes Conjecture (Conjecture V.1) are trivial for this example. The difficulty in proving the second necessary condition: that at least two of the competitive modes compete.

Now, the intersections between each of the squared frequency functions need to be calculated. For simplicity, let us say that splitting parameters c_x, c_y, and c_z are all equal to zero. The resulting intersections are listed below, with the corresponding calculations able to be found in Appendix A.

The solution for $g_x(x,y,z;0) = g_y(x,y,z;0)$ is

$$
z = \begin{cases} \dfrac{x+x^2\tanh(x)}{\tanh(x)-x\operatorname{sech}^2(x)} + \dfrac{x\tanh(x)\ln(\cosh(\beta y))}{\beta\tanh(x)y - \beta x\operatorname{sech}^2(x)y} & x, y \neq 0 \\ \dfrac{x+x^2\tanh(x)}{\tanh(x)-x\operatorname{sech}^2(x)} & x \neq 0, y = 0 \end{cases}
\tag{48}
$$

Notice that no solution is defined for $x = 0$. Thus, the solution is divided into two path-continuous surfaces: one for $x > 0$ and one for $x < 0$. Collectively, we call these surfaces G_{xy}.

The solution for $g_x(x,y,z;0) = g_z(x,y,z;0)$ is

$$
z = \begin{cases} \dfrac{x}{\tanh(x)} + x^2 + x\tanh(\beta y) & x \neq 0 \\ 1 & x = 0 \end{cases}
\tag{49}
$$

Thus, the solution is a path-continuous surface over all $x, y \in \mathbb{R}^2$ which we call G_{xz}.

The solution for $g_y(x, y, z; 0) = g_z(x, y, z; 0)$ is

$$z = \begin{cases} \sinh(x)\cosh(x)\left(\tanh(\beta y) - \dfrac{\ln(\cosh(\beta y))}{\beta y}\right) & y \neq 0 \\ 0 & y = 0 \end{cases} \tag{50}$$

Thus, the solution is a path-continuous surface over all $x, y \in \mathbb{R}^2$ which we call G_{yz}.

Plotting these intersection surfaces results in the Figure 28. Let us focus on just one of

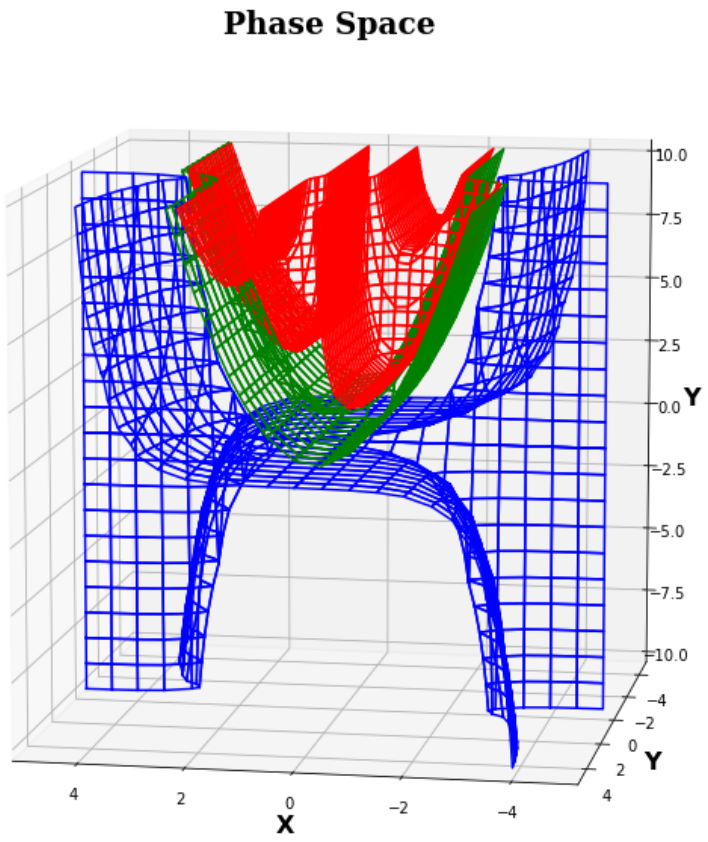

Figure 28: *The intersection surfaces G_{xy} (in red), G_{xz} (in green), and G_{yz} (in blue). The surfaces were approximated using an adaptive Marching Cube Algorithm. See Appendix C for coding details.*

these surfaces, and plot it separately along with the modified Wimol-Banlue Attractor in Figure 29. This shows that the Wimol-Banlue Attractor repeatedly intersects the surface G_{yz} described by Equation (50), indicating at least two of the competitive modes could be

competing.

To prove the additional requirement that these squared frequency functions intersect positively, we take a single trajectory in the strange attractor and calculate the squared frequency functions of the Wimol-Banlue System over this trajectory. The results are given in Figure 30. As one can see, most if not all intersections between each of the three g functions happens when these g functions take on positive values. This proves that at least two of the competitive modes do indeed compete.

This provides even more evidence that the Competitive Modes Conjecture using the splitting defined in Definition VI.1 may indeed be true, not only for multipolynomial dynamical systems but also other systems as well.

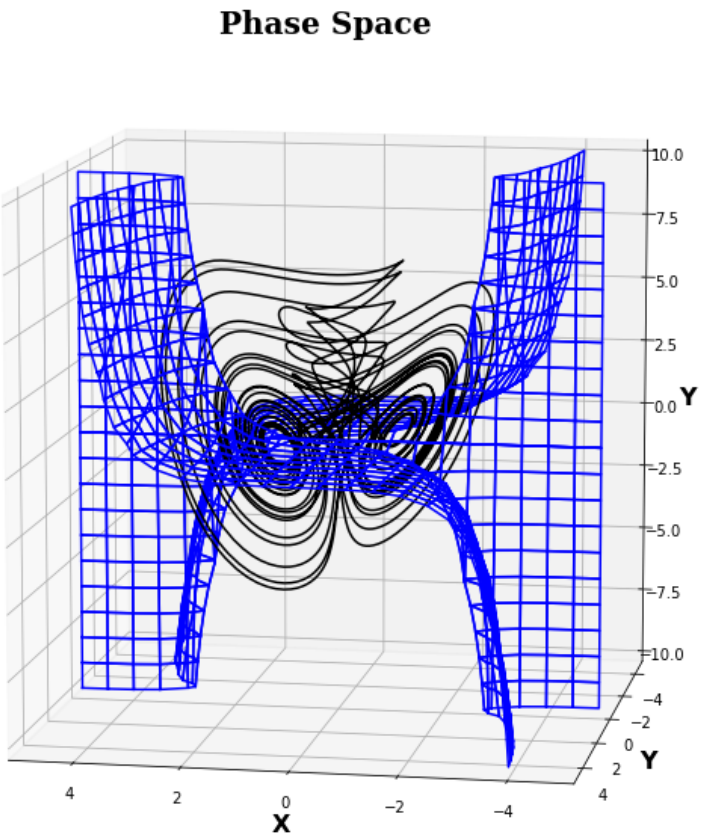

Figure 29: *The modified Wimol-Banlue Attractor (with parameter values $\alpha = 2$ and $\beta = 10$), along with the surface G_{yz} described in Equation* (50) *(in blue). The surface was approximated using an adaptive Marching Cube Algorithm. See Appendix C for coding details.*

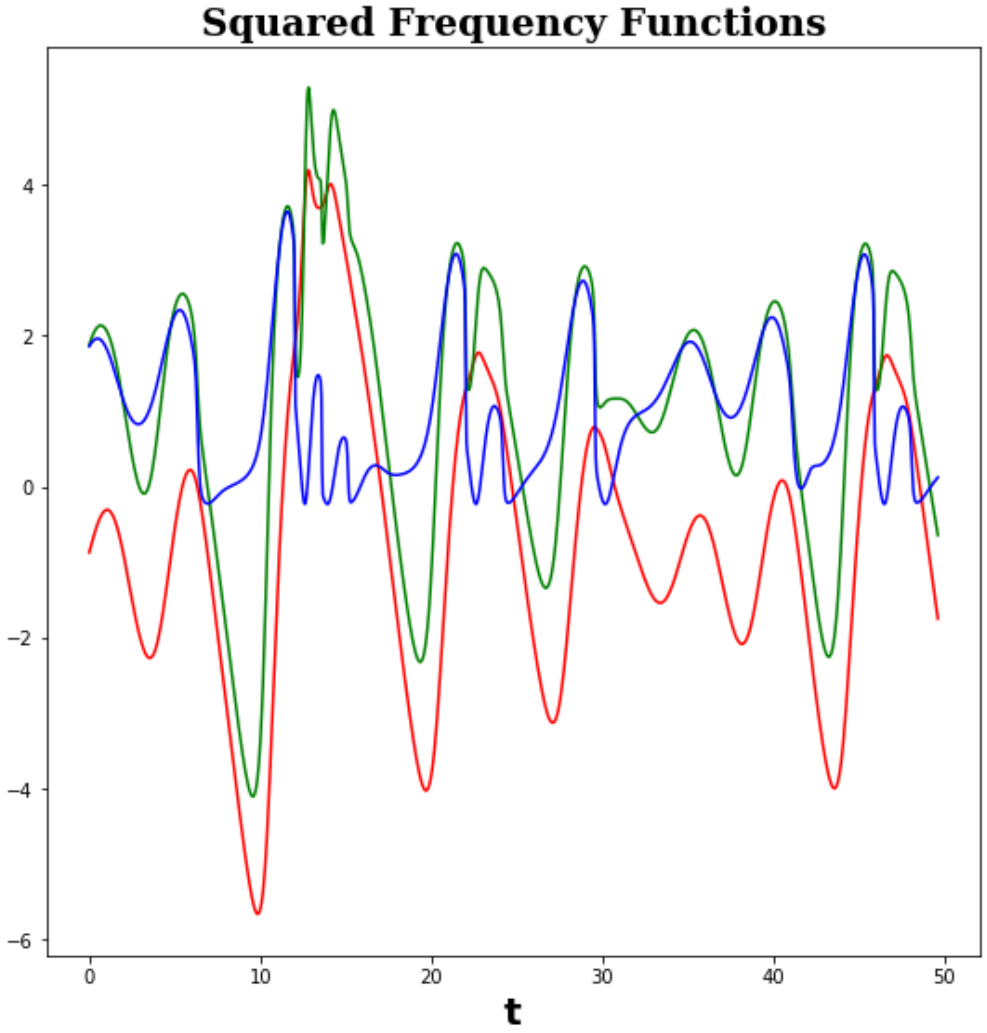

Figure 30: *The squared frequency functions g_x (in red), g_y (in green), and g_z (in blue) applied to a random trajectory in the Wimol-Banlue Attractor, where $\alpha = 2$ and $\beta = 10$. The splitting parameters in this situation are $c_x, c_y, c_z = 0$. Notice that g_x, g_y, and g_z intersect on a regular basis, and that most if not all intersections occur when g_x, g_y, and g_z take on positive values. This means that the modified Wimol-Banlue Attractor consistently intersects the intersection sets G^+_{xy}, G^+_{xz}, and G^+_{yz} as defined in Equation 31 from Section V.*

VIII. Discussing Issues with the Splitting of Functions

Using Theorem VI.4, we can define the unique splittings of many different basic mathematical functions, as shown in Table 1. However, the astute reader will immediately recognize a leering issue: how do we define splitting parameter c? Up till now, c has been taken arbitrarily, but this approach is rarely worthwhile. There are two requisites to consider.

1. c must be chosen so that forcing function h is well-defined.
2. c must be chosen so that it does not cause issues for the Competitive Modes Conjecture. This is to say, the choice of c does not affect the validity of the Competitive Modes Conjecture when a chaotic dynamical system is applied to it (assuming the conjecture is true).

Let us discuss each of these requisites thoroughly.

Obviously, the first requisite is necessary in order to avoid ill-defined forcing functions and squared frequency functions. Per Lemma VI.1, requiring that the forcing function h be well-defined is equivalent to requiring that the set $\{\mathbf{x} \in D_i^n : \mathrm{x}_i = c\}$ is not empty, where D_i^n is the domain of the function we wish to split as defined in Equation (32).

As simple as this requisite is, fulfilling it can be meddlesome. At first glance, one would suggest to simply set c equal to 0. Indeed, this choice would have many benefits, as described below, and the authors suggest to use this assumption if at all possible.

- First of all, this choice in $c = 0$ would be elegant, which is something that all mathematicians strive for.
- All previous literature on the subject has focused on multipolynomial chaotic dynamical systems. Corollary VI.5 shows that choosing c to be 0 would result in forcing and squared frequency functions that are identical to previous literature's methodology when applied to multipolynomial systems.

Obviously, we would not be having this discussion if there was not at least one glaring issue: not all differentiable functions have a domain D_i^n where the subset $\{\mathbf{x} \in D_i^n : \mathrm{x}_i = 0\}$ is nonempty. For instance, the reciprocal function is not defined on 0.

Now, one could simply mandate that the Competitive Modes Conjecture only deals with systems that can be split with splitting parameter $c = 0$. However, mathematicians love to expound on matters that were previously seen as uncomfortable, impractical, or downright impossible. No one would have discovered the sheer usefulness of complex numbers if no one ever thought to take the square root of a negative number. As such, we dare to ask the question: can we split a function with a splitting parameter $c \neq 0$ and still acquire useful results concerning the Competitive Modes Conjecture?

A simple preliminary question would be: does changing the value of the splitting parameter change the corresponding forcing and squared frequency functions?

Lemma VIII.1 (Splittings of Multilinear Functions)**.** *Suppose function $f : D_i^n \to \mathbb{R}$ is linear with respect to the i-th dimension x_i of its input variable $\mathbf{x}$. Say f can be split with respect to i-th dimension and splitting parameter $c_1 \in \mathbb{R}$ into corresponding forcing function h_1 and squared frequency function g_1. Say that f can also be split with respect to i-th dimension and splitting parameter $c_2 \in \mathbb{R}\backslash\{c_1\}$ into corresponding forcing function h_2 and squared frequency function g_2. Then $g_1 \equiv g_2$.*

Proof. Since f is linear in x_i, we know that for some continuous functions $A : \mathbb{R}^{n-1} \to \mathbb{R}$ and $B : \mathbb{R}^{n-1} \to \mathbb{R}$,

$$f(\mathbf{x}) = A(\mathfrak{p}_i(\mathbf{x}))\mathrm{x}_i + B(\mathfrak{p}_i(\mathbf{x}))$$

Then using Corollary VI.5,

$$\begin{aligned} h_1(\mathfrak{p}_i(\mathbf{x}); c_1) &= A(\mathfrak{p}_i(\mathbf{x}))c_1 + B(\mathfrak{p}_i(\mathbf{x})) \\ g_1(\mathbf{x}; c_1) &= -A(\mathfrak{p}_i(\mathbf{x})) \\ h_2(\mathfrak{p}_i(\mathbf{x}); c_2) &= A(\mathfrak{p}_i(\mathbf{x}))c_2 + B(\mathfrak{p}_i(\mathbf{x})) \\ g_2(\mathbf{x}; c_2) &= -A(\mathfrak{p}_i(\mathbf{x})) \end{aligned}$$

As such, $g_1 \equiv g_2$. □

Because of this, we know that in certain situations, the choice of splitting parameter c will never matter. In fact, the Lorenz System, defined back in Section II in Equation (4), is an example of these situations. Looking at the resulting squared frequency functions in Equation (34), notice that c_x, c_y, and c_z do not appear in functions g_x, g_y, and g_z, respectively.

Of course, there are a plethora of cases where the choice of splitting parameter does matter. Take for instance the two simple functions f_1 and f_2.

$$\begin{aligned} f_1(x, y) &= -x(x^2 + y^2) \\ f_2(x, y) &= -\alpha y, \ \alpha \in \mathbb{R}_{>0} \end{aligned}$$

Using Theorem VI.4, let us split these two equations, one with respect to x and splitting parameter $c_x \in \mathbb{R}$, and the other with respect to y and splitting parameter $c_y \in \mathbb{R}$.

$$\begin{aligned} f_1(x, y) &= h_1(y; c_x) - (x - c_x)g_1(x, y; c_x) \\ f_2(x, y) &= h_2(x; c_y) - (y - c_y)g_2(x, y; c_x) \\ h_1(y; c_x) &= -c_x(c_x^2 + y^2) \\ h_2(x; c_y) &= -\alpha c_y \\ g_1(x, y; c_x) &= x^2 + c_x x + c_x^2 + y^2 \\ g_2(x, y; c_y) &= \alpha \end{aligned}$$

As a result, functions g_1 and g_2 are equal to one another when

$$(x + c_x/2)^2 + y^2 = \alpha - 3c_x^2/4 \tag{51}$$

Obviously, Equation (51) is similar to the equation of a circle. For convenience, let us define a new function concerning the radius of such a circle.

$$R(c_x) = \alpha - 3c_x^2/4$$

When R is positive, then the intersection of g_x and g_y represented in Equation (51) is a real circle with center $(-c_x/2, 0)$ and radius $\sqrt{R(c_x)}$. This only occurs when $|c_x| < \sqrt{4\alpha/3}$.

If $|c_x| = \sqrt{4\alpha/3}$, then function R is zero and the intersection of g_x and g_y represented in Equation (51) is the single point $(-c_x/2, 0)$.

Finally, if $|c_x| > \sqrt{4\alpha/3}$, then function R is negative and g_x and g_y do not intersect at all in real space.

As one can see, the competitive nature of even a simple example can have wildly varying behavior. For some values of c_x, g_1 and g_2 intersect on a path-continuous 1-dimensional closed set in $\mathbb{R}^2$. For other values, g_1 and g_2 only intersect in a single point, and for still other values, the squared frequency functions do not intersect at all in the real 2-dimensional plane.

The all-important question that then arises from this is: for what values of splitting parameter c does one arbitrary competitive mode compete with another? In an attempt to bring light to this important matter, we will need to delve a little into Differential Geometry.

IX. Manifold Theory and Basic Differential Geometry

To answer the questions posed at the end of Section VIII, let us first understand some theory of a different branch of mathematics: Differential Geometry. The concept of a manifold is crucial here, and as such will be defined thoroughly for future reference; in order to do so, we must define the concept of a diffeomorphism.

Definition IX.1 (Diffeomorphism)**.** *A differentiable map $\phi : A \to B$ with $A \subseteq \mathbb{R}^n$, $B \subseteq \mathbb{R}^m$ is a diffeomorphism if ϕ is a bijection between A and B and the inverse ϕ^{-1} is also differentiable [19][24].*

Now we can define a differentiable manifold.

Definition IX.2 (Differentiable Manifold)**.** *Set $M \subseteq \mathbb{R}^n$ is a k-dimensional differentiable manifold if for every point $p \in M$ there exists an open neighborhood $N_p \subseteq M$ that is diffeomorphic to some open set $U_p \subseteq \mathbb{R}^k$. If instead for every point $p \in M$ there exists an open neighborhood $N_p \subseteq M$ that is diffeomorphic to some open set $U_p \subseteq \{\mathbf{x} \in \mathbb{R}^k : \mathrm{x}_1 \geq 0\}$, then M is called a k-dimensional differentiable manifold with boundary. The diffeomorphism $\phi_p : U_p \to N_p$ is called the local parameterization of N_p, and its inverse ϕ_p^{-1} is the coordinate system on N_p [19][24].*

For the reader's convenience, we will denote a k-dimensional differentiable manifold simply as a k-manifold. Furthermore, if M is a manifold with boundary, then ∂M denotes the boundary of M, while $int(M)$ denotes the interior of M [19][24].

Intuitively, a k-manifold is a piece of the $\mathbb{R}^k$-plane that has been smoothly stretched, curved, moved, and otherwise molded while inside of a higher dimensional ambient space. This is a very general definition, and frankly may seem a bit vague. However, this is all what a manifold is. In fact, any sort of smooth geometric object, regardless of what finite dimension it is in, can usually be described as a manifold. The important detail is that manifolds have some semblance of smoothness[7], allowing for some concept of differentiation to be defined over it. But in order to do so, we must define tangent spaces over manifolds [19][24].

Definition IX.3 (Tangent Spaces of a Manifold)**.** *Say we have a k-dimensional differentiable manifold $M \subseteq \mathbb{R}^n$. Take point $p \in M$; this point per definition has some open neighborhood $N_p \subseteq M$ which is diffeomorphic to some open set U_p of $\mathbb{R}^k$ (or of the upper halfspace H_k if M is a manifold with boundary) via local parametrization ϕ. The tangent space T_pM of M at p is the k-dimensional linear space defined as*

$$T_pM \equiv span\left\{\lim_{h\to 0}\left(\frac{\phi(\phi^{-1}(p)+hv)-p}{h}\right) : v \in U_p\right\}$$

Note that this definition is independent of our choice of ϕ [19][24]

[7] The authors realize that most texts refer to smooth functions as being of class $\mathcal{C}^\infty$. In this text they are not nearly so restrictive, and simply refer to a smooth function as being of class $\mathcal{C}^1$.

Intuitively, $T_pN + p$ is the set of vectors that are locally tangent to M at point p. We can then use the tangent space of M at p to define the directional derivatives at point p, and building the calculus associated with manifold M from there on [19][24].

Manifolds can intersect each other, and can do so in a number of ways. Here we discuss the idea behind manifolds intersecting transversely.

Definition IX.4 (Transversality of Manifolds)**.** *Say we have two differentiable manifolds $M_1, M_2 \subset \mathbb{R}^n$. M_1 intersects M_2 transversely at $p \in M_1 \cap M_2$ if the span of T_pM_1 and T_pM_2 equals the ambient space $\mathbb{R}^n$. If M_1 and M_2 intersect transversely for all points in $M_1 \cap M_2$, then M_1 and M_2 are said to be transverse to each other [19][24].*

Bringing these mathematical concepts into something a bit more applicable to the everyday mathematician, we will provide a very useful lemma relating differentiable functions to manifolds. The authors found this lemma in [24] and changed it only slightly to better suit their purposes.

Lemma IX.1. *Say $U_1 \subseteq \mathbb{R}^n$ and $U_2 \subseteq \mathbb{R}^m$ are open sets. If $\mathbf{f} : U_1 \to U_2$ is a $\mathcal{C}^1(U_1)$ function, then $G_f = \{(\mathbf{x}, \mathbf{f}(\mathbf{x})) \in \mathbb{R}^{n+m} : \mathbf{x} \in U_1\}$ is a n-manifold [24].*

Proof. Define function $\phi : U_1 \times U_2 \to U_1$ with $\phi(\mathbf{x}, \mathbf{f}(\mathbf{x})) = \mathbf{x}$. The inverse of $\phi|_{G_f}$ is $\varphi : U_1 \to G_f$ with $\varphi(\mathbf{x}) = (\mathbf{x}, \mathbf{f}(\mathbf{x}))$. Notice that $\phi|_{G_f}$ is a diffeomorphism, since

$$D\phi|_{G_f} = \begin{bmatrix} 1 & 0 & \dots & 0 & 0 & 0 & \dots & 0 \\ 0 & 1 & \dots & 0 & 0 & 0 & \dots & 0 \\ \vdots & \vdots & \ddots & \vdots & \vdots & \vdots & \ddots & \vdots \\ 0 & 0 & \dots & 1 & 0 & 0 & \dots & 0 \end{bmatrix} \in \mathbb{R}^{n \times (n+m)}$$

$$D\varphi = \begin{bmatrix} 1 & 0 & \dots & 0 \\ 0 & 1 & \dots & 0 \\ \vdots & \vdots & \ddots & \vdots \\ 0 & 0 & \dots & 1 \\ \partial f_1/\partial \mathrm{x}_1 & \partial f_1/\partial \mathrm{x}_2 & \dots & \partial f_1/\partial \mathrm{x}_n \\ \partial f_2/\partial \mathrm{x}_1 & \partial f_2/\partial \mathrm{x}_2 & \dots & \partial f_2/\partial \mathrm{x}_n \\ \vdots & \vdots & \ddots & \vdots \\ \partial f_m/\partial \mathrm{x}_1 & \partial f_m/\partial \mathrm{x}_2 & \dots & \partial f_m/\partial \mathrm{x}_n \end{bmatrix} \in \mathbb{R}^{(n+m) \times n}$$

Thus G_f is entirely diffeomorphic to an open subset of U_1, making it a differentiable manifold with dimension $dim(U_1) = n$. □

As a result of this lemma, we have the follow corollary that will become quite useful to us when studying dynamical systems.

Corollary IX.2 (Solutions to Systems of Differential Equations)**.** *Say we have an n-dimensional autonomous system of differential equations $\dot{\mathbf{x}}(t) = \mathbf{F}(\mathbf{x}(t))$ with $\mathbf{F} \in \mathcal{C}^0(\mathbf{x})$. Then the solution $\{(t, \mathbf{x}(t)) \in \mathbb{R}^{n+1} : t \in \mathbb{R}\}$ of the system with arbitrary initial condition is a 1-manifold.*

This lemma can be useful in certain circumstances, but for our purposes we wish to focus on specifically the phase space, which excludes the temporal dimension. What can we say about the nature of a trajectory of the dynamical system when projected onto the phase space?

Lemma IX.3 (Projected Partial Solutions to Systems of Differential Equations)**.** *Say we have an n-dimensional autonomous system of differential equations* $\dot{\mathbf{x}}(t) = \mathbf{F}(\mathbf{x}(t))$ *with* $\mathbf{F} \in \mathcal{C}^0(\mathbf{x})$*. Say we have a partial solution* $\{(t, \mathbf{x}(t)) \in \mathbb{R}^{n+1} : t \in [a, b],\ a < b\}$ *of the system with initial condition* $\mathbf{x}_0 \in \mathbb{R}^n$ *and* $a, b \in \mathbb{R}$*.*

- *If* $\mathbf{x}_0$ *is not an equilibrium point and the partial solution is periodic, then the partial solution projected onto the phase space is a 1-manifold.*
- *If* $\mathbf{x}_0$ *is not an equilibrium point and the partial solution is aperiodic, then the partial solution projected onto the phase space is a 1-manifold with boundary.*

Proof. Let us begin with the lemma's first statement. If $\mathbf{x}_0$ is not an equilibrium point of the system and the partial solution is periodic, then the partial solution must be a subset of a periodic attractor with a period $T > 0$. Because of its smoothness, periodicity, and non-self-transversal nature, the partial solution projected onto the phase space is locally diffeomorphic to the open unit 1-ball in $\mathbb{R}^1$ and is thus a 1-manifold.

If however $\mathbf{x}_0$ is not an equilibrium point of the system and the partial solution is aperiodic, then there must exist some minimal Euclidean distance between every pair of distinct points in the projected partial solution. Because of its smoothness and non-self-transversal nature, the projected partial solution is locally diffeomorphic to the open unit half 1-ball in $\mathbb{R}^1$ and is thus a 1-manifold with boundary.

□

This completes the mathematical basis needed to understand the following Theorem.

Theorem IX.4 (Splitting Parameter Perturbation Theorem)**.** *Say we have compact sets $X \in \mathbb{R}^n$ and $C \in \mathbb{R}^m$ with interiors $int(X), int(C) \neq \emptyset$. Say we have an n-dimensional autonomous system of differential equations $\dot{\mathbf{x}}(t) = \mathbf{F}(\mathbf{x}(t))$ with $\mathbf{x} \in X$, $t \in \mathbb{R}$, and $\mathbf{F} \in \mathcal{C}^1(\mathbf{x})$. For some initial value $\mathbf{x}_0$ that is not an equilibrium point, the partial solution to the system over temporal domain $[0, T]$ with $T \in \mathbb{R}_{>0}$ is defined as $\psi : [0, T] \to X$. Then the partial solution projected onto the phase space is defined as*

$$\Psi \equiv \{\psi(t) : t \in [0, T]\} \in \mathbb{R}^n$$

Assume without loss of generality that Ψ is aperiodic. Furthermore, say we have some other function $G : X \times C \to \mathbb{R}$. For arbitrary $\mathbf{c} \in C$, define $M_{\mathbf{c}} \equiv \{\mathbf{x} \in X : G(\mathbf{x}, \mathbf{c}) = 0\}$. If

- *$\forall \mathbf{c} \in C$, $M_{\mathbf{c}}$ is a connected nonempty $(n-1)$-dimensional manifold with boundary $\partial M_{\mathbf{c}}$*
- *$\forall \mathbf{c} \in C$, $\partial M_{\mathbf{c}} \cap int(X) = \emptyset$*
- *$M \equiv \bigcup_{\mathbf{c} \in C} M_{\mathbf{c}}$ is a path-continuous set.*
- *Ψ intersects $M_{\mathbf{c}^*}$ transversely at some point $\mathbf{x}^* \in int(\Psi) \cap int(M_{\mathbf{c}^*})$ for some $\mathbf{c}^* \in C$*

then for small enough $r > 0$, Ψ will also intersect $M_{\mathbf{c}}$ with $||\mathbf{c} - \mathbf{c}^*|| < r$.

Proof. First, notice that due to Corollary IX.3, Ψ is a 1-dimensional differentiable manifold with boundary, where $\partial\Psi = \{\mathbf{x}(0), \mathbf{x}(T)\} \subset X$.

For reference,

$$B_n(\mathbf{a}, \rho) \equiv \{\mathbf{x} \in \mathbb{R}^n : ||\mathbf{x} - \mathbf{a}|| < \rho\} \text{ where } \mathbf{a} \in \mathbb{R}^n,\ \rho > 0$$

Suppose that for some $\mathbf{c}^* \in C$, Ψ intersects $M_{\mathbf{c}}$ transversely at some point $\mathbf{x}^* \in int(\Psi) \cap int(M_{\mathbf{c}}) \subseteq int(X)$. Then there must exist an $r_1 > 0$ so that $B_n(\mathbf{x}^*, r_1) \cap M_{\mathbf{c}^*} \subseteq int(M_{\mathbf{c}^*})$, $B_n(\mathbf{x}^*, r_1) \cap \Psi \subseteq int(\Psi)$, and $B_n(\mathbf{x}^*, r_1) \cap \Psi$ is connected.

Define the set

$$D(\rho) \equiv \left[\bigcup_{\mathbf{x} \in M_{\mathbf{c}^*}} B_n(\mathbf{x}, \rho)\right] \cap B_n(\mathbf{x}^*, r_1)$$

Take $r_2 \in (0, r_1)$ so that Ψ intersects $\partial D(r_2) \backslash \big(\partial D(r_2) \cap \partial B_n(\mathbf{x}^*, r_1)\big)$ twice, once on one "side" of $M_{\mathbf{c}^*}$ and once on the other "side". This r_2 must exist because of the transversality of the intersection between Ψ and $M_{\mathbf{c}^*}$.

Then due to the continuity of M, there must exist an $r_3 > 0$ so that $\forall |\varepsilon| < r_3$, the set $N_{\mathbf{c}^*+\varepsilon} \equiv M_{\mathbf{c}^*+\varepsilon} \cap B_n(\mathbf{x}^*, r_1)$ has the following properties.

$$N_{\mathbf{c}^*+\varepsilon} \subseteq int(M_{\mathbf{c}^*+\varepsilon}) \cap D(r_2)$$
$$N_{\mathbf{c}^*+\varepsilon} \neq \emptyset$$

Because of this, the set $N_{\mathbf{c}^*+\varepsilon}$ has no boundaries or holes in $B_n(\mathbf{x}^*, r_1)$. Furthermore, both $N_{\mathbf{c}^*+\varepsilon}$ and Ψ are path-continuous and entirely enclosed in $D(r_2) \subset B_n(\mathbf{x}^*, r_1)$. Thus Ψ must intersect $N_{\mathbf{c}^*+\varepsilon}$ as some point inside $D(r_2)$, meaning that Ψ intersects $M_{\mathbf{c}^*+\varepsilon}$. □

We can use Theorem IX.4 to conclude the following. Let us say we have a system of second-order differential equations $\ddot{\mathbf{x}} = \mathbf{f}(\mathbf{x})$, where $f_i : D_i^n \to \mathbb{R}$ (D_i^n defined as in Equation (32) in Section VI). Assume that the corresponding dynamical system has a k-Hausdorff-dimensional attractor with $k > 1$ in some compact subset X.

Assume (without loss of generality) that f_1 and f_2 are differentiable functions. If f_1 can be split with respect to the first dimension and splitting parameter $c_1 \in \mathbb{R}$, and f_2 can be split with respect to the second dimension and splitting parameter $c_2 \in \mathbb{R}$, then

$$
\begin{aligned}
f_1(\mathbf{x}) &= h_1(\mathfrak{p}_1(\mathbf{x}); c_1) - (\mathrm{x}_1 - \mathrm{c}_1) g_1(\mathbf{x}; c_1) \\
h_1(\mathfrak{p}_1(\mathbf{x}); c_1) &= f_1(\mathbf{x})|_{\mathrm{x}_1 = c_1} \\
g_1(\mathbf{x}; c_1) &= \begin{cases} \dfrac{f_1(\mathbf{x})|_{\mathrm{x}_1 = c_1} - f_1(\mathbf{x})}{\mathrm{x}_1 - c_1} & \mathrm{x}_1 \neq c_1 \\ -\dfrac{\partial f_1(\mathbf{x})}{\partial \mathrm{x}_1}\Big|_{\mathrm{x}_1 = c_1} & \mathrm{x}_1 = c_1 \end{cases} \\
f_2(\mathbf{x}) &= h_2(\mathfrak{p}_2(\mathbf{x}); c_2) - (\mathrm{x}_2 - \mathrm{c}_2) g_2(\mathbf{x}; c_2) \\
h_2(\mathfrak{p}_2(\mathbf{x}); c_2) &= f_2(\mathbf{x})|_{\mathrm{x}_2 = c_2} \\
g_2(\mathbf{x}; c_2) &= \begin{cases} \dfrac{f_2(\mathbf{x})|_{\mathrm{x}_2 = c_2} - f_2(\mathbf{x})}{\mathrm{x}_2 - c_2} & \mathrm{x}_2 \neq c_2 \\ -\dfrac{\partial f_2(\mathbf{x})}{\partial \mathrm{x}_2}\Big|_{\mathrm{x}_2 = c_2} & \mathrm{x}_2 = c_2 \end{cases}
\end{aligned}
$$

Define the function $G(\mathbf{x}, c_1, c_2) \equiv g_1(\mathbf{x}; c_1) - g_2(\mathbf{x}; c_2)$, and suppose it fulfills the requirements stated in Theorem IX.4. If a solution in the dynamical system's attractor intersects the resulting manifold $\{\mathbf{x} \in D^n : G(\mathbf{x}; c_1, c_2) = 0\}$, then for small enough $\varepsilon_1, \varepsilon_2 \in \mathbb{R}$, the solution will still intersect the manifold $\{\mathbf{x} \in D^n : G(\mathbf{x}; c_1 + \varepsilon_1, c_2 + \varepsilon_2) = 0\}$.

This proves that under small perturbations and under certain conditions, a splitting of a function as defined in Definition VI.1 will not change the competitive nature of the corresponding squared frequency functions.

X. Examples of the Splitting Parameter Perturbation Theorem

Let us visualize the results from Theorem IX.4 with an example. Previously, we looked at the modified Wimol-Banlue Attractor in Section VII with splitting parameters $c_x, c_y, c_z = 0$. However, now we need to analyze the modified Wimol-Banlue System using arbitrary splitting parameters. Thankfully, Appendix A provides us with a thorough analysis thereof.

Referring to Equation (46) in Section VII, our modification of the Wimol-Banlue Attractor is

$$\begin{cases} \dot{x} &= y - x \\ \dot{y} &= -z\tanh(x) \\ \dot{z} &= -\alpha + xy + \frac{1}{\beta}\ln(2\cosh(\beta y)) \end{cases}$$

with $\alpha > 0$ and $\beta >> 1$. The corresponding forcing functions and squared frequency functions are

$$\begin{aligned} h_x(y,z;c_x) &= c_x - y - z\tanh(c_x) \\ h_y(x,z;c_y) &= \operatorname{sech}^2(x)(x-c_y)z + \tanh(x)\left(\alpha - xc_y - \frac{1}{\beta}\ln(2\cosh(\beta c_y))\right) \\ h_z(x,y;c_z) &= y^2 - xy - (x+\tanh(\beta y))\tanh(x)c_z \\ g_x(x,y,z;c_x) &= \begin{cases} -1 + z\left(\dfrac{\tanh(x)-\tanh(c_x)}{x-c_x}\right) & x \neq c_x \\ -1 + \operatorname{sech}^2(c_x)z & x = c_x \end{cases} \\ g_y(x,y,z;c_y) &= \begin{cases} \tanh(x)x + \operatorname{sech}^2(x)z + \dfrac{\tanh(x)}{\beta(y-c_y)}\ln\left(\dfrac{\cosh(\beta y)}{\cosh(\beta c_y)}\right) & y \neq c_y \\ \tanh(x)x + \operatorname{sech}^2(x)z + \tanh(x)\tanh(\beta c_y) & y = c_y \end{cases} \\ g_z(x,y,z;c_z) &= (x+\tanh(\beta y))\tanh(x) \end{aligned}$$

Using Theorem IX.4, we would like to prove that for some $c_x, c_y, c_z \in \mathbb{R}$, the Wimol-Banlue Attractor will intersect the set $\{(x,y,z) \in \mathbb{R}^3 : g_y(x,y,z;c_y) = g_z(x,y,z;c_z)\}$ transversely.

First let us define out sets.

$$\begin{aligned} X &\equiv \{(x,y,z) \in \mathbb{R}^3\} \\ C &\equiv \{(c_y,c_z) \in \mathbb{R}^2\} \\ M_{c_y,c_z} &\equiv \{(x,y,z) \in \mathbb{R}^3 : g_y(x,y,z;c_y) = g_z(x,y,z;c_z)\} \\ M &\equiv \bigcup_{c_y,c_z \in \mathbb{R}} M_{c_y,c_z} \end{aligned}$$

To use Theorem IX.4, we must first prove that M_{c_y,c_z} is a connected 2-manifold for arbitrary $c_y, c_z \in \mathbb{R}$. M_{c_y,c_z} can be rewritten as the set

$$M_{c_y,c_z} \equiv \{(x, y, G(x, y, c_y, c_z)) \in \mathbb{R}^3\}$$

where

$$G(x, y, c_y, c_z) = \begin{cases} \sinh(x)\cosh(x)\tanh(\beta y) - \left(\dfrac{\sinh(x)\cosh(x)}{\beta(y - c_y)}\right) \ln\left(\dfrac{\cosh(\beta y)}{\cosh(\beta c_y)}\right) & y \neq c_y \\ 0 & y = c_y \end{cases}$$

This follows from the calculations done in Equations (68) and (69) from Appendix A. Function G is trivially continuous in x and c_z. Proving that G is continuous in y and c_y is not as straightforward, but can be relatively easily proven.

Taking c_y as fixed, function G is trivially continuous in $y \neq c_y$. So now what remains is proving that G is continuous in $y = c_y$. Using L'Hopital's theorem, we see that

$$\begin{aligned} \lim_{y \to c_y} G(x, y, c_y, c_z) &= \sinh(x)\cosh(x) \lim_{y \to c_y} \tanh(\beta y) \\ &\quad - \sinh(x)\cosh(x) \lim_{y \to c_y} \left(\frac{\ln(\cosh(\beta y)/\cosh(\beta c_y))}{\beta(y - c_y)}\right) \\ &= \sinh(x)\cosh(x)\tanh(\beta c_y) - \sinh(x)\cosh(x)\tanh(\beta c_y) \\ &= G(x, c_y, c_y, c_z) \end{aligned}$$

Similarly, function G is again trivially continuous in $c_y \neq y$ for fixed y. So now what remains is proving that G is continuous in $c_y = y$. Using L'Hopital's theorem, we again see that

$$\begin{aligned} \lim_{c_y \to y} G(x, y, c_y, c_z) &= \sinh(x)\cosh(x)\tanh(\beta y) \\ &\quad - \sinh(x)\cosh(x) \lim_{c_y \to y} \left(\frac{\ln(\cosh(\beta y)/\cosh(\beta c_y))}{\beta(y - c_y)}\right) \\ &= \sinh(x)\cosh(x)\tanh(\beta y) - \sinh(x)\cosh(x)\tanh(\beta y) \\ &= G(x, y, y, c_z) \end{aligned}$$

Thus, we can conclude $G \in \mathcal{C}^0(x, y, c_y, c_z)$.

Function G is also differentiable in x and y, with partial derivatives given by

$$\frac{\partial G}{\partial x} = \begin{cases} \cosh(2x)\tanh(\beta y) - \left(\dfrac{\cosh(2x)}{\beta(y-c_y)}\right)\ln\left(\dfrac{\cosh(\beta y)}{\cosh(\beta c_y)}\right) & y \neq c_y \\ 0 & y = c_y \end{cases}$$

$$\frac{\partial G}{\partial y} = \begin{cases} \sinh(x)\cosh(x)\left(\beta\,\mathrm{sech}^2(\beta y) - \dfrac{\tanh(\beta y)}{y-c_y} + \dfrac{\ln(\cosh(\beta y)/\cosh(\beta c_y))}{\beta(y-c_y)^2}\right) & y \neq c_y \\ \dfrac{\beta}{2}\sinh(x)\cosh(x)\,\mathrm{sech}^2(\beta c_y) & y = c_y \end{cases}$$

Moreover, $\partial G/\partial x$ and $\partial G/\partial y$ are trivially continuous in x and c_z. Proving that both derivatives are continuous in y and c_y is a little more involved.

First off, let us prove that $\partial G/\partial x$ is continuous in y. Taking c_y fixed, $\partial G/\partial x$ is trivially continuous in $y \neq c_y$. Using L'Hopital's Theorem again, we see that $\partial G/\partial x$ is indeed continuous in $y = c_y$.

$$\begin{aligned} \lim_{y\to c_y}\frac{\partial G(x,y,c_y,c_z)}{\partial x} &= \cosh(2x)\lim_{y\to c_y}\tanh(\beta y) - \cosh(2x)\lim_{y\to c_y}\left(\frac{\ln(\cosh(\beta y)/\cosh(\beta c_y))}{\beta(y-c_y)}\right) \\ &= \cosh(2x)\tanh(\beta c_y) - \cosh(2x)\tanh(\beta c_y) \\ &= \frac{\partial G(x,c_y,c_y,c_z)}{\partial x} \end{aligned}$$

Similarly, function $\partial G/\partial x$ is again trivially continuous in $c_y \neq y$ for fixed y. Using L'Hopital's Theorem again, we see that $\partial G/\partial x$ is indeed continuous in $c_y = y$.

$$\begin{aligned} \lim_{c_y\to y}\frac{\partial G(x,y,c_y,c_z)}{\partial x} &= \cosh(2x)\tanh(\beta y) - \cosh(2x)\lim_{c_y\to y}\left(\frac{\ln(\cosh(\beta y)/\cosh(\beta c_y))}{\beta(y-c_y)}\right) \\ &= \cosh(2x)\tanh(\beta y) - \cosh(2x)\tanh(\beta y) \\ &= \frac{\partial G(x,y,y,c_z)}{\partial x} \end{aligned}$$

We can conclude that $\partial G/\partial x \in \mathcal{C}^0(x,y,c_y,c_z)$.

We also wish to prove that $\partial G/\partial y$ is continuous. We have already concluded that $\partial G/\partial y$ is trivially continuous in x and c_z. Proving that the function is continuous in y and c_y is not so easy.

For c_y fixed, function $\partial G/\partial y$ is continuous over $y \neq c_y$. Proving that $\partial G/\partial y$ is continuous

in $y = c_y$ requires L'Hopital's Theorem as before.

$$\begin{aligned}\lim_{y\to c_y}\frac{\partial G(x,y,c_y,c_z)}{\partial y} &= \sinh(x)\cosh(x)\lim_{y\to c_y}\left(\beta\,\mathrm{sech}^2(\beta y)-\frac{\tanh(\beta y)}{y-c_y}+\frac{\ln(\cosh(\beta y)/\cosh(\beta c_y))}{\beta(y-c_y)^2}\right)\\ &= \sinh(x)\cosh(x)\left(\beta\,\mathrm{sech}^2(\beta c_y)-\frac{\beta}{2}\mathrm{sech}^2(\beta c_y)\right)\\ &= \frac{\partial G(x,c_y,c_y,c_z)}{\partial y}\end{aligned}$$

Similarly, function $\partial G/\partial y$ is again trivially continuous in $c_y \neq y$ for fixed y. Using L'Hopital's Theorem again, we see that $\partial G/\partial y$ is indeed continuous in $c_y = y$.

$$\begin{aligned}\lim_{c_y\to y}\frac{\partial G(x,y,c_y,c_z)}{\partial y} &= \sinh(x)\cosh(x)\lim_{c_y\to y}\left(\beta\,\mathrm{sech}^2(\beta y)-\frac{\tanh(\beta y)}{y-c_y}+\frac{\ln(\cosh(\beta y)/\cosh(\beta c_y))}{\beta(y-c_y)^2}\right)\\ &= \sinh(x)\cosh(x)\left(\beta\,\mathrm{sech}^2(\beta y)-\frac{\beta}{2}\mathrm{sech}^2(\beta y)\right)\\ &= \frac{\partial G(x,y,y,c_z)}{\partial y}\end{aligned}$$

We can again conclude that $\partial G/\partial y \in \mathcal{C}^0(x, y, c_y, c_z)$.

In conclusion, function $G \in \mathcal{C}^0(x, y, c_y, c_z)$ that is at least continuous differentiable in x and y. Since $G, \partial G/\partial x, \partial G/\partial y \in \mathcal{C}^0(x, y, c_y, c_z)$, we can conclude that, for arbitrary $c_y, c_z \in \mathbb{R}$, M_{c_y,c_z} is a connected 2-manifold using Lemma IX.1. Of particular note, since G is defined over every coordinate pair $(x, y) \in \mathbb{R}^2$ for arbitrary c_y and c_z, $\partial M_{c_y,c_z} \cap int(X) = \emptyset$

What is left to prove is that set M is path-continuous. This can also easily be proven since we can rewrite M as

$$M = \{(x, y, G(x, y, c_y, c_z), c_y, c_z) \in \mathbb{R}^5\}$$

Since function $G \in \mathcal{C}^0(x, y, c_y, c_z)$, set M must be a path-continuous set.

To prove the last condition of Theorem IX.4, recall our previous work on the modified Wimol-Banlue Attractor in Section VII. It so happened that for splitting parameters $c_x, c_y, c_z = 0$, the modified Wimol-Banlue Attractor repeatedly intersects the set $\{(x, y, z) \in \mathbb{R}^3 : g_y(x, y, z; 0) = g_z(x, y, z; 0)\}$ (see Figure 29). Moreover, this intersection is transverse for at least some point in the phase space.

Now we can finally use Theorem IX.4 to conclude that there exists a $r > 0$ so that for all $||(c_y, c_z)|| < r$, the Wimol-Banlue Attractor will also intersect the intersection between

$g_y(x, y, z; c_y)$ and $g_z(x, y, z; c_z)$ transversely. In other words, if the squared frequency functions compete for one set of splitting parameters, then they will compete for certain other sets of splitting parameters as well.

XI. Conclusions

Chaotic strange attractors have a certain sense of unpredictability in them, proving that the smallest changes in data can render entire models unreliable. Since the discovery of the first chaotic attractor by Lorenz [12][31], more and more processes have been discovered to contain a strange attractor. Therefore, to understand chaotic strange attractors is a matter of great importance for the progress of science as a whole. The Competitive Modes Conjecture is an attempt at doing just that.

This paper is not meant to prove or disprove the Competitive Modes Conjecture by any means, but simply to provide an in-depth analysis into what it is, when it can be useful, and provide mathematical structure to some of the vagueness that previous literature on the subject has failed to address. The largest contribution this paper has to offer is found in Section VI, where the concept of the splitting a function is rigorously defined in Definition VI.1 and proven to exist under a set of basic assumptions in Theorem VI.4.

In light of this, the authors ultimately propose a new formulation for the Competitive Modes Conjecture.

Conjecture XI.1 (Competitive Modes Conjecture)**.** *Suppose we have a autonomous n-dimensional system of differential equations of the form* $\dot{\mathbf{x}} = \mathbf{F}(\mathbf{x})$ *that can be differentiated with respect to time into* $\ddot{\mathbf{x}} = \mathbf{f}(\mathbf{x})$*. Suppose for all* $i \in \{1, 2, \cdots, n\}$*,* f_i *can be split with respect to the* i*th dimension and splitting parameter* $c_i = 0$[8] *according to Definition VI.1 into forcing function* h_i *and squared frequency function* g_i*. Furthermore, suppose this system produces a chaotic attractor in the phase space. This leads to the following results.*

- $n > 2$*;*
- *For some distinct* $i, j \in \{1, 2, \cdots, n\}$*, squared frequency functions* g_i *and* g_j *over some arbitrary trajectory* $\mathbf{x}(\cdot)$ *in the system's attractor are repeatedly competitive or nearly competitive*
- *for some* $i \in \{1, 2, \cdots, n\}$*, squared frequency function* g_i *over some arbitrary trajectory* $\mathbf{x}(\cdot)$ *in the system's attractor is not constant with respect to time;*
- *for some* $i \in \{1, 2, \cdots, n\}$*, forcing function* h_i *is not constant with respect to all variables* x_j*, where* $j \in \{1, 2, \cdots, i-1, i+1, \cdots, n\}$

This formulation removes much of the ambiguity of the original formulation, allowing for mathematicians to have a firm footing for any potential future research. Furthermore, the original was only applicable to multipolynomial systems; this new formulation allows for many more interesting systems, including many non-multipolynomial ones.

[8] More research is needed to see what affect varying c_i would have the conjecture.

XII. Future Research

In this section, we briefly discuss future research opportunities into this field of mathematics.

Splitting Parameter C

The main question that still lingers is what the optimal value of splitting parameter c should be in Definition VI.1 on page 59. Corollary VI.5 seems to suggest that the best option would be setting c equal to zero, but Table 1 and Section VIII then conclude that not all functions are splittable. This does not necessarily have to be an issue; there is no universal law that requires all possible functions to be splittable. Theorem IX.4 on page 94 does try to rectify this somewhat, but the theorem is rather restrictive and gives no indication as to which parameter values are optimal.

As such, more research needs to be done into the interdependency between the splitting of a function and the splitting parameter itself. However, as it stands, it is the authors' personal conclusion that the best option is setting the parameter equal to zero and accepting the consequences: perhaps some functions just can not be split using Definition VI.1.

Difference Systems

Perhaps a much more exciting area of research is applying the Competitive Modes Conjecture to difference systems instead of dynamical systems. As far as the authors are aware, this is a completely untapped field, and no research has be done whatsoever concerning this subject. And yet, difference and dynamical systems can be so similar; both types of systems can even contain chaotic attractors. Perhaps applying the conjecture to difference systems will reveal something dynamical systems can not.

As a quick example, let us examine the Hénon Attractor. Michel Hénon presented a two-dimensional nonlinear difference system in 1976 that contains a strange attractor [20]. The system is given as

$$\begin{cases} x_{n+1} = 1 - \alpha x_n^2 + y_n \\ y_{n+1} = \beta x_n \end{cases} \tag{52}$$

Using this, we can conclude the following.

$$\begin{cases} x_{n+2} = 1 - \alpha(1 - \alpha x_n^2 + y_n)^2 + \beta x_n \\ y_{n+2} = \beta - \alpha\beta x_n^2 + \beta y_n \end{cases} \tag{53}$$

In a way similar to Lemma VI.5, we could "split" this system into its constituent "forcing"

functions and "squared frequency" functions. Here we use splitting parameters $c_x, c_y = 0$.

$$\begin{aligned} h_x(y_n;0) &= 1-\alpha-2\alpha y_n-\alpha y_n^2 \\ g_x(x_n,y_n;0) &= \alpha^3 x_n^3-\beta-2\alpha^2 x_n-2\alpha^2 x_n y_n \\ h_y(x_n;0) &= \beta(1-\alpha x_n^2) \\ g_y(x_n,y_n;0) &= -\beta \end{aligned} \tag{54}$$

The solution to the equation $g_x(x_n, y_n; 0) = g_y(x_n, y_n; 0)$ is given by

$$G_{xy} \equiv \{(x_n, y_n) \in \mathbb{R}^2 : \alpha^2 x_n = 0,\ y_n = \alpha x_n^2/2 - 1\} \tag{55}$$

Plotting this intersection set in 2-dimensional phase space in Figure 31 along with the Hénon Attractor, we see that the attractor and the set do indeed intersect. This is corroborated with the evidence that g_x and g_y plotted over a sequence $\{(x_n, y_n) \in \mathbb{R}^2 : n \in \mathbb{N}\}$ do compete with each other on a regular basis (see Figure 32). What is interesting though is that the two "squared frequency functions" are only equal to each other when they are strictly negative, which is markedly different from dynamical systems.

As we can see, this provides evidence that the Competitive Modes Conjecture, or at least a modified version thereof, may be applicable to difference systems as well as dynamical systems. Clearly the research in this field is far from complete.

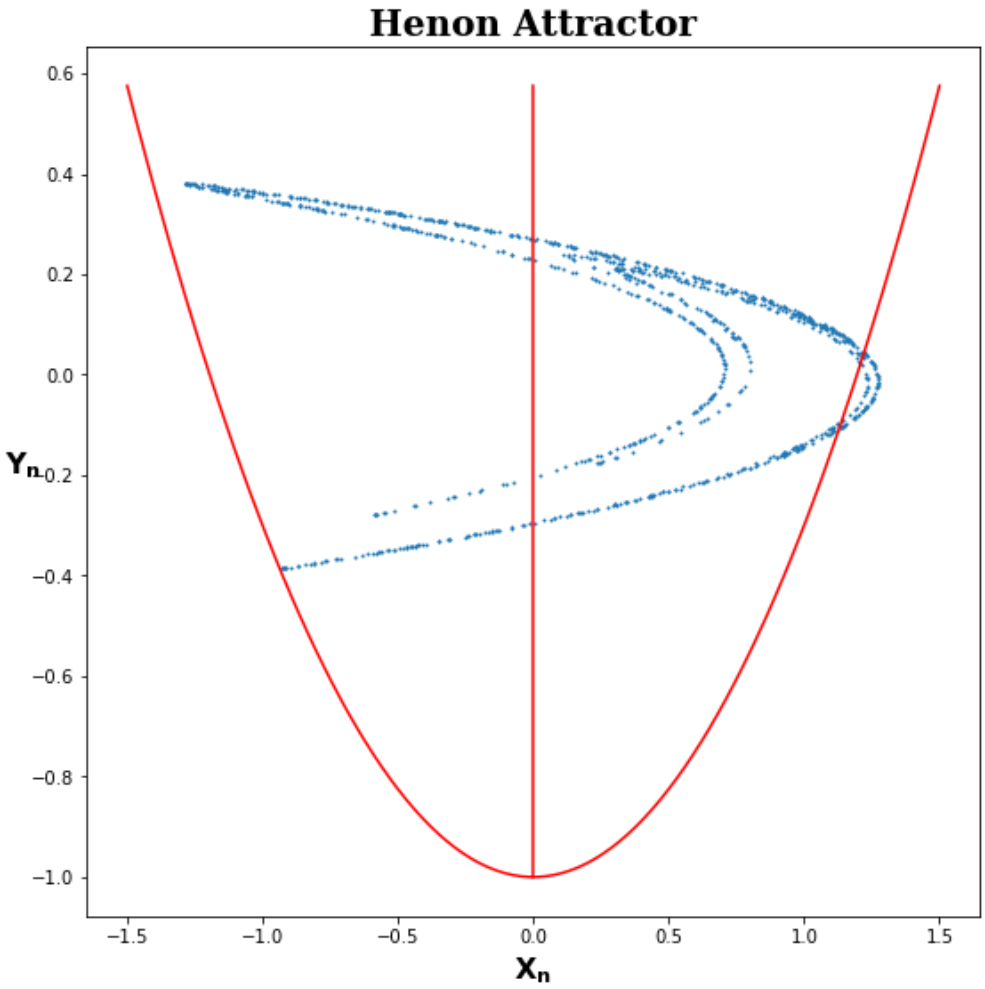

Figure 31: *The Hénon Attractor, along with the expressions in Equation* (55)*. Here,* $\alpha = 1.4$ *and* $\beta = 0.3$ *[20]. The trajectory used to plot the attractor has an initial position* $(x_0 = 0.2929376, y_0 = 0.2388)$*.*

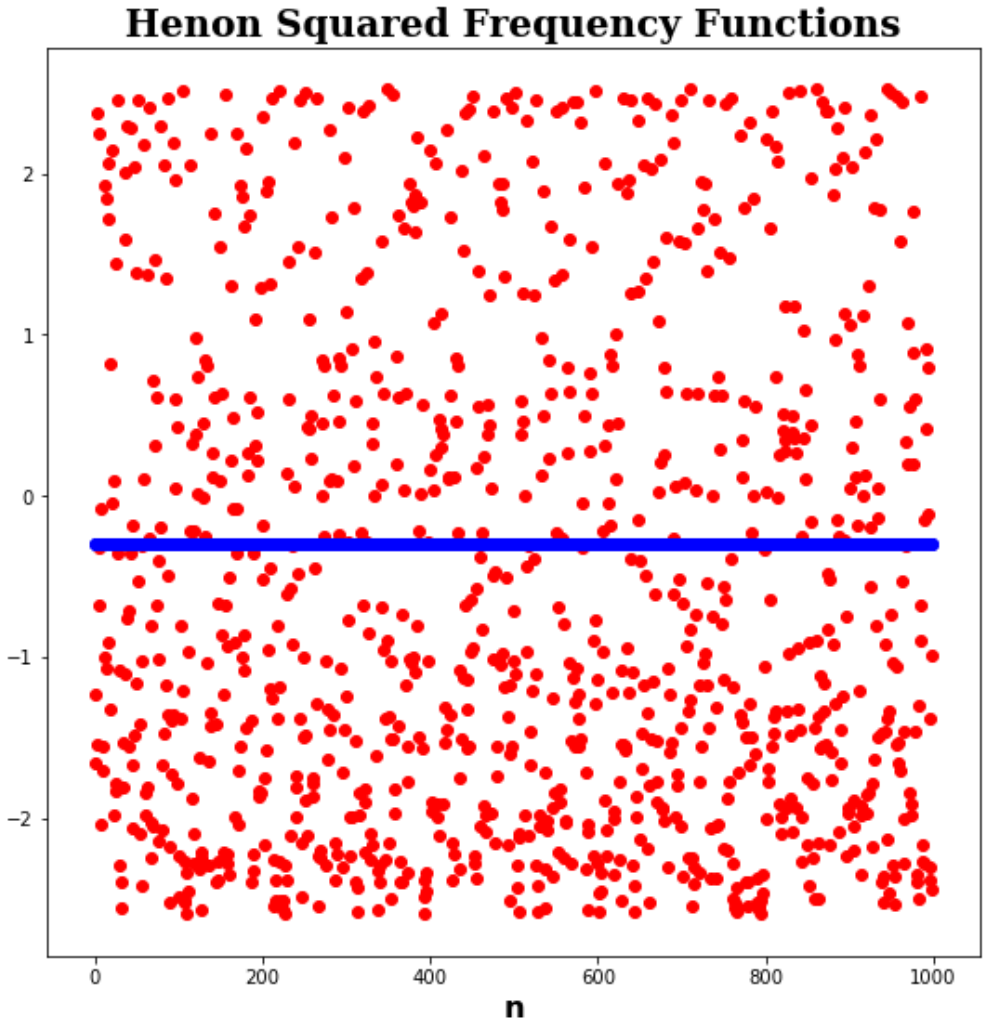

Figure 32: *The squared frequency functions* $g_x(x_n, y_n; 0)$ *and* $g_y(x_n, y_n; 0)$ *from Equation* (54) *over a trajectory in the Hénon Attractor with an initial position* $(x_0 = 0.2929376, y_0 = 0.2388)$*. Here,* $\alpha = 1.4$ *and* $\beta = 0.3$ *[20]. Notice that these two functions do intersect on a regular basis.*

Potential Counter Example of the Conjecture

After more research, it has come to the attention of the authors that in defining the Competitive Modes Conjecture more accurately in Definition XI.1, it may have resulted in a counter example of the conjecture. Let us have a look again at the Chua System defined by Equation 6 in Section II. Under the right set of parameters, the Chua Attractor exhibits a self-excited attractor around the origin, known as the Chua's Double Scroll Attractor [7][26][30]. Modifying the Chua Attractor to smoothly approximate the piece-wise linear function f from Equation 7 as was done in Section VII preserves this strange attractor.

For the reader's convenience, the necessary mathematics is succinctly shown below.

$$\begin{cases} \dot{x} = \alpha(y - x - f(x)) \\ \dot{y} = x - y + z \\ \dot{z} = -\beta y \end{cases}$$

where

$$f_{appr}(x) = \begin{cases} m_1 x + (m_1 - m_0) & x < -2 \\ \dfrac{(m_1 - m_0)x^7}{1024} + \dfrac{3(m_0 - m_1)x^5}{128} + \dfrac{13(m_1 - m_0)x^3}{64} + m_0 x & x \in [-2, 2] \\ m_1 x + (m_0 - m_1) & x > 2 \end{cases}$$

Then a self-excited attractor is formed around the origin, as shown in Figure 33. The Lyapunov Spectrum shown in Figure 34, with a maximal Lyapunov Exponent of 0.287532, reveals that the modified Double Scroll Chua Attractor is indeed chaotic. Differentiating the system leads to the 2nd order system of differential equations.

$$\begin{cases} \ddot{x} = \alpha(x - y + z) - \alpha^2(y - x - f_{appr}(x))(1 + f'_{appr}(x)) \\ \ddot{y} = -(1 + \alpha)x + (\alpha - \beta + 1)y - z - \alpha f_{appr}(x) \\ \ddot{z} = -\beta(x - y + z) \end{cases}$$

Then we calculate the proper partial derivatives.

$$\begin{cases} \partial\ddot{x}/\partial x = \alpha - \alpha^2(y - x - f_{appr}(x))f''_{appr}(x) + \alpha^2(1 + f'_{appr}(x))^2 \\ \partial\ddot{y}/\partial y = \alpha - \beta + 1 \\ \partial\ddot{z}/\partial z = -\beta \end{cases}$$

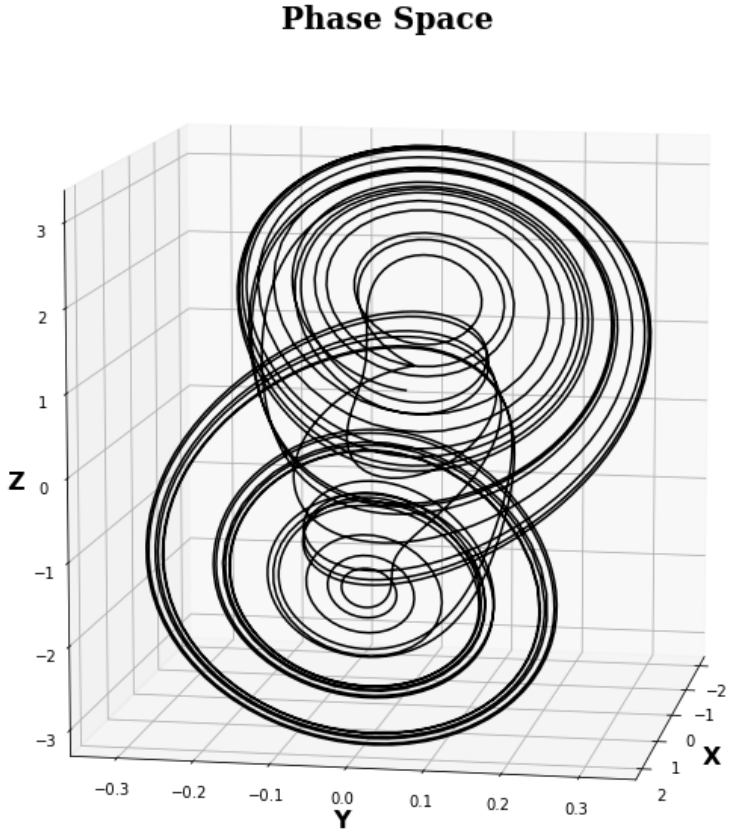

Figure 33: *The modified self-excited Chua Attractor, approximating f with f_{appr} as described in Equation* (42)*. Parameter values are $\alpha = 15.60$, $\beta = 28$, $m_0 = -1.15$, and $m_1 = -0.7$ [30]. The attractor was approximated using an adaptive explicit RK4 numerical integration technique over a time span of 60 time units using an initial position of (-1.0898, -0.0165, 0.32548). See Appendix C for coding details.*

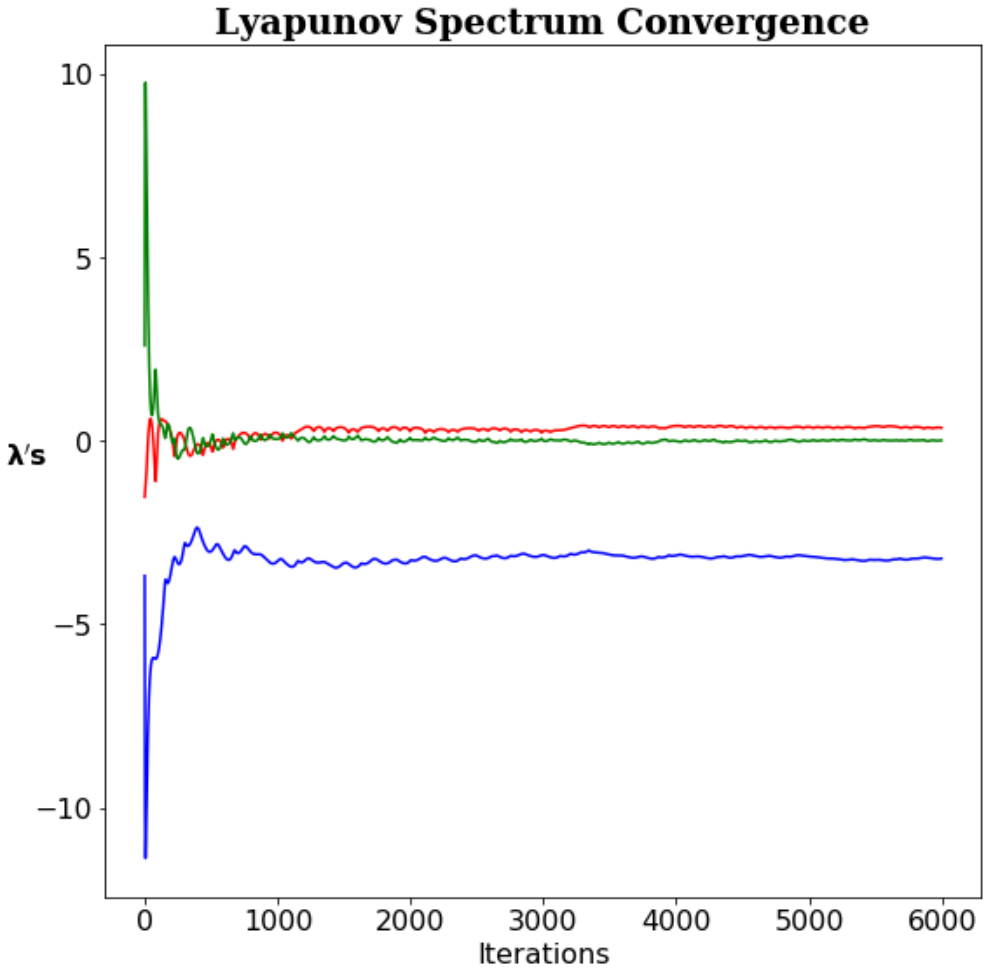

Figure 34: *The convergence of the Lyapunov Spectrum of the self-excited modified Double Scroll Chua Attractor, approximating f with f_{appr} as described in Equation* (42)*. According to our calculations, the spectrum is approximately (0.287532, -0.026106, -3.037632). See Appendix C for coding details.*

Since $\partial\ddot{x}/\partial x$, $\partial\ddot{y}/\partial y$, and $\partial\ddot{z}/\partial z$ are all continuous over all of $\mathbb{R}^3$, we can use Theorem VI.4.

$$
\begin{aligned}
h_x(y,z;c_x) &= \alpha(c_x - y + z) - \alpha^2(y - c_x - f_{appr}(c_x))(1 + f'_{appr}(c_x)) \\
g_x(x,y,z:c_x) &= \begin{cases} -\alpha(1+\alpha) - \alpha^2\left(\dfrac{f_{appr}(x) - f_{appr}(c_x)}{x - c_x}\right) \\ \quad +\alpha^2\left(\dfrac{(y - x - f_{appr}(x))f'_{appr}(x) - (y - c_x - f_{appr}(c_x))f'_{appr}(c_x))}{x - c_x}\right) & x \neq c_x \\ -\alpha - \alpha^2(1 + f'_{appr}(c_x))^2 + \alpha^2(y - c_x - f_{appr}(c_x))f''_{appr}(c_x) & x = c_x \end{cases} \\
h_y(x,z;c_y) &= -(1+\alpha)x + (\alpha - \beta + 1)c_y - z - \alpha f_{appr}(x) \\
g_y(x,y,z:c_y) &= \beta - \alpha - 1 \\
h_z(x,y;c_z) &= -\beta(x - y + c_z) \\
g_z(x,y,z:c_z) &= \beta
\end{aligned}
$$

Like before, we first set g_x and g_y equal to each other. The result is then split into two cases. When $x \neq c_x$, then

$$
\begin{aligned}
\alpha^2(f'_{appr}(x) - f'_{appr}(c_x))y =& (\alpha^2 + \beta - 1)(x - c_x) + \alpha^2(f_{appr}(x) - f_{appr}(c_x)) \\
&+ \alpha^2(x + f_{appr}(x))f'_{appr}(x) - \alpha^2(c_x + f_{appr}(c_x))f'_{appr}(c_x)
\end{aligned} \tag{56}
$$

and when $x = c_x$, then

$$
\alpha^2 f''_{appr}(c_x)y = \beta - 1 + \alpha^2(c_x + f_{appr}(c_x))f''_{appr}(c_x) + \alpha^2(1 + f'_{appr}(c_x))^2 \tag{57}
$$

As such, the intersection g_x and g_y describes a 2-dimensional real surface in the 3-dimensional phase space, which we call G_{xy}. The continuity of this surface depends on f_{appr}, f'_{appr}, and f''_{appr}, specifically when $x = c_x$.

Next, we set g_x and g_z equal to each other, the result again being split into two situations. When $x \neq c_x$, then

$$
\begin{aligned}
\alpha^2(f'_{appr}(x) - f'_{appr}(c_x))y =& (\alpha^2 + \alpha + \beta)(x - c_x) + \alpha^2(f_{appr}(x) - f_{appr}(c_x)) \\
&+ \alpha^2(x + f_{appr}(x))f'_{appr}(x) - \alpha^2(c_x + f_{appr}(c_x))f'_{appr}(c_x)
\end{aligned} \tag{58}
$$

and when $x = c_x$, then

$$
\alpha^2 f''_{appr}(c_x)y = \alpha + \beta + \alpha^2(c_x + f_{appr}(c_x))f''_{appr}(c_x) + \alpha^2(1 + f'_{appr}(c_x))^2 \tag{59}
$$

As a result, the intersection between g_x and g_z describes a 2-dimensional real surface in the 3-dimensional phase space, which we call G_{xz}. Again, the continuity of this surface depends on f_{appr}, f'_{appr}, and f''_{appr}, specifically when $x = c_x$.

And finally, we set g_y and g_z equal to each other, resulting in the simple requisite

$$
\alpha = 1
$$

Generally, α will not meet this requisite. As a result, generally there is no intersection of g_y and g_z in the phase space and $G_{yz} = \emptyset$.

The intersections between the squared frequency functions can be plotted. It is easier to understand the behavior of these intersections from a top-down aerial view (a projection of the 3-dimensional phase space onto the 2-dimensional $x - y$ plane). This is because Equations (56), (57), (58), and (59) do not include the variable z. The projected intersections are plotted in Figure 35. The splitting parameters in this situation are $c_x, c_y, c_z = 0$.

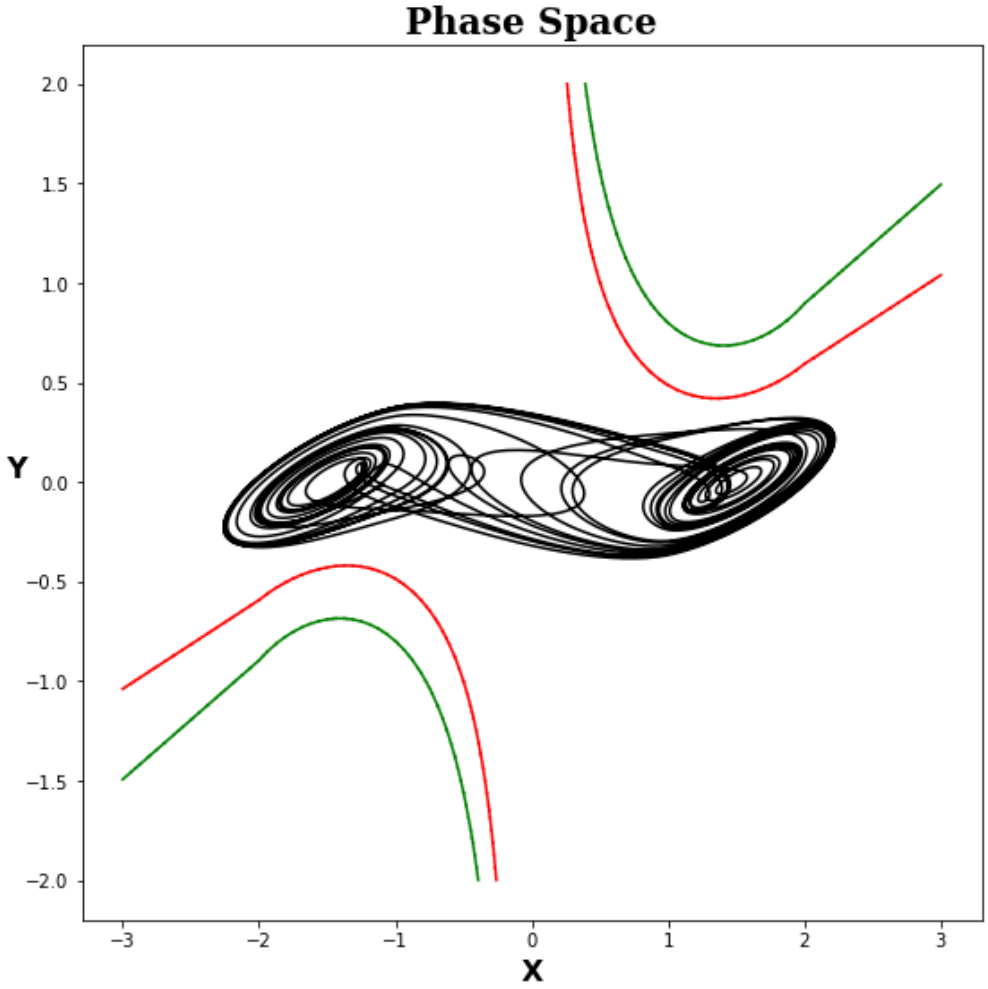

Figure 35: *The modified self-excited Chua Attractor, along with the projected intersection surfaces G_{xy} (in red) and G_{xz} (in green). The splitting parameters in this situation are $c_x, c_y, c_z = 0$. The surfaces were approximated using an adaptive Marching Square Algorithm. See Appendix C for coding details.*

From Figure 35 something interesting is revealed: although the modified self-excited Chua Attractor is indeed chaotic, the attractor does not intersect the surfaces G_{xy} or G_{xz}. This

seems to then indicate the the Competitive Modes Conjecture is incorrect.

To see the phenomenon from a different angle , we take a single trajectory in the strange attractor and calculate the squared frequency functions of the Double Scroll Chua System over this trajectory. The results are given in Figure 36. As one can see, none of the three g functions intersect at all.

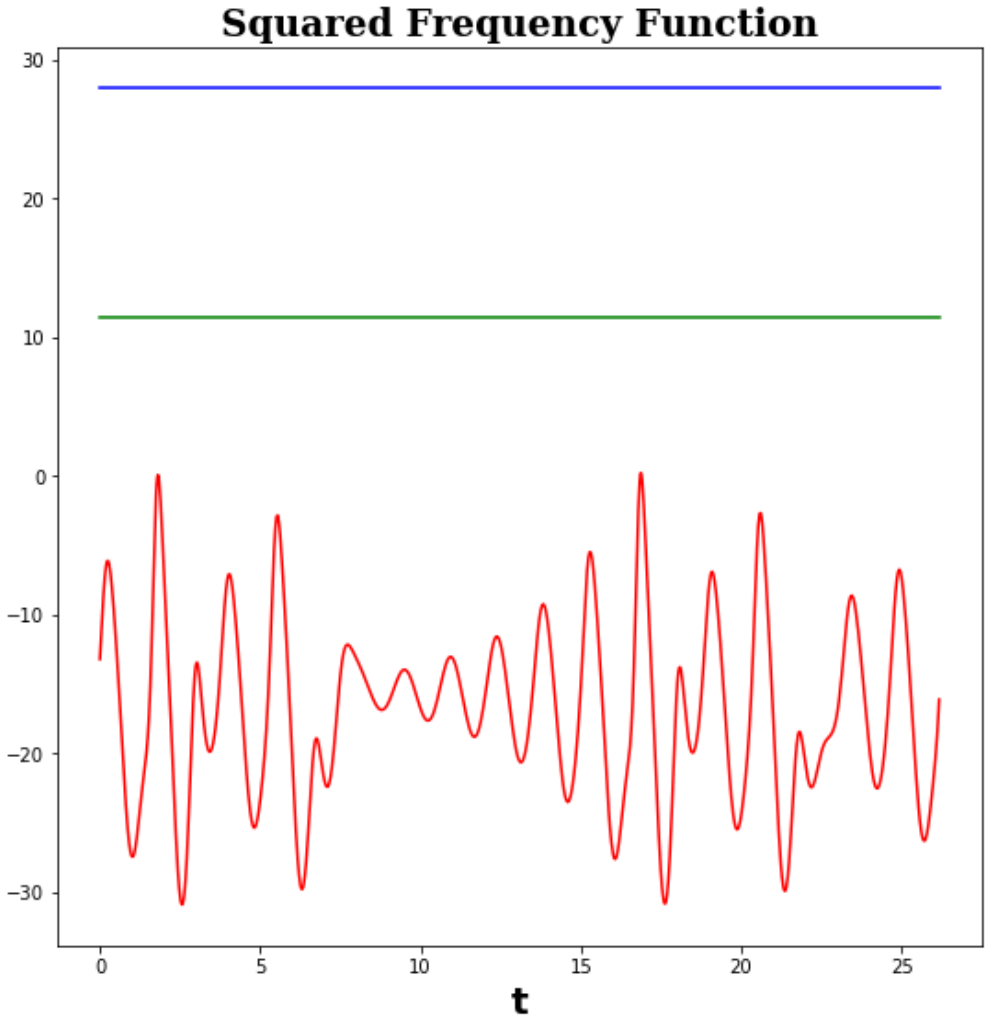

Figure 36: *The squared frequency functions g_x (in red), g_y (in green), and g_z (in blue) applied to a random trajectory in the Double Scroll Chua Attractor, where $\alpha = 15.60$, $\beta = 28$, $m_0 = -1.15$, $m_1 = -0.7$. The splitting parameters in this situation are $c_x, c_y, c_z = 0$. Notice that g_x, g_y, and g_z do not intersect at all.*

There are several explanations for this phenomenon, indicating there are a few areas of research yet to be explored.

- There could be an error present in the mathematics of the example that, despite the authors' most sincere efforts, has avoided detection. Third party validation can verify whether this is true or not.
- Our more-rigorous definition of the splitting of a function (Definition VI.1) has somehow introduced a fatality into the Competitive Modes Conjecture. Our definition would then have to be reworked to include an as-of-yet unknown requirement that will save the conjecture. This would require a deep understanding of the origins of the theory with special application to dynamical systems. Unfortunately, this is beyond the scope of this paper.
- In the counter example, the squared frequency functions do not compete directly, but could be considered nearly competitive. Remember that the conjecture does allow for this. The problem is then discerning what "nearly competitive" means mathematically. What is "near" enough for competition to take place, and do the counter example's squared frequency functions compete "near" enough? This nearness concept is rather arbitrary and needs further investigation.
- The Competitive Modes Conjecture is simply incorrect and requires revision.

In conclusion, the Chua Double Scroll Attractor seems to be a counter example of the conjecture; the question is why. Whatever the answer may be, it will provide invaluable insight into the study of chaos.

References

[1] K. Astrom and R. Murray. *Feedback Systems: An Introduction for Scientists and Engineers*, chapter 8, pages 229–262. Princeton University Press, 2009. ISBN 978-0-691-13576-2. URL http://www.cds.caltech.edu/~murray/books/AM05/pdf/am08-complete_22Feb09.pdf.

[2] A. B. Ayoub. The central conic sections revisited. *Mathematics Magazine*, 66(5):322–325, 1993. URL https://www.jstor.org/stable/2690513?seq=1.

[3] M. Cencini, F. Cecconi, and A. Vulpiani. *Chaos: From Simple Models to Complex Systems*, volume 17 of *Series on Advanced in Statistical Mechanics*. World Scientific Publishing Co. Pte. Ltd., 2009. ISBN 978-981-4277-65-5.

[4] G. Chen, P. Yu, and W. Yao. Analysis on topological properties of the lorenz and the chen attractors using gcm. *International Journal of Bifurcation and Chaos*, 17(8):2791–2796, 2007. URL https://www.worldscientific.com/doi/10.1142/S0218127407018762.

[5] S.R. Choudhury and R.A. Van Gorder. Classification of chaotic regimes in the t system by use of competitive modes. *International Journal of Bifurcation and Chaos*, 20 (11):3785–3793, 2010. URL https://www.worldscientific.com/doi/abs/10.1142/S0218127410028033.

[6] S.R. Choudhury and R.A. Van Gorder. Competitive modes as reliable predictors of chaos versus hyperchaos and as geometric mappings accurately delimiting attractors. *Nonlinear Dynamics*, 69(4):2255–2267, 2012. URL https://link.springer.com/article/10.1007/s11071-012-0424-0.

[7] L. O. Chua, M. Komuro, and T. Matsumoto. The double scroll family. *IEEE Transactions on Circuits and Systems*, 33(11):1072–1118, 1986. URL https://ieeexplore.ieee.org/document/1085869.

[8] Z. Daugherty. Math 202: Calculus 2: Section 24 rotating conic sections: Rotation of axes, 2016. URL https://zdaugherty.ccnysites.cuny.edu/teaching/m202s16/resources/conic-rotation.pdf.

[9] M. Davison, C. Essex, P. Yu, and W. Yao. Competitive modes and their application. *International Journal of Bifurcation and Chaos*, 16(3):497–522, 2006. URL https://www.worldscientific.com/doi/abs/10.1142/S0218127406014976.

[10] Harvard University-Mathematics Department. Lagrange multipliers, 2009. URL http://legacy-www.math.harvard.edu/archive/21a_spring_09/PDF/11-08-Lagrange-Multipliers.pdf.

[11] Robert Devaney. *An Introduction to Chaotic Dynamical Systems*. Westview Press, 2003. ISBN 978-0813340852.

[12] E. Doedel, B. Krauskopf, and H. Osinga. Global bifurcations of the lorenz manifold. *Nonlinearity*, 19(12):2947–2972, 2006. URL https://iopscience.iop.org/article/10.1088/0951-7715/19/12/013/meta.

[13] J.P. Eckmann and D. Ruelle. Ergodic theory of chaos and strange attractors. *Reviews of Modern Physics*, 57(3):617–656, 1985. URL https://journals.aps.org/rmp/abstract/10.1103/RevModPhys.57.617.

[14] C. Essex, P. Yu, and W. Yao. Estimation of chaotic parameter regimes via generalized competitive modes approach. *Communications in Nonlinear Science and Numerical Simulation*, 7(4):197–205, 2002. URL https://www.sciencedirect.com/science/article/abs/pii/S1007570402000217.

[15] K. Falconer. *Fractal Geometry: Mathematical Foundations and Applications*. John Wiley & Sons Ltd, 2 edition, 2003. ISBN 978-0-470-84861-8.

[16] T. Feagin. High-order m-symmetric Runge-Kutta methods. In *Proceeding of the 23rd Biennial Conference on Numerical Analysis*, Strathclyde University, Glasgow, Scotland, June 2009. URL http://sce.uhcl.edu/rungekutta/.

[17] T. Feagin. High-order explicit Runge-Kutta methods using m-symmetry. *Neural, Parallel and Scientific Computations*, 20(4):437–458, 2012.

[18] Mitchell Feigenbaum. Quantitative universality for a class of nonlinear transformations. *Journal of Statistical Physics*, 19(1):25–52, 1978. URL https://link.springer.com/article/10.1007/BF01020332.

[19] G. Haller. *Chaos Near Resonance*, volume 138, chapter A, pages 371–389. Springer, 1999. URL https://link.springer.com/book/10.1007/978-1-4612-1508-0.

[20] M. Henon. A two-dimensional mapping with a strange attractor. *Communications in Mathematical Physics*, 50(1):69–77, 1976. URL https://link.springer.com/article/10.1007/BF01608556.

[21] N. Kuznetsov and G. Leonov. Hidden attractors in dynamical systems. from hidden oscillations in hilbert-kolmogorov, aizerman, and kalman problems to hidden chaotic attractors in chua's circuits. *International Journal of Bifurcation and Chaos*, 23(1), 2013. URL https://www.worldscientific.com/doi/pdf/10.1142/S0218127413300024.

[22] N. Kuznetsov and G. Leonov. Hidden attractors in dynamical systems: systems with no equilibria multistability and coexisting attractors. *19th IFAC World Congress Proceedings*, 47(3):5445–5454, 2014. URL https://www.sciencedirect.com/science/article/pii/S1474667016424614.

[23] N. Kuznetsov, O. Kuznetsova, G. Leonov, and V. Vagaitsev. Analytical-numerical localization of hidden attractors in electrical chua's circuit. *Lecture Notes in Electrical Engineering*, 174:149–158, 2013. URL https://link.springer.com/chapter/10.1007%2F978-3-642-31353-0_11.

[24] J. Lawson. Chapter 2: Manifolds. Louisiana State University, 2006. URL https://www.math.lsu.edu/~lawson/Chapter2.pdf.

[25] B. Mandelbrot. *Fractals: Form, Chance, and Dimension*. W. H. Freeman and Company, 1 (augmented) edition, 1977. ISBN 978-0-7167-0473-7.

[26] T. Matsumoto. A chaotic attractor from chua's circuit. *IEEE Transactions on Circuits and Systems*, 31(12):1055–1058, 1984. URL https://people.eecs.berkeley.edu/~chua/papers/Matsumoto84.pdf.

[27] Lawrence Perko. *Differential Equations and Dynamical Systems*, volume 7 of *Texts in Applied Mathematics*. Springer-Verlag New York, 3 edition, 2009. ISBN 978-0-387-95116-4.

[28] Z. Roupas. Phase space geometry and chaotic attractors in dissipative nambu mechanics. *Journal of Physics A: Mathematical and Theoretical*, 45(19), 2012. URL https://iopscience.iop.org/article/10.1088/1751-8113/45/19/195101.

[29] W. San-Um and B. Srisuchinwong. A high-chaoticity high-complexity modified diffusionless lorenz system. pages 561–565, 2011.

[30] Valentin Siderskiy. Chua's circuit diagrams, equations, simulations and how to build. URL http://www.chuacircuits.com/.

[31] C. Sparrow. An introduction to the lorenz equations. *IEEE Transactions on Circuits and Systems*, 30(8):533–542, 1983. URL https://ieeexplore.ieee.org/document/1085400.

[32] L. Takhtajan. On foundation of the generalized nambu mechanics. *Communications in Mathmatical Physics*, 160(2):295–315, 1994. URL https://link.springer.com/article/10.1007/BF02103278.

[33] R. Taylor. Attractors: Nonstrange to chaotic. *Society for Industrial and Applied Mathematics*, 2011. URL https://www.researchgate.net/publication/275400091_Attractors_Nonstrange_to_Chaotic/references.

[34] W. Tucker. A rigorous ode solver and smale's 14th problem. *Foundations of Computational Mathematics*, 2(1):53–117, 2002. URL http://www2.math.uu.se/~warwick/main/rodes.html.

[35] F.H. van der Meulen. Statistical inference lecture 1: The probability space and random variables, 2018.

[36] Ferdinand Verhulst. *Nonlinear Differential Equations and Dynamical Systems*. Universitext. Springer-Verlag Berlin Heidelberg, 2 edition, 2000. ISBN 978-3-540-60934-6.

[37] P. Yu. *Edited Series on Advances in Nonlinear Science and Complexity*, volume 1, chapter 1, pages 1–125. Elsevier B.V., 2006. URL `https://www.sciencedirect.com/science/article/pii/S157469090601001X`.

A. Intersections of the G Functions of the Modified Wimol-Banlue System

In this Appendix, we calculate the intersections between the squared frequency functions of the modified Wimol-Banlue dynamical system found in Equation (9) in Section II. This analysis is referenced in Sections VII and X.

The modified Wimol-Banlue dynamical system has the form

$$\begin{cases} \dot{x} &= y - x \\ \dot{y} &= -z\tanh(x) \\ \dot{z} &= -\alpha + xy + \frac{1}{\beta}\ln(2\cosh(\beta y)) \end{cases}$$

where $\alpha, \beta > 0$. Differentiating this system with respect to time leads to

$$\begin{cases} \ddot{x} &= x - y - z\tanh(x) \\ \ddot{y} &= \operatorname{sech}^2(x)(x-y)z + \tanh(x)\left(\alpha - xy - \frac{1}{\beta}\ln(2\cosh(\beta y))\right) \\ \ddot{z} &= y^2 - xy - (x + \tanh(\beta y))\tanh(x)z \end{cases}$$

Then we can calculate the proper partial derivatives as follows.

$$\begin{cases} \partial\ddot{x}/\partial x = 1 - z\operatorname{sech}^2(x) \\ \partial\ddot{y}/\partial y = -\operatorname{sech}^2(x)z - \tanh(x)\,(x + \tanh(\beta y)) \\ \partial\ddot{z}/\partial z = -(x + \tanh(\beta y))\tanh(x) \end{cases}$$

Since $\partial\ddot{x}/\partial x$, $\partial\ddot{y}/\partial y$, and $\partial\ddot{z}/\partial z$ are continuous over all of $\mathbb{R}^3$, we can use Theorem VI.4 to split $\ddot{x}$, $\ddot{y}$, and $\ddot{z}$ using splitting parameters c_x, c_y, and c_z, respectively.

$$\begin{aligned} h_x(y,z;c_x) &= c_x - y - z\tanh(c_x) \\ h_y(x,z;c_y) &= \operatorname{sech}^2(x)(x-c_y)z + \tanh(x)\left(\alpha - xc_y - \frac{1}{\beta}\ln(2\cosh(\beta c_y))\right) \\ h_z(x,y;c_z) &= y^2 - xy - (x + \tanh(\beta y))\tanh(x)c_z \\ g_x(x,y,z;c_x) &= \begin{cases} -1 + z\left(\dfrac{\tanh(x) - \tanh(c_x)}{x - c_x}\right) & x \neq c_x \\ -1 + \operatorname{sech}^2(c_x)z & x = c_x \end{cases} \\ g_y(x,y,z;c_y) &= \begin{cases} x\tanh(x) + \operatorname{sech}^2(x)z + \dfrac{\tanh(x)}{\beta(y-c_y)}\ln\left(\dfrac{\cosh(\beta y)}{\cosh(\beta c_y)}\right) & y \neq c_y \\ x\tanh(x) + \operatorname{sech}^2(x)z + \tanh(x)\tanh(\beta c_y) & y = c_y \end{cases} \\ g_z(x,y,z;c_z) &= (x + \tanh(\beta y))\tanh(x) \end{aligned}$$

Now we set each other the squared frequency functions g_x, g_y, and g_z equal to each other and calculate the results.

$g_x(x, y, z; c_x) = g_y(x, y, z; c_y)$ **where** $x \neq c_x$ **and** $y \neq c_y$

First, we set g_x and g_y equal to each other for $x \neq c_x$ and $y \neq c_y$.

$$z\left(\frac{\tanh(x) - \tanh(c_x)}{x - c_x} - \operatorname{sech}^2(x)\right) = 1 + x\tanh(x) + \frac{\tanh(x)}{\beta(y - c_y)}\ln\left(\frac{\cosh(\beta y)}{\cosh(\beta c_y)}\right) \tag{60}$$

A natural reaction would be to isolate variable z in the left-hand-side. This is only possible if $\tanh(x) - \tanh(c_x) \neq \operatorname{sech}^2(x)(x - c_x)$. As a result,

$$\begin{aligned} z =& \frac{(1 + x\tanh(x))\,(x - c_x)}{\tanh(x) - \tanh(c_x) - \operatorname{sech}^2(x)(x - c_x)} \\ &+ \frac{\tanh(x)(x - c_x)}{\beta(y - c_y)\big(\tanh(x) - \tanh(c_x) - \operatorname{sech}^2(x)(x - c_x)\big)}\ln\left(\frac{\cosh(\beta y)}{\cosh(\beta c_y)}\right) \end{aligned}$$

If however $\tanh(x) - \tanh(c_x) = \operatorname{sech}^2(x)(x - c_x)$, then x, y, c_x and c_y must follow the equation

$$0 = 1 + x\tanh(x) + \frac{\tanh(x)}{\beta(y - c_y)}\ln\left(\frac{\cosh(\beta y)}{\cosh(\beta c_y)}\right) \tag{61}$$

for a solution to even exist. The following lemma prohibits this.

Lemma A.1.

$$\left\{(x, y) \in \mathbb{R}^2 : 0 = 1 + x\tanh(x) + \frac{\tanh(x)}{\beta(y - c_y)}\ln\left(\frac{\cosh(\beta y)}{\cosh(\beta c_y)}\right),\ y \neq c_y\right\} = \emptyset \tag{62}$$

Proof. First off, notice that

$$\begin{aligned} &\forall x \geq 0,\ x\tanh(x) \geq 0 \\ &\forall x < 0,\ x\tanh(x) = -|x|\tanh(-|x|) = |x|\tanh(|x|) > 0 \end{aligned}$$

Thus, $x\tanh(x)$ is greater than or equal to 0 for all real values of x.

Now comes the difficult part: proving that for arbitrary $c_y \in \mathbb{R}$

$$\psi(y; c_y) \equiv \frac{1}{\beta(y - c_y)}\ln\left(\frac{\cosh(\beta y)}{\cosh(\beta c_y)}\right) \in (-1, 1)\ \forall y \in \mathbb{R}\backslash\{c_y\}$$

Step one is to ascertain the limits of ψ for arbitrary c_y. This is a relatively simple calculation, using L'Hopital's Theorem to prove that

$$\lim_{y \to \pm\infty} \frac{1}{\beta(y - c_y)}\ln\left(\frac{\cosh(\beta y)}{\cosh(\beta c_y)}\right) = \lim_{y \to \pm\infty} \tanh(\beta y) = \pm 1$$

The only step that remains is to prove that ψ is an increasing function in y, which is equivalent to proving that the derivative of ψ with respect to y is non-negative for all values of y and c_y.

The derivative of ψ with respect to y, defined for arbitrary $c_y \in \mathbb{R}$ and for all $y \neq c_y$, is

$$\frac{\partial \psi(y; c_y)}{\partial y} = \frac{\beta \tanh(\beta y)(y - c_y) - \ln(\cosh(\beta y)) + \ln(\cosh(\beta c_y))}{\beta (y - c_y)^2}$$

Since the denominator is always positive ($\beta > 0$), we only have to focus on the numerator, which consists of two functions. Obviously, to prove that $\partial \psi(y; c_y)/\partial y$ is non-negative, one must prove that $\beta \tanh(\beta y)(y - c_y) \geq \ln(\cosh(\beta y)) - \ln(\cosh(\beta c_y))$.

The first thing one should notice is what is expressed in the limits below.

$$\lim_{y \to c_y} \Big(\beta \tanh(y)(y - c_y) - \ln\big(\cosh(\beta y) / \cosh(\beta c_y) \big) \Big) = 0$$

Furthermore, the numerator is a differentiable function, and as such we express the derivative of the numerator of $\partial \psi(y; c_y)/\partial y$ as follows.

$$\frac{\partial}{\partial y} \left[\beta \tanh(\beta y)(y - c_y) - \ln \left(\frac{\cosh(\beta y)}{\cosh(\beta c_y)} \right) \right] = \beta^2 \operatorname{sech}^2(\beta y)(y - c_y)$$

Then, since the numerator of $\partial \psi(y; c_y)/\partial y$ limits to zero at the point $y = c_y$, and the derivative of the numerator is positive for all $y > c_y$, we can conclude that

$$\forall y > c_y, \ \beta \tanh(y)(y - c_y) > \ln \left(\frac{\cosh(\beta y)}{\cosh(\beta c_y)} \right)$$

Furthermore, since the numerator of $\partial \psi(y; c_y)/\partial y$ limits to zero at the point $y = c_y$, and the derivative of the numerator is negative for all $y < c_y$, we can conclude that

$$\forall y < c_y, \ \beta \tanh(y)(y - c_y) > \ln \left(\frac{\cosh(\beta y)}{\cosh(\beta c_y)} \right)$$

Thus, we have concluded that for all $y \neq c_y$, the numerator and concurrently all of $\partial \psi(y; c_y)/\partial y$ is non-negative.

Therefore, since $\lim_{y \to -\infty} \psi(y; c_y) = -1$, $\lim_{y \to \infty} \psi(y; c_y) = +1$, and $\partial \psi(y; c_y)/\partial y \geq 0$, we can conclude that for arbitrary $c_y \in \mathbb{R}$,

$$\psi(y; c_y) \in (-1, 1) \ \forall y \neq c_y$$

Now to wrap things up, we go back to Equation (61).

$$\begin{aligned} 1 + x\tanh(x) + \frac{\tanh(x)}{\beta(y - c_y)} \ln\left(\frac{\cosh(\beta y)}{\cosh(\beta c_y)}\right) &> 1 + x\tanh(x) - \tanh(x) \\ &> 1 + x\tanh(x) - 1 \\ &\geq 0 \end{aligned}$$

Hence, we have proven that Equation (61) has no solutions for arbitrary $c_y \in \mathbb{R}$ if $y \neq c_y$. □

Because of Lemma A.1, we can conclude that for $x \neq c_x$ and $y \neq c_y$, $g_x(x, y, z; c_x) = g_y(x, y, z; c_y)$ when $\tanh(x) - \tanh(c_x) \neq \operatorname{sech}^2(x)(x - c_x)$.

$g_x(x, y, z; c_x) = g_y(x, y, z; c_y)$ where $x \neq c_x$ and $y = c_y$

Next, we set g_x equal to g_y for $x \neq c_x$ and $y = c_y$. Under these assumptions, the following equation is the result.

$$z\left(\frac{\tanh(x) - \tanh(c_x)}{x - c_x} - \operatorname{sech}^2(x)\right) = 1 + x\tanh(x) + \tanh(x)\tanh(\beta c_y) \tag{63}$$

Like before, we would like to isolate variable z in the left-hand-side. This is only possible if $\tanh(x) - \tanh(c_x) \neq \operatorname{sech}^2(x)(x - c_x)$. As a result,

$$z = \frac{(x - c_x) + x\tanh(x)(x - c_x) + \tanh(x)\tanh(\beta c_y)(x - c_x)}{\tanh(x) - \tanh(c_x) - \operatorname{sech}^2(x)(x - c_x)}$$

If however $\tanh(x) - \tanh(c_x) = \operatorname{sech}^2(x)(x - c_x)$, then for a solution to even exist, variables x, c_x, and c_y must follow the equation. The following lemma again prohibits this.

Lemma A.2.

$$\{x \in \mathbb{R} : 0 = 1 + x\tanh(x) + \tanh(x)\tanh(\beta c_y)\} = \emptyset$$

Proof. The proof is much simpler than that of the previous subsection.

We have already proven previously that $x\tanh(x) \geq 0$ for all $x \in \mathbb{R}$. We also know that $\tanh(x) \in (-1, 1)$ for all $x \in \mathbb{R}$ and similarly that $\tanh(\beta c_y) \in (-1, 1)$ for all $c_y \in \mathbb{R}$. Then we can finish off this quick proof with the following inequality.

$$1 + x\tanh(x) + \tanh(x)\tanh(\beta c_y) > 1 + x\tanh(x) - 1 \geq 0$$

□

Because of Lemma A.2, we can conclude that for $x \neq c_x$ and $y = c_y$, $g_x(x, c_y, z; c_x) = g_y(x, c_y, z; c_y)$ when $\tanh(x) - \tanh(c_x) \neq \operatorname{sech}^2(x)(x - c_x)$.

$g_x(x, y, z; c_x) = g_y(x, y, z; c_y)$ **where** $x = c_x$ **and** $y \neq c_y$

Next, we set g_x equal to g_y for $x = c_x$ and $y \neq c_y$. Under these assumptions, an equation is the result.

$$0 = 1 + c_x \tanh(c_x) + \frac{\tanh(c_x)}{\beta(y - c_y)} \ln\left(\frac{\cosh(\beta y)}{\cosh(\beta c_y)}\right) \tag{64}$$

According to Lemma A.1, solutions to this equation do not exist.

$g_x(x, y, z; c_x) = g_y(x, y, z; c_y)$ **where** $x = c_x$ **and** $y = c_y$

Continuing on, we set g_x equal to g_y for $x = c_x$ and $y = c_y$. Under these assumptions, the result is

$$0 = 1 + c_x \tanh(c_x) + \tanh(c_x) \tanh(\beta c_y)) \tag{65}$$

According to Lemma A.2, the equation has no solutions and cannot be solved for any real selection of c_x and c_y.

$g_x(x, y, z; c_x) = g_z(x, y, z; c_z)$ **where** $x \neq c_x$

Continuing on this extensive analysis, setting g_x equal to g_z with $x \neq c_x$ results in the equation

$$z(\tanh(x) - \tanh(c_x)) = (x - c_x) + (x - c_x)(x + \tanh(\beta y)) \tanh(x) \tag{66}$$

Notice that if $x \neq c_x$, then $\tanh(x) \neq \tanh(c_x)$; Equation (66) can be freely rewritten as

$$z = \frac{x - c_x}{\tanh(x) - \tanh(c_x)} + \frac{(x - c_x)x \tanh(x)}{\tanh(x) - \tanh(c_x)} + \frac{(x - c_x) \tanh(x) \tanh(\beta y)}{\tanh(x) - \tanh(c_x)}$$

$g_x(x, y, z; c_x) = g_z(x, y, z; c_z)$ **where** $x = c_x$

Next, we set g_x equal to g_z with $x = c_x$, with the resulting equation as follows.

$$z \operatorname{sech}^2(c_x) = 1 + c_x \tanh(c_x) + \tanh(c_x) \tanh(\beta y) \tag{67}$$

Since $\operatorname{sech}^2(c_x) > 0$ for all $c_x \in \mathbb{R}$, this equation can be freely rewritten to

$$z = \cosh^2(c_x) + c_x \sinh(c_x) \cosh(c_x) + \sinh(c_x) \cosh(c_x) \tanh(\beta y)$$

$g_y(x, y, z; c_y) = g_z(x, y, z; c_z)$ **where** $y \neq c_y$

Getting close to completing this section of the analysis on the modified Wimol-Banlue system, we set g_y equal to g_z with $y \neq c_y$. The resulting equation is equal to

$$z \operatorname{sech}^2(x) = \tanh(x) \tanh(\beta y) - \frac{\tanh(x)}{\beta(y - c_y)} \ln\left(\frac{\cosh(\beta y)}{\cosh(\beta c_y)}\right) \tag{68}$$

Since $\operatorname{sech}^2(x) > 0$ for all $x \in \mathbb{R}$, this equation can be freely rewritten as

$$z = \sinh(x)\cosh(x)\tanh(\beta y) - \frac{\sinh(x)\cosh(x)}{\beta(y - c_y)} \ln\left(\frac{\cosh(\beta y)}{\cosh(\beta c_y)}\right)$$

$g_y(x, y, z; c_y) = g_z(x, y, z; c_z)$ **where** $y = c_y$

Finally, we set g_y equal to g_z with $y = c_y$. The resulting equation is equal to

$$z \operatorname{sech}^2(x) = 0 \tag{69}$$

Simplifying this equation, regardless of choice for any splitting parameter, concludes in the simple planer equation in 3-dimensional phase space.

$$z = 0$$

B. Calculations involving the Conic Section Equation

In this Appendix, we relay the proof that for $A, C \in \mathbb{R}$, $B \in \mathbb{R}\backslash\{0\}$

$$Ax^2 + Bxy + Cy^2 = \left(\frac{A+C}{2} + \frac{\sqrt{(A-C)^2+B^2}}{2}\right)\chi^2 + \left(\frac{A+C}{2} - \frac{\sqrt{(A-C)^2+B^2}}{2}\right)\omega^2 \tag{70}$$

where for $\cot(2\theta) = (A-C)/B$

$$\begin{bmatrix}\chi\\ \omega\end{bmatrix} = \begin{bmatrix}\cos(\theta) & \sin(\theta)\\ -\sin(\theta) & \cos(\theta)\end{bmatrix}\begin{bmatrix}x\\ y\end{bmatrix}$$

This transformation is used in constructing the standard canonical form of the conic sections equation; more information can be found at [2][8].

Please note that to prove the validity of this transformation, we will need the equivalence relation

$$\cot(2\theta) = \frac{A-C}{B} \Leftrightarrow B\cos(2\theta) - (A-C)\sin(2\theta) = 0$$

Let us start with the inverse of the bijective change of variables [8].

$$\begin{bmatrix}x\\ y\end{bmatrix} = \begin{bmatrix}\cos(\theta) & -\sin(\theta)\\ \sin(\theta) & \cos(\theta)\end{bmatrix}\begin{bmatrix}\chi\\ \omega\end{bmatrix}$$

Inserting these equations into Equation (70) results in the following [8].

$$\begin{aligned}&A\left(\chi^2\cos^2(\theta) - 2\chi\omega\cos(\theta)\sin(\theta) + \omega^2\sin^2(\theta)\right)\\ &+ B\left(\chi^2\cos(\theta)\sin(\theta) + \chi\omega\cos^2(\theta) - \chi\omega\sin^2(\theta) - \omega^2\cos(\theta)\sin(\theta)\right)\\ &+ C\left(\chi^2\sin^2(\theta) + 2\chi\omega\cos(\theta)\sin(\theta) + \omega^2\cos^2(\theta)\right)\end{aligned}$$

Rewriting this expression moves us closer to our desired outcome.

$$\begin{aligned}&\left(A\cos^2(\theta) + C\sin^2(\theta) + B\cos(\theta)\sin(\theta)\right)\chi^2\\ &+ \left(B\cos^2(\theta) - B\sin^2(\theta) + 2(C-A)\cos(\theta)\sin(\theta)\right)\chi\omega\\ &+ \left(A\sin^2(\theta) + C\cos^2(\theta) - B\cos(\theta)\sin(\theta)\right)\omega^2\end{aligned}$$

The $\chi\omega$-term of the expression above can be simplified to zero [8].

$$\left(B\cos^2(\theta) - B\sin^2(\theta) + 2(C-A)\cos(\theta)\sin(\theta)\right) = B\cos(2\theta) - (A-C)\sin(2\theta) = 0$$

Furthermore, we need to calculate the value of a few trigonometric functions.

$$\sin(2\theta) = \frac{B}{\sqrt{(A-C)^2 + B^2}}$$
$$\cos(2\theta) = \frac{A-C}{\sqrt{(A-C)^2 + B^2}}$$
$$\sin^2(\theta) = \frac{1-\cos(2\theta)}{2} = \frac{\sqrt{(A-C)^2 + B^2} - (A-C)}{2\sqrt{(A-C)^2 + B^2}}$$
$$\cos^2(\theta) = \frac{1+\cos(2\theta)}{2} = \frac{\sqrt{(A-C)^2 + B^2} + (A-C)}{2\sqrt{(A-C)^2 + B^2}}$$
$$\sin(\theta)\cos(\theta) = \frac{\sin(2\theta)}{2} = \frac{B}{2\sqrt{(A-C)^2 + B^2}}$$

Thus Equation (70) can be rewritten as

$$\left(\frac{(A+C)\sqrt{(A-C)^2 + B^2} + (A-C)^2 + B^2}{2\sqrt{(A-C)^2 + B^2}}\right)\chi^2 + \left(\frac{(A+C)\sqrt{(A-C)^2 + B^2} - (A-C)^2 - B^2}{2\sqrt{(A-C)^2 + B^2}}\right)\omega^2$$

which can be further reduced to

$$\left(\frac{(A+C)}{2} + \frac{\sqrt{(A-C)^2 + B^2}}{2}\right)\chi^2 + \left(\frac{(A+C)}{2} - \frac{\sqrt{(A-C)^2 + B^2}}{2}\right)\omega^2$$

which completes the proof [8].

C. Coding involved in Numerical Calculations

Including the raw code in this paper would increase the page-count significantly; the code is thousands of lines long. Instead, one can find the necessary python package located in the Github repository `https://github.com/HugoReijm/Toolbox`.

The python package, named toolbox, has a simple structure. Besides the obligatory __init__.py file, the package includes a number of "toolbox" files, each files designated for a particular field of mathematics. Currently, the four toolbox files are

- generaltoolbox, used for general mathematical concepts such as differentiation, integration, and function plotting
- matrixtoolbox, used for mathematics involving linear algebra, such as calculating the Jacobian and implementation of several matrix-vector equation solvers
- continuoustoolbox, used specifically for differential systems of equations and continuous dynamical systems.
- discretetoolbox, used specifically for difference systems

For full clarity, we now give a brief overview of the individual toolbox files. Every method of each file is described, including each of its arguments.

The code was written was the specific goal in mind of not being heavily dependent on specialized packages and modules. Any basic python editor should already have the prerequisites needed to run the toolbox package code. As such, most of the toolbox code is self-written, with a structure focusing on understandability.

generaltoolbox

- colors: returns equidistantly-spaced colors for plotting
  - N (integer): number of requested colors
- hammersley: returns pseudo-random Hammersley points
  - N (integer): number of requested points
  - dim (integer): dimension of requested points
  - points (boolean): formats output pointwise, otherwise formats coordinate-wise; defaults to False
- differentiate: differentiates a function in a point with respect to a dimension
  - f (method): function $\mathbb{R}^n \to \mathbb{R}$ to be differentiated
  - x (list): point in which f is differentiated
  - args (list): extra arguments for f; defaults to [ ]
  - kwargs (dictionary): extra keyword arguments for f; defaults to {}
  - h (float): step size of numerical differentiation; defaults to 1e-3
  - variableDim (integer): dimension over which f is differentiated in x; defaults to 1
- integrate: integrates a function over a finite domain
  - f (method): function $\mathbb{R} \to \mathbb{R}$ to be integrated
  - start (float): lower bound of integration domain
  - stop (float): upper bound of integration domain
  - args (list): extra arguments for f; defaults to [ ]
  - kwargs (dictionary): extra keyword arguments for f; defaults to {}
  - mode (string): selects from the following numerical integration techniques
    - mode = "gauss", "kronrod" selects the Gauss-Kronrod Quadrature (default)
    - mode $\neq$ "gauss", "kronrod" selects the Trapezium Quadrature
  - maxlevel (integer): sets maximum level of iterations if method is adaptive; defaults to 5
  - errtol (float): error tolerance used for verification if method is adaptive; defaults to 1e-3
  - adapt (boolean): dictates whether method uses an adaptive algorithm or not; defaults to True
- multiIntegrate: integrates a function over a finite multidimensional domain
  - f (method): function $\mathbb{R}^n \to \mathbb{R}$ to be integrated
  - start (list): lower bounds of integration domain
  - stop (list): upper bounds of integration domain
  - args (list): extra arguments for f; defaults to [ ]
  - kwargs (dictionary): extra keyword arguments for f; defaults to {}
  - N (integer): number of pseudo-random points used for multidimensional Monte-Carlo numerical integration; defaults to 1e3

- interpolate: interpolates temporally-advancing data into a temporally-equidistant set
  - sol (list of lists): set of n-dimensional temporally-advancing data formatted coordinate-wise
  - t (list): corresponding temporal data
  - N (integer): size of resulting interpolated data
- newtonRaphson: generic n-dimensional real root-finding algorithm
  - f (method): function $\mathbb{R}^n \to \mathbb{R}$ of which whose roots are requested
  - start (list): lower bounds of domain
  - stop (list): upper bounds of domain
  - delta (list): size per dimension of each subdomain
  - args (list): extra arguments for f; defaults to [ ]
  - kwargs (dictionary): extra keyword arguments for f: defaults to {}
  - errtol (float): error tolerance used for verification; defaults to 1e-3
  - neighborhoodRange (float): tolerance used for determining uniqueness of output per subdomain; defaults to 1e-2
  - maxlevel (integer): sets maximum level of iterations; defaults to 50
  - speed (float): weight used to speed up or slow down convergence; defaults to 1.0
- pointplot: determines roots of function using Marching Line Algorithm
  - f (method): explicit or implicit function $\mathbb{R} \to \mathbb{R}$ of which whose roots are requested
  - start (float): lower bound of domain
  - stop (float): upper bound of domain
  - delta (float): size of subdomains
  - args (list): extra arguments of f; defaults to [ ]
  - kwargs (dictionary): extra keyword arguments of f; defaults to {}
  - adapt (boolean): dictates whether method uses an adaptive algorithm or not; defaults to True
  - maxlevel (integer): sets maximum level of iterations if method is adaptive; defaults to 10
  - mode (string): selects from the following interpolation techniques
    - mode = "cubic" selects the cubic interpolation method
    - mode = "quadratic" selects the quadratic interpolation method
    - mode $\neq$ "cubic", "quadratic" selects the linear interpolation method
  - plotbool (boolean): dictates whether output should be plotted; defaults to True
  - plotaxis (axis): pre-existing axis to plot the output in if plotbool is True; defaults to None
  - colormap (colormap): colormap to plot output with, if any; defaults to None
  - color (list or string): color to plot output with if colormap is None; defaults to "black"
  - alpha (float): alpha value to plot output with; defaults to 1.0

- plot2D: plots explicit function with 1-dimensional input
  - f (method): function $\mathbb{R} \to \mathbb{R}$ to be plotted
  - start (float): lower bound of domain
  - stop (float): upper bound of domain
  - delta (float): step-size used for plotting through domain
  - args (list): extra arguments for f; defaults to [ ]
  - kwargs (dictionary): extra keyword arguments for f; defaults to {}
  - limit (list): limits the lower and upper value of function output; defaults to [None, None]
  - dependentvar (string): selects from the following axes corresponds to output
    - dependentvar = "x" selects x-axis
    - dependentvar $\neq$ "x" selects y-axis (default)
  - mode (string): selects from the following types of graphs
    - mode = "polar" selects a polar graph
    - mode $\neq$ "polar" selects a Cartesian graph (default)
  - plotaxis (axis): pre-existing axis to plot output in; defaults to None
  - color (list or string): color to plot output with; defaults to "black"
  - alpha (float): alpha value to plot output with; defaults to 1.0
- lineplot: determines the roots of function using Marching Square Algorithm
  - f (method): explicit or implicit function $\mathbb{R}^2 \to \mathbb{R}$ of which whose roots are requested
  - start (list): lower bounds of domain
  - stop (list): upper bounds of domain
  - delta (list): size per dimension of subdomains
  - args (list): extra arguments of f; defaults to [ ]
  - kwargs (dictionary): extra keyword arguments of f; defaults to {}
  - adapt (boolean): dictates whether method uses an adaptive algorithm or not; defaults to True
  - maxlevel (integer): sets maximum level of iterations if method is adaptive; defaults to 5
  - mode (string): selects from the following interpolation techniques
    - mode = "cubic" selects the cubic interpolation method
    - mode = "quadratic" selects the quadratic interpolation method
    - mode $\neq$ "cubic", "quadratic" selects the linear interpolation method
  - plotbool (boolean): dictates whether output should be plotted; defaults to True
  - plotaxis (axis): pre-existing axis to plot the output in if plotbool is True; defaults to None
  - wireframe (boolean): dictates whether to plot output using a wireframe or just using a point cloud; defaults to True
  - colormap (colormap): colormap to plot output with, if any; defaults to None

- color (list or string): color to plot output with if colormap is None; defaults to "black"
- alpha (float): alpha value to plot output with; defaults to 1.0

- plot3D: plots explicit function with 2-dimensional input
  - f (method): function $\mathbb{R}^2 \to \mathbb{R}$ to be plotted
  - start (list): lower bounds of domain
  - stop (list): upper bounds of domain
  - delta (list): step-size used for plotting through domain per dimension
  - args (list): extra arguments for f; defaults to [ ]
  - kwargs (dictionary): extra keyword arguments for f; defaults to {}
  - limit (list): limits the lower and upper value of function output; defaults to [None, None]
  - dependentvar (string): selects from the following axes corresponds to output
    - dependentvar = "x" selects x-axis
    - dependentvar = "y" selects y-axis
    - dependentvar $\neq$ "x", "y" selects z-axis (default)
  - plotaxis (axis): pre-existing axis to plot output in; defaults to None
  - wireframe (boolean): plots output using a wireframe, otherwise plots using polygonal surface reconstruction; defaults to False
  - colormap (colormap): colormap to plot output with, if any; defaults to None
  - color (list or string): color to plot output with is colormap is None; defaults to "black"
  - alpha (float): alpha value to plot output with; defaults to 1.0

- surfaceplot: determines the roots of function using Marching Cube Algorithm
  - f (method): explicit or implicit function $\mathbb{R}^3 \to \mathbb{R}$ of which whose roots are requested
  - start (list): lower bounds of domain
  - stop (list): upper bounds of domain
  - delta (list): size per dimension of subdomains
  - args (list): extra arguments of f; defaults to [ ]
  - kwargs (dictionary): extra keyword arguments of f; defaults to {}
  - adapt (boolean): dictates whether method uses an adaptive algorithm or not; defaults to True
  - maxlevel (integer): sets maximum level of iterations if method is adaptive; defaults to 3
  - mode (string): selects from the following interpolation techniques
    - mode = "cubic" selects the cubic interpolation method
    - mode = "quadratic" selects the quadratic interpolation method
    - mode $\neq$ "cubic", "quadratic" selects the linear interpolation method
  - plotbool (boolean): dictates whether output should be plotted; defaults to True

- plotaxis (axis): pre-existing axis to plot the output in if plotbool is True; defaults to None
- surface (boolean): dictates whether to plot output using a polygonal surface reconstruction or not
- wireframe (boolean): dictates whether to plot output using a wireframe or not
- colormap (colormap): colormap to plot output with, if any; defaults to None
- color (list or string): color to plot output with if colormap is None; defaults to "black"
- alpha (float): alpha value to plot output with; defaults to 1.0

matrixtoolbox

- jacobian: calculates the Jacobian of a function at a point
  - f (method): function $\mathbb{R}^n \to \mathbb{R}^m$ of which whose Jacobian is requested
  - vect (list): point in which the Jacobian of f is calculated
  - h (float): step-size of numerical differentiation; defaults to 1e-6
  - args (list): extra arguments for f; defaults to [ ]
  - kwargs (dictionary): extra keyword arguments for f; defaults to {}
- grammSchmidt: orthogonalizes set of vectors
  - vectors (list of lists): list of vectors to be orthogonalized
  - tol (float): zero tolerance; defaults to 1e-6
  - normalize (boolean): normalizes orthogonalized vectors; defaults to True
  - clean (boolean): removes vectors whose norm falls under the zero tolerance; defaults to True
- jacobi: matrix-vector equation solver using Jacobi iteration
  - A (list of lists): matrix in $\mathbb{R}^{n\times m}$ of equation A*x=b
  - b (list): vector in $\mathbb{R}^n$ of equation A*x=b
  - errtol (float): error tolerance used for verification; defaults to 1e-6
  - maxlevel (integer): sets maximum level of iterations; defaults to 1000
  - x0 (list): optional first guess at solution of equation A*x=b; defaults to None
  - omega (float): weight for optional weighted Jacobi iterations; defaults to 1.0
  - inform (boolean): informs user of convergence and viability of output; defaults to False
- sor: matrix-vector equation solver using Successive Over-Relaxation
  - A (list of lists): matrix in $\mathbb{R}^{n\times m}$ of equation A*x=b
  - b (list): vector in $\mathbb{R}^n$ of equation A*x=b
  - errtol (float): error tolerance used for verification; defaults to 1e-6
  - maxlevel (integer): sets maximum level of iterations; defaults to 1000
  - x0 (list): optional first guess at solution of equation A*x=b; defaults to None
  - omega (float): weight for optional weighted Successive Over-Relaxation iterations; defaults to 1.0
  - inform (boolean): informs user of convergence and viability of output; defaults to False
- cg: matrix-vector equation solver using Conjugate Gradient Algorithm
  - A (list of lists): matrix in $\mathbb{R}^{n\times m}$ of equation A*x=b
  - b (list): vector in $\mathbb{R}^n$ of equation A*x=b
  - errtol (float): error tolerance used for verification; defaults to 1e-6
  - maxlevel (integer): sets maximum level of iterations; defaults to 1000
  - x0 (list): optional first guess at solution of equation A*x=b; defaults to None

- inform (boolean): informs user of convergence and viability of output; defaults to False

- lu: matrix-vector equation solver using LU-decomposition
  - A (list of lists): matrix in $\mathbb{R}^{n \times m}$ of equation A*x=b
  - b (list): vector in $\mathbb{R}^{n}$ of equation A*x=b
  - tol (float): zero tolerance; defaults to 1e-6
  - symbol (boolean): allows for symbolic solving of matrix-vector equation
  - inform (boolean): informs user of viability of output; defaults to False

continuoustoolbox

- poincareSection: calculates a Poincare Section of a trajectory of a dynamical system
  - sol (list of lists): trajectory of dynamical system formatted coordinate-wise
  - planeCoords (list): point on the n-1 dimensional plane used for the Poincare Section in n-dimensional phase space
  - planeParams (list): normal vector of the n-1 dimensional plane used for the Poincare Section in n-dimensional phase space
- lyapunovSpectrum: calculates the Lyapunov Spectrum of a trajectory of a dynamical system
  - sol (list of lists): trajectory of dynamical system formatted coordinate-wise
  - t (list): corresponding temporal data
  - f (method): system of differential equations controlling the trajectory of dynamical system
  - args (list): extra arguments for f; defaults to [ ]
  - kwargs (dictionary): extra keyword arguments for f; defaults to {}
  - dist (float): initial distance between initial positions at each iteration of algorithm; defaults to 1e-6
  - K (integer): number of Lyapunov Exponents to be calculated; defaults to 1
  - easy (boolean): dictates whether to use easy RK4 or hard RK14 integration; defaults to True
  - plotbool (boolean): dictates whether output should be plotted; defaults to False
  - plotaxis (axis): pre-existing axis to plot the output in if plotbool is True; defaults to None
  - savefigName (string): saves plot of output under savefigName.png if plotbool is True; defaults to None
- rungeKutta: generic n-dimensional explicit Runge Kutta numerical integration algorithm
  - a (list of lists): a matrix of Butcher Tableau
  - b (list): b vector of Butcher Tableau
  - c (list): c vector of Butcher Tableau
  - f (method): system of differential equations controlling dynamical system
  - vect0 (list): initial position of trajectory
  - args (list): extra arguments for f
  - kwargs (dictionary): extra keyword arguments of f
  - start (list): lower bounds of domain in phase space
  - stop (list): upper bounds of domain in phase space
  - tstart (float): lower bound of temporal domain
  - tstop (float): upper bound of temporal domain
  - deltat (float): time step used in numerical integration

  - inform (boolean): informs user of viability of output
  - rev (boolean): reverses the direction of dynamical system
  - autonomous (boolean): indicates whether dynamical system is autonomous or not
  - adapt (boolean): dictates whether method uses an adaptive algorithm or not
- euler: n-dimensional explicit forward Euler numerical integration algorithm
  - f (method): system of differential equations controlling dynamical system
  - vect0 (list): initial position of trajectory
  - start (list): lower bounds of domain in phase space
  - stop (list): upper bounds of domain in phase space
  - tstart (float): lower bound of temporal domain
  - tstop (float): upper bound of temporal domain
  - deltat (float): time step used in numerical integration
  - args (list): extra arguments for f; defaults to [ ]
  - kwargs (dictionary): extra keyword arguments of f; defaults to {}
  - inform (boolean): informs user of viability of output; defaults to True
  - rev (boolean): reverses the direction of dynamical system; defaults to False
  - autonomous (boolean): indicates whether dynamical system is autonomous or not; defaults to True
  - adapt (boolean): dictates whether method uses an adaptive algorithm or not; defaults to False
- rk2: n-dimensional explicit Runge Kutta 2 numerical integration algorithm
  - f (method): system of differential equations controlling dynamical system
  - vect0 (list): initial position of trajectory
  - start (list): lower bounds of domain in phase space
  - stop (list): upper bounds of domain in phase space
  - tstart (float): lower bound of temporal domain
  - tstop (float): upper bound of temporal domain
  - deltat (float): time step used in numerical integration
  - args (list): extra arguments for f; defaults to [ ]
  - kwargs (dictionary): extra keyword arguments of f; defaults to {}
  - inform (boolean): informs user of viability of output; defaults to True
  - rev (boolean): reverses the direction of dynamical system; defaults to False
  - autonomous (boolean): indicates whether dynamical system is autonomous or not; defaults to True
  - adapt (boolean): dictates whether method uses an adaptive algorithm or not; defaults to False
- rk4: n-dimensional explicit Runge Kutta 4 numerical integration algorithm
  - f (method): system of differential equations controlling dynamical system
  - vect0 (list): initial position of trajectory
  - start (list): lower bounds of domain in phase space

  - stop (list): upper bounds of domain in phase space
  - tstart (float): lower bound of temporal domain
  - tstop (float): upper bound of temporal domain
  - deltat (float): time step used in numerical integration
  - args (list): extra arguments for f; defaults to [ ]
  - kwargs (dictionary): extra keyword arguments of f; defaults to {}
  - inform (boolean): informs user of viability of output; defaults to True
  - rev (boolean): reverses the direction of dynamical system; defaults to False
  - autonomous (boolean): indicates whether dynamical system is autonomous or not; defaults to True
  - adapt (boolean): dictates whether method uses an adaptive algorithm or not; defaults to False

- rk12: n-dimensional explicit Runge Kutta 12 numerical integration algorithm
  - f (method): system of differential equations controlling dynamical system
  - vect0 (list): initial position of trajectory
  - start (list): lower bounds of domain in phase space
  - stop (list): upper bounds of domain in phase space
  - tstart (float): lower bound of temporal domain
  - tstop (float): upper bound of temporal domain
  - deltat (float): time step used in numerical integration
  - args (list): extra arguments for f; defaults to [ ]
  - kwargs (dictionary): extra keyword arguments of f; defaults to {}
  - inform (boolean): informs user of viability of output; defaults to True
  - rev (boolean): reverses the direction of dynamical system; defaults to False
  - autonomous (boolean): indicates whether dynamical system is autonomous or not; defaults to True
  - adapt (boolean): dictates whether method uses an adaptive algorithm or not; defaults to False

- rk14: n-dimensional explicit Runge Kutta 14 numerical integration algorithm
  - f (method): system of differential equations controlling dynamical system
  - vect0 (list): initial position of trajectory
  - start (list): lower bounds of domain in phase space
  - stop (list): upper bounds of domain in phase space
  - tstart (float): lower bound of temporal domain
  - tstop (float): upper bound of temporal domain
  - deltat (float): time step used in numerical integration
  - args (list): extra arguments for f; defaults to [ ]
  - kwargs (dictionary): extra keyword arguments of f; defaults to {}
  - inform (boolean): informs user of viability of output; defaults to True
  - rev (boolean): reverses the direction of dynamical system; defaults to False

  - autonomous (boolean): indicates whether dynamical system is autonomous or not; defaults to True
  - adapt (boolean): dictates whether method uses an adaptive algorithm or not; defaults to False

- verlet: n-dimensional explicit Verlet numerical integration algorithm
  - f (method): system of differential equations controlling dynamical system
  - vect0 (list): initial position of trajectory
  - start (list): lower bounds of domain in phase space
  - stop (list): upper bounds of domain in phase space
  - tstart (float): lower bound of temporal domain
  - tstop (float): upper bound of temporal domain
  - deltat (float): time step used in numerical integration
  - args (list): extra arguments for f; defaults to [ ]
  - kwargs (dictionary): extra keyword arguments of f; defaults to {}
  - inform (boolean): informs user of viability of output; defaults to True
  - rev (boolean): reverses the direction of dynamical system; defaults to False
  - adapt (boolean): dictates whether method uses an adaptive algorithm or not; defaults to False

- eulerTableau: forward Euler numerical integration algorithm Butcher Tableau
- rk2Tableau: Runge Kutta 2 numerical integration algorithm Butcher Tableau
- rk4Tableau: Runge Kutta 4 numerical integration algorithm Butcher Tableau
- rk12Tableau: Runge Kutta 12 numerical integration algorithm Butcher Tableau
- rk14Tableau: Runge Kutta 14 numerical integration algorithm Butcher Tableau

discretetoolbox

- generate: generate a sequence of points dictated by a difference system
  - f (method): difference system
  - vect0 (list): initial position of sequence
  - N (integer): size of outputted sequence
  - args (list): extra arguments for f; defaults to [ ]
  - kwargs (dictionary): extra keyword arguments for f; defaults to {}
- lyapunovSpectrum: calculates the Lyapunov Spectrum of a sequence of a difference system
  - sol (list of lists): sequence of difference system formatted coordinate-wise
  - f (method): difference system
  - args (list): extra arguments for f; defaults to [ ]
  - kwargs (dictionary): extra keyword arguments for f; defaults to {}
  - dist (float): initial distance between initial positions at each iteration of algorithm; defaults to 1e-6
  - K (integer): number of Lyapunov Exponents to be calculated; defaults to 1
  - plotbool (boolean): dictates whether output should be plotted; defaults to False
  - plotaxis (axis): pre-existing axis to plot the output in if plotbool is True; defaults to None
  - savefigName (string): saves plot of output under savefigName.png if plotbool is True; defaults to None